Fluidized Segregation of a Bidisperse Particulate Mixture in a Nonuniform Annular Geometry

by

Rajesh Bilimoria

Bachelor of Science, Engineering and Applied Science
California Institute of Technology, 1993

Submitted to the Department of Mechanical Engineering
in Partial Fulfillment of the Requirements for the Degree of

MASTER OF SCIENCE IN MECHANICAL ENGINEERING

at the

MASSACHUSETTS INSTITUTE OF TECHNOLOGY

May 1995

Signature of Author _____
Department of Mechanical Engineering
12 May 1995

Certified by _____
Carl R. Peterson
Professor of Mechanical Engineering
Thesis Supervisor

Accepted by _____
Ain A. Sonin
Chairman, Graduate Committee

Fluidized Segregation of a Bidisperse Particulate Mixture in a Nonuniform Annular Geometry

by

Rajesh Bilimoria

Submitted to the Department of Mechanical Engineering in May, 1995
in partial fulfillment of the requirements for the degree of
Master of Science in Mechanical Engineering

ABSTRACT

An apparatus is designed and fabricated for conducting experiments concerning fluidized segregation to verify a proposed design concept for a more efficient comminution machine. Previous studies have found that the fines distribute the intended crushing load imposed by the machine on the particle bed; thus, the load that must be applied to crush the larger particles increases. By removing the fines as they are produced, smaller loads may be applied to achieve crushing. The proposed design incorporates size-dependent material transport and comminution into a single, continuous process. This integration can provide increased comminution efficiency by removing the fines as soon as they are produced. To effect removal of the fines, fluidization will be employed. An upward water jet will carry away only particles that are smaller than a threshold size, which is controlled by the velocity of the fluid.

In order to implement the above concepts, a machine design has been proposed. The design features a nonuniform annular gap, which is the space between two cylinders. The inner cylinder revolves around its own axis, which in turn revolves about the axis of the outer cylinder. The resulting geometry is a gap that appears to converge and diverge in time, when viewed from any fixed point on the cylinder. The converging-diverging motion of the walls will provide the motion necessary for comminution, and the cylindrical implementation will allow a the machine to operate continuously.

An apparatus has been designed and constructed to conduct experiments that will determine the efficacy of fluidized segregation in the nonuniform annular geometry under simulated crushing conditions. The device simulates the kinematic behavior of the proposed concept and provides facilities for observation and data acquisition. In addition, a set of experiments has been designed to explore the operating space of the apparatus. Data acquired from the apparatus is to be captured on SVHS videotape, from which it is post-digitized and analyzed with computer image analysis tools.

Thesis Supervisor: Carl R. Peterson
Title: Professor of Mechanical Engineering

Acknowledgments

Many people have contributed to this work. Professor Carl Peterson has provided the necessary support and guidance during the different phases of this project. Working with such a skilled designer has been an invaluable part of my education. Professors Frank McClintock and Harri Kytömaa offered additional ideas during the initial design work on this thesis. Fellow graduate students Stefano Schiaffino and Mick Wisnewski provided assistance in the Fluid Mechanics Laboratory.

Many people on the staff at MIT were very helpful. Dick Fenner provided significant logistical assistance. Norman Berube was very helpful when machining tasks arose. Julie Drennan and Dot Cavanaugh provided assistance with the many administrative matters that demanded attention.

My officemates made my work at MIT more enjoyable. Kristen Bohlke, José Arocha, and Amy Smith made 3-438B nicer place to work. Kristen helped the many hours of the final semester pass more quickly. José shared my interest in industrial design and other things visual and provided many enjoyable conversations. Amy's experience and knowledge was an invaluable resource for all of those little questions.

Finally, I would also like to thank my parents and my sister for their constant support during my education.

This work was made possible in part by a grant from the United States Department of Energy.

Contents

Abstract 3

Acknowledgments 5

Contents 7

Figures 9

Chapter 1 Background and Motivation 11
1.1 Overview of Comminution Processes 11
1.1.1 Primary Crushing 12
1.1.2 Secondary Crushing 12
1.1.3 Fine Grinding 12
1.2 Motivations for a Different Design 13
1.3 The New Design Concept 13
1.4 Previous Work in the Comminution Program: Particle Fracture in Beds 17
1.4.1 Efficiency and Efficiency Metrics 18
1.4.2 Optimal Bed Compression 18
1.4.3 Optimal Bed Thickness 19
1.4.4 Recommendations 19
1.5 Previous Work in the Comminution Program: Particle Fluidization and Segregation 19
1.5.1 Steady Fluidization of Fine Particles Within a Coarse Matrix 20
1.5.2 Impulsive Fluidization of a Bidisperse Mixture 20
1.5.3 Impulsive Fluidization of a Bidisperse Mixture Between Outwardly Moving Walls 21
1.5.4 Discussion of Previous Fluidization/Segregation Work 22
1.6 Organization 22

Chapter 2 Design of An Apparatus for Fluidized Segregation of a Bidisperse Particulate Mixture in a Nonuniform Annular Geometry 25
2.1 Apparatus Objectives 25
2.2 Experimental Apparatus 26
2.2.1 Test Section Geometry & Kinematics 29
2.2.2 Power System 32
2.2.3 Structure 32
2.2.4 Fluid System 33
2.2.5 Observation 34
2.2.6 Parameters 35
2.2.7 Alternatives Considered 35
2.2.8 Sample Data 36

Chapter 3 Discussion **41**
3.1 Preliminary Data Interpretation 41
3.2 Apparatus Idealizations *v.* Actual Practice 42
3.3 Fluidization Time *v.* Settling Zone 42
3.4 Issues Not Addressed By This Apparatus 42

Chapter 4 Conclusions **45**
4.1 Summary 45
4.2 Future Work 45
4.2.1 Hardware Completion 45
4.2.2 Experimentation Recommendations 46

Appendix A Assembly & Disassembly Instructions **51**
A.1 Disassembly 51
A.2 Assembly 51

Appendix B Resources **53**

Appendix C Engineering Drawings **55**

Bibliography **87**

Figures

Figure 1.1. A plan view and section of the proposed machine geometry. 14
Figure 1.2. Plan and side views of the unwrapped machine geometry. 16
Figure 1.3. Conical machine geometry (section view).. 17
Figure 2.1. The apparatus. 27
Figure 2.2. A schematic illustration of the apparatus 28
Figure 2.3. The test section of the apparatus 29
Figure 2.4. An isometric illustration of the apparatus. 30
Figure 2.5. A cross section of the test section of the apparatus.. 31
Figure 2.6. Isometric illustration of the nozzle employed in the apparatus. 33
Figure 2.7. A sample image set. Images were captured at a rate of one fps 38
Figure 2.8. Images of the test section as the jet flow begins.. 39
Figure 4.1. An isometric illustration of a new nozzle design. 46

Chapter 1

Background and Motivation

The purpose of this research program is to determine the efficacy of fluidized segregation for use in industrial comminution devices. The mining, pharmaceutical, and food processing industries are among those that employ comminution as an industrial process. Unfortunately, current comminution processes consume large amounts of energy and are, additionally, quite inefficient. The energy not contributing to particle fracture is lost to machine wear, noise, and heat. Upon first examination, the comminution process appears to be inherently inefficient; as small particles are formed from the crushing of larger particles, they distribute the crushing load on the remaining large particles. Thus, the load that must be applied to the crushing bed to achieve the stress concentrations required for particle fracture increases. If the smaller particles were removed as they were created, however, the loads applied by the crushing chamber would remain concentrated and the previously mentioned inefficiency would not arise. In current devices for crushing large fragments of material, gravity is used to attempt to remove the fines; however, gravity-driven removal systems often clog when fine particles are being produced.

The goal of this research is to interpret the results of previous studies on fluidized segregation and apply those to the development of a comminution device that simultaneously segregates particles while it comminutes them. Fluidized segregation uses an upward water flow to separate the fine particles from the coarse particles in the comminution chamber. Since only coarse particles remain to be crushed in such a device, the major inefficiency is removed, and thus the force required to crush a particular size of particle remains constant. Fluidized segregation provides a mechanism to achieve fine particle removal. Additionally, only particles that have reached a particular size threshold are carried away by the upward water flow, since the terminal velocity of a particle is proportional to particle diameter. Particles are only resident in the comminution chamber as long as they are larger than the desired diameter. Potential benefits include energy conservation, reduced machine wear, increased productivity, and, perhaps, better product uniformity.

This work involves the design and fabrication of an experimental apparatus to observe fluidized segregation in the proposed machine geometry. In this work, idealizations were made to facilitate experimentation and observation. The experiments to be conducted with this apparatus focus upon particle segregation. Comminution could be performed in this geometry, while coarse material transport (into the machine) may present more challenging problems to be solved before the proposed concept can be successfully executed.

The proposed design is intended for fine crushing of particles to 20 μ, as is required for the deep cleaning of coal or beneficiation of oil shale or other materials.

1.1 Overview of Comminution Processes

Comminution refers to processes involving grinding and crushing. Reduced materials are produced either for further reduction or as end products. A comminution system may consist of several stages, each of which achieves a level of particle size reduction. The number

of stages in a comminution process is dependent upon the quantity of material to be processed, the rate at which it must be processed, the hardness of the material, and the amount of reduction required. Although the number of stages can vary from process to process, there are three main categories into which stages fall: primary, secondary, and fine grinding. Each of the categories is described below.

1.1.1 Primary Crushing

As indicated by its name, primary crushing is the first stage of comminution. In some sense, this processing stage can be thought of as preparatory; primary crushers reduce large fragments of blasted rock to sizes suitable for handling by secondary crushing equipment and transfer equipment. There are three main types of primary crushers: jaw crushers, gyratory crushers, and impact crushers. Descriptions of these types of machines, as well as their relative strengths and weaknesses follow.

Jaw crushers are the simplest type of primary crusher. In a jaw crusher, the rock to be crushed is simply squeezed between a stationary and a movable jaw. The surfaces of the jaws are tapered to facilitate the grasping of the rock. Although various angles have been experimented with, most jaw crushers implement a crushing angle of 27°. Jaw crushers are pressure, as opposed to impact, crushing machines.

Gyratory crushers feature a cone in a housing. The media to be ground resides between the cone and the housing. The cone is mounted on a shaft; one end of the shaft is held stationary, while the other is eccentrically rotated. Gyratory crushers possess several advantages over other crushing mechanisms, including: the largest unrestricted feed opening available, a high range of sizes and capacities where rates of between 600 and 6,000 tons per hour are required, and the absence of required feed control (Mular & Bhappu, 1980).

Impact crushers effect material reduction through the impact of the material to be crushed with fixed or free-swinging hammers revolving about a central rotor. Kinetic energy imparted to the particles results in reduction when the particles impact breaking plates or the hammers. Both rotor speed and friability affect the proportion of fines produced; higher speeds or friabilities yield higher proportions of fines. Impact crushers offer several advantages over compression crushers, including: lower installed capital costs per ton of capacity, more cubical product, and finer product gradation. Disadvantages include high maintenance costs and the amount of testing of the feed material required before use. (Mular & Bhappu, 1980).

1.1.2 Secondary Crushing

Secondary crushing can include a number of stages; it includes all the stages following primary crushing that precede fine grinding, the final stage of comminution. The most common type of machine for these stages is the cone crusher. The cone crusher is similar to the gyratory crushers mentioned above, with the following key distinction: the base of the cone moves through a larger distance and gyrates at much faster speeds. The combined effect is that finer products result, in part because the higher gyratory speeds make the crushing process more like impact crushing, rather than pressure crushing. The size of the product is related to the stroke (eccentricity) of the base of the cone.

1.1.3 Fine Grinding

Grinding is the final phase of comminution. Grinding is usually performed in rotating drums where grinding media reduce the product through impact, attrition, and

abrasion mechanisms. Several types of media are available: the product itself (autogeneous milling), natural or manufactured media. Natural and manufactured media exist in both metallic (steel or iron rods or balls) and non-metallic types (pebbles). Due to the abrasive nature of the process, machine wear is a serious problem. Additional problems include the large capital cost of grinding machinery and the large quantities of power consumed in grinding processes.

1.2 Motivations for a Different Design

Comminution processes, in general, are extremely inefficient. Considerable energy is consumed by machine wear, noise, and heat, none of which are desirable. A report from the National Academy of Sciences (1981) notes that comminution processes consume two percent of the electrical power produced in the United States; in the rest of the world, the figure is five percent. In order to discuss comminution efficiency, a metric must be utilized. One metric compares the energy required for comminution to the energy associated with the new surface created. Under such a metric, the efficiency of current industrial processes ranges from one percent to two percent. The extremely low efficiencies and large amount of energy consumed by comminution processes motivate more efficient machine designs.

Material transport has not been addressed as an important issue related to comminution. Specifically, the transport of the fines can have serious performance implications, since the presence of fines contributes to additional friction and rubbing during comminution. Additionally, the smaller particles distribute the crushing load over the larger particles, necessitating the need for larger forces (Laffey, 1987). Given the fines' detrimental impact on comminution processes, it is clear that they should be removed as they are formed.

At the center of this research is an idea for a comminution machine designed so that the functions of crushing and material transport are both addressed. By removing the fines upon their formation, the negative effects of the fines on comminution efficiency would be minimized, and comminution efficiency would increase. In turn, comminution productivity would be improved.

1.3 The New Design Concept

The design that motivates this work has undergone some conceptual development. It is the goal of the Comminution Program, and this work, to implement these concepts. The design concept embodies two main components: fluidized segregation and a circumferentially changing gap, each of which is discussed below.

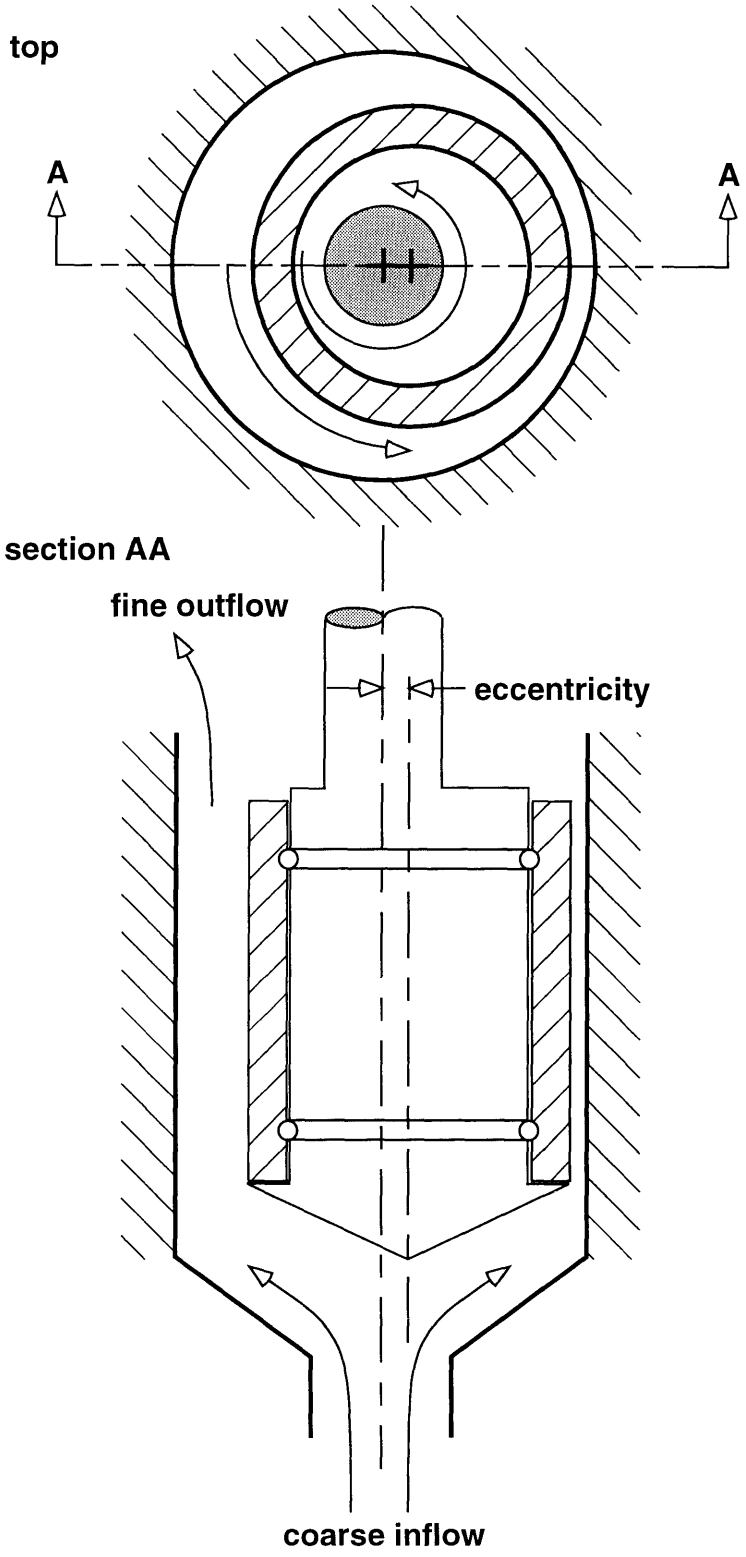

Figure 1.1. A plan view and section of the idealized machine geometry.

Fluidization involves the propulsion of particles by fluid flow, and is dependent upon their size. The underlying principle behind fluidization is that of terminal velocity and its proportional relationship to particle diameter. The working fluid velocity is such that particles of and smaller than a certain diameter are carried upward with the fluid. The diameter of particles carried away is determined by the velocity of the fluid, and is thus controllable. In gyratory or jaw crushers, material transport is effected by means of gravity; particles that are smaller than the smallest opening of the crusher pass through; larger particles remain to be crushed. Unfortunately, such systems fail when fine particles are desired as an end product; surface forces retain the particles, the small opening in the flow-through area clogs, and no material flows out. In this area, fluidization is superior, since clogging cannot occur. Another potential advantage is that the entire transport of material can be achieved with fluidization; the coarse/fines mixture could be fluidized in, and the fines could be fluidized out. Additionally, wet fluidization prevents very fine particles from becoming airborne; the particles are suspended in the working fluid and, as slurries, are more easily handled. The transport issues discussed here have not been explored experimentally and warrant further investigation. These issues are discussed in chapter three.

The circumferentially changing gap is a feature of the geometry of the design concept. While a cylindrical geometry is represented here, as well as in the experimental test section, it is not a fixture of the design; rather, it is a simplification that facilitates the construction and analysis of the test section and the design concept. The geometry of the crushing section is another area of the concept that can, and should, be refined before such a device were designed for production. Figures 1.1 and 1.2 illustrate the general design concept into which we would integrate material transport operations to remove the fine particles. The kinematic motion of the system is similar to that of a planetary gear system, *i.e.* the inner crushing surface can be thought of as rolling (not slipping) on the outer crushing surface (or on the imaginary surface of the cylinder with a radius equal to the radius of the inner member plus the eccentricity). This kinematic relationship is achieved through the eccentric rotation of the inner member and produces an annular geometry in which the circumferential gap is changing, *i.e.* at any fixed point on the outer crushing surface, the gap appears to shrink and grow. Where the gap is narrowing (until the minimum gap is reached), crushing is occurring; in the region following that the walls are diverging and material is expanded and agitated. This is the region in which fluidized segregation would occur. The crushing zone is illustrated in Figure 1.2. Fluidization and wall expansion must occur in concert such that as the comminution gap narrows, new coarse material has been introduced into the crushing zone. Crushing will be facilitated by the irregular shape of the actual particles, as they will bind in the gap and be crushed.

This experiment, while being the most complex of those in the Comminution Program, is still an idealization of the design concept in several respects. These idealizations will affect the interpretation of our results and will be discussed further in the chapter three. Experiments are based upon the behavior of a bidisperse particle mixture, in a cylindrical geometry. Of course, in practice, many more than two sizes of particles would be encountered, and rather than being spherical, their shapes would likely be irregular. Additionally, the geometry of the test section, here circular, might be replaced by a conical or more complex crushing chamber in actual practice. Finally, the scale of the experiment must be addressed. The quantities of media this experiment accommodates are on the order of one kilogram, while industrial applications would involve much larger quantities of material. In spite of these limitations, there is much to observe from this experiment. The idealizations we have made allow us to more clearly see the phenomena occurring in this very complex regime.

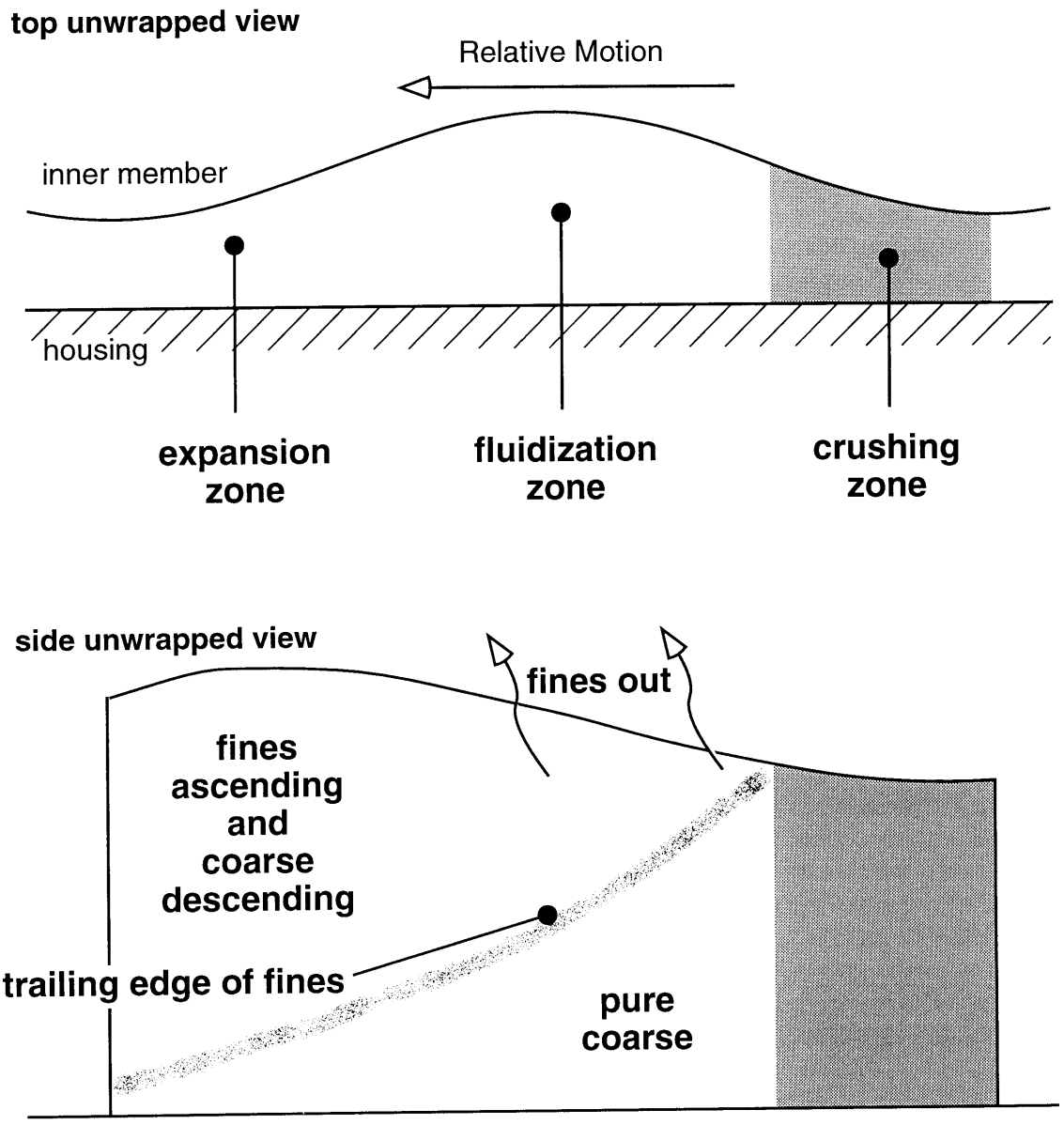

Figure 1.2. Plan and side views of the unwrapped machine geometry.

The eccentricity which produces the circumferentially changing gap directly affects the comminution efficiency by determining the bed compression the device produces. Ghaddar (1991) shows that maximum comminution efficiency can be achieved with a bed compression of 22%. This compression ratio corresponds to

$$\frac{\delta_{min}}{\delta_c} \cong 0.78 \tag{1.1}$$

where δ_{min} denotes the minimum gap width and δ_c denotes the gap width at which crushing begins.

In order to achieve maximum comminution efficiency, a thin bed arrangement would be best. To facilitate this a conical geometry is proposed (see Figure 1.3); the inner

member is a cone that subtends a narrower angle than the outer member, which is also a cone. The inner member could oscillate vertically to produce converging-diverging walls, but, since this would entail a very large force as crushing occurs simultaneously over the entire area, a nutating central cone (like that of a gyratory crusher) is still the preferred design. The conical geometry would allow for a decreasing fluid velocity in the forward direction (increasing cross section passages), even though the gap between opposite walls is diminishing in that direction. An inclined geometry may also offer segregation benefits (Savage and Lun, 1988), although this mechanism has not been explored in high solid fractions, such as those that occur in comminution.

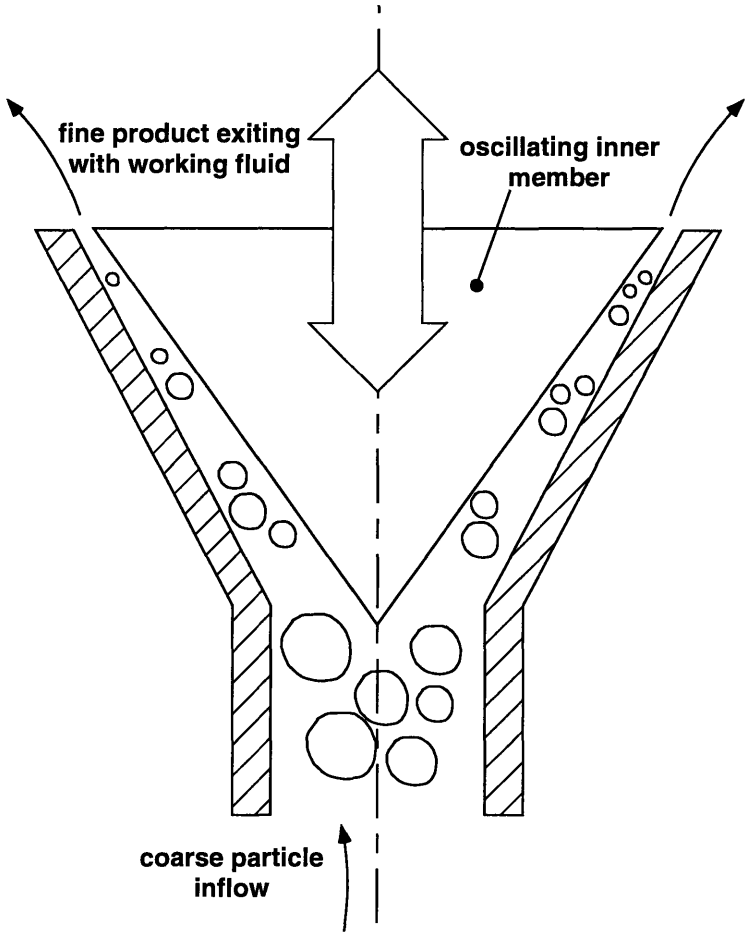

Figure 1.3. Conical machine geometry (section view). The fluid velocity decreases as it nears the top of the section due to the decreasing area. The decreasing velocity restricts the size of particles that can be carried upward by the flow. Comminution is achieved as the inner conical member oscillates vertically.

1.4 Previous Work in the Comminution Program: Particle Fracture in Beds

A significant segment of the work in this program was devoted to the phenomena related to particle fracture. These investigations (Ghaddar, Pflueger, Laffey, Larson) comprised theoretical and empirical studies, as well as computer simulations, and provided

insight into bed and loading conditions. The objective of this phase of the research was to determine and apply these insights to optimize (maximize) particle fracture in the crushing bed.

As in the current work, glass particles were used in these experiments. Glass beads are readily available in a variety of sizes and have been used by other authors, facilitating data comparisons. Spherical particles eliminate the effects of shape complexity, allowing a better understanding of the phenomena at work.

1.4.1 Efficiency and Efficiency Metrics

As noted earlier, an efficiency metric is necessary to evaluate the performance of a comminution device. Ghaddar developed a simple, yet effective, model that compares the energy required (per particle) to crush particles in a bed configuration to the energy required (per particle) to crush the particles in a two-point-load configuration.

$$\eta_b \equiv \frac{E_{two\ point\ load}}{E_{bed}} \tag{1.2}$$

Where η_b denotes the comminution efficiency for the bed, $E_{two\ point\ load}$ denotes the energy required per particle to crush particles in a two point load configuration, and E_{bed} denotes the energy required per particle to crush particles in a bed configuration.

The equation is based on two observations. First, that the energy required to crush an individual particle in a two point configuration is the minimum energy required in a practical mechanical device. Second, that only a small fraction of the input to the bed is actually useful energy that contributes to fracture. The rest of the energy is either stored in the constituents of the system due to elastic deformation, or transferred into undesired forms due to friction, rearrangement of the bed configuration, plastic deformation, and heat generation.

This simple model has limitations. Ghaddar notes that this model only considers primary fractures of full-sized spheres in a bed of initial uniform size, and that this could limit the value of the comminution efficiency, since it ignores useful subsequent fracturing of the resulting fragments that may take place. However, Ghaddar argues and demonstrates, that dominant bed behavior, at least up to the compression stroke of maximum efficiency, is represented by this model.

1.4.2 Optimal Bed Compression

Bed compression is the amount of compression of the crushing chamber as a percentage of the original bed height. Both Ghaddar and Misra find that the optimum compression ratio lies in the range of 18 to 22%, *i.e.*, the bed is 0.78 times as thick after compression as it was before compression. Ghaddar notes that the existence of an optimal region of compression ranges implies that the number of broken particles is not linearly proportional to the input energy. These experiments were conducted with a one-inch bed thickness. Misra also notes that fracture efficiency reaches its maximum when the bed is compressed to an amount at which point the original inter-particle voids become filled with fine products from the primary crushing, and beyond which the required loading rises rapidly.

The system in which the current experiments are conducted can simulate compression ratios ranging from 0 to 100%, by adjusting the eccentricity of the inner cylinder.

When no compression occurs, the bed thickness is 0.75 inches. The apparatus is discussed in greater detail in chapter two.

1.4.3 Optimal Bed Thickness

In addition to the existence of an optimal compression ratio, there exists an optimum region for the bed thickness. Fracture efficiency, as we have defined it, is 100% in a two point load system. Misra notes that fracture efficiency decreases sharply until beds are three particles deep, at which point the rate of efficiency reduction decreases slowly as the bed thickness increases. The maximum achievable efficiency approaches 35% as the bed thickness increases (up to 25 particle diameters). The productivity improvements offered by deeper beds may outweigh the increased efficiency of very thin beds, since the efficiency loss increases slowly after a depth of approximately three particle diameters.

1.4.4 Recommendations

Fracture efficiency is practically unaffected by compression rate and presence of shear loading, but is adversely affected by the presence of excessive amounts of fines. Therefore, crushing energy can be better utilized with prompt removal of the fines and segregation of coarse particles before crushing, which effectively reduces the number of inter particle contacts and the resulting friction loss and "blunting" effect on the load. A controlled fluidized transport system can effectively remove the fines by elutriation while segregating the coarse particles by size, smaller ones occupying the upper layers within the crushing zone. This prompted the study of the fluidization behavior of binary size mixtures of particles (representing the fines and coarse fractions in the crushing zone). The results demonstrated the superiority of water over air as a working fluid, columnar vertical beds over tapered and or inclined beds for better segregation quality and shorter over taller beds for faster segregation. Noting that this recommendation contradicts previous work in the literature, a conical test section should be constructed to determine its utility in this regime.

1.5 Previous Work in the Comminution Program: Particle Fluidization and Segregation

The second phase of the Comminution Program investigated the phenomena related to fluidized transport and segregation of the crushed media. As with the previous work on the fracture mechanics of particles, the goal of the early experiments in fluidization and segregation was to gain understanding of the phenomena that will be important in implementing the final concept. Fluidization could be also be used for transport of the uncrushed product into the comminution chamber, however, that aspect of performance has not been investigated.

The fluidization and segregation work in the Comminution Program consists of three projects that investigated steady and impulsive fluidization in a constant area test section, impulsive fluidization with an outwardly moving wall, and this project, which investigates fluidized segregation in the concept geometry. The initial work in a constant area test section validates the possibility of employing fluidization for material transport. The work in the test section with an outwardly moving wall was a first-order approximation to the converging diverging walls of the concept device with an annular gap. The outwardly moving wall approximated the diverging section of the annular gap.

1.5.1 *Steady Fluidization of Fine Particles Within a Coarse Matrix*

The first section of work in fluidization consisted of experiments in which a bi-disperse mixture of particles was subjected to a steady fluid flow. From these experiments and the following analysis, it was observed that if the upward liquid flow is just above the incipient fluidization condition, the fines will form a fluidized bed within the coarse particles, and the height of the fluidized region will depend on the liquid velocity. It is important to note that fines approximately larger that 0.1 of the coarse particle diameter will be unable to percolate through the coarse packed bed. (Percolation is unimportant if flow rates are sufficient to fluidize the entire bed, both the coarse and the fines.) Fluidization conditions of the fine particles can be predicted by the means of an extension of the general correlations proposed by Richardson and Zaki (Schiaffino, 1993), and developed for mono-disperse particles fluidized in vertical channels. The extension of such general relationships is obtained with the correction of one of the empirical coefficients proposed by Richardson and Zaki, and the introduction of a hydraulic diameter for the channel. This diameter represents an effective size of the passages formed by the coarse particle bed an can be related to the coarse be concentration and coarse particle diameter by the following equation.

$$D = \frac{4 \times \textit{Coarse Pore Volume}}{\textit{Wet Surface of Coarse Medium}} = \frac{2(1-\nu_c)d_c}{3\nu_c} \tag{1.3}$$

ν_c denotes coarse concentration (dimensionless), d_c denotes coarse particle diameter. These modifications capture the hindering effects of the coarse matrix on the fluidization of the fine bed, while still retaining the generality and simplicity of the original framework. (Schiaffino, 1993)

1.5.2 *Impulsive Fluidization of a Bidisperse Mixture*

Experiments conducted to study the effects of impulsive fluidization revealed that the behavior of the bed under impulsive fluidization condition can not be predicted on the basis of the understanding of the steady fluidization case. Segregation is achieved as the result of a different mechanism. Upon impulsive injection of the flow, the particle bed is lifted as a "plug" and a raining occurs at the bottom. A coarse particle-free region is formed where segregation takes place. The fine particles are kept fluidized in this region, while the coarse particles precipitate and accumulate at the bottom. The process reveals its sudden nature when the void region progresses to the top of the rising bed, and the fine particles break through in an apparently unstable manner. (Schiaffino, 1993)

When the liquid velocity is higher than the terminal velocity of each single fine sphere, complete segregation between the two species can be achieved. For lower liquid velocities, segregation is still achieved, but with a partial removal of the fine particles. The same mechanism is also able to provide segregation with size ratios larger than 0.1 for which simple percolation of the fines is not possible.

Based upon these results, as well as the steady fluidization results, Schiaffino makes design recommendations for the new machine, while noting that further experiments with moving walls (discussed below) will be important in these considerations. Complete removal of fines can be obtained when the fluid velocity is higher than the terminal velocity of the fine particulate. If only elevated fines removal is desired, it is not recommended to operate the machine with flow rates much higher than the fines terminal velocity. However,

segregation speed increases with faster flow rates. When fast segregation speed is desired, fluid velocities two to three times the terminal velocity of the fine products should be used.

Since the proposed design involves a rotating machine, angular frequency is an important consideration. Schiaffino offers the following observations. The machine frequency must be chosen in such a way that the bed is allowed to be completely separated. Successive strokes should take place only after the plug breakage has occurred and the coarse particles left are collected again at the bottom of the machine. From the segregation time results, the machine operating frequency must be based on the initial bed height and liquid flow rate. The bed height is directly related to the material output requested. Within the observed behaviors, higher beds are associated with higher removal speed per unit bed height, and are attractive from this point of view. Beds of excessive height could be limited by resistance considerations for the crushing members, and by the need to allow for larger bed expansions before achieving segregation. The above recommendation are only valid for bed heights of less than 40 particle diameters, as the previous studies did not investigate taller beds, which may exhibit different behavior.

Schiaffino notes that for 40 particle-diameter-high beds, with fluid velocities two to three times the terminal velocities of the fines, the total segregation time is approximately three seconds. Further, he observes that high machine frequencies may result in the development of secondary flows that would interfere with the desired segregation. Bearing these considerations in mind, a machine frequency of 15-20 rpm, which allows a crushing period of 3-4 seconds, is suggested.

These recommendations are for configurations which include the current experiment parameters. Bed heights are less than forty particle diameters, particles sizes are 3 mm (coarse) and 0.2 mm (fine).

1.5.3 Impulsive Fluidization of a Bidisperse Mixture Between Outwardly Moving Walls

Following the experiments conducted in constant-area rectangular test sections, experiments were conducted in constant width rectangular test section, which grew in depth. This configuration was intended as first order approximation to the geometry of the proposed design, where a the inner member is moving away from a particular point on the outer member.

In the moving wall experiments, there were seven experimental parameters: coarse particle diameter, fine particle diameter, bed height, wall displacement, wall velocity, flow rate, and wall/flow delay. Each of these parameters can be translated into a parameter for the current experiment; this correlation is discussed in section 2.3. In the experiments, Wisnewski varied two parameters: the inlet flow rate and the wall velocity. The remaining parameters were constant during all of the experiments. Coarse particles were 3.0 mm in diameter, while fine particles were 0.2 mm in diameter.

Wisnewski established three design criteria (as dependent variables) to evaluate the different sets of operating parameters:

1. clearing speed, defined as the final bed height divided by the process time (h_f/t_{pr});
2. fines removal fraction at process time (t_{pr});
3. maximum height of the fluidized segregation process.

Process time, t_{pr}, is defined as the time from the beginning of fluidization until the final coarse particles that were fluidized settle at the pile of coarse at the bottom. Wisnewski observes that clearing speed is an important design criterion, as higher clearing speeds allow

higher production rates, since the machine could operate at higher frequencies. The fines removal fraction is a measure of the efficiency of the process; more fines in the remaining coarse material inhibits breakage in the next crushing cycle, also slowing production. The maximum height of the process determines how much space is required for the process; lower maximum heights permit smaller machines and reduced chances of ejecting the coarse material (63).

Wisnewski determined that the best operating configuration consisted of that at which both the inlet flow rate and wall velocity were maximized within the limitations of his apparatus (at 36 000 mm^3/s and 8.5 mm/s, respectively). With these parameter values, a clearing speed of 33.9 mm/s, a fines removal fraction of 89.7%, and a maximum height of h_0 (the bed does not increase in height) were achieved. These results were the best of experiments conducted. However, Wisnewski recommends that higher flow rates and wall velocities be investigated, since a better set of operating parameters may lie outside the range of his experiments.

1.5.4 Discussion of Previous Fluidization/Segregation Work

The work discussed above has provided significant insight into the behavior of fluidized particles. These insights were considered in the design of the current experiments, however, there are significant differences between the different test sections that affect the validity of the design recommendations proposed above. None of the previous work has explored the impact of the cyclical nature of the machine upon performance or of the two- or three-dimensional flow within practical devices.

The geometry of the test section in the current experiment is a vertical annular gap. Locally, where the gap is at its minimum width, the rectangular test section with a moving wall is a reasonable approximation of the geometry. However, in the rectangular section experiments, the entire area of the test section is fluidized. In the current experiment, the impulsive flow would arrive after the minimum gap, and would thus allow the bed to expand laterally, in addition to vertically, since there are no vertical walls around the jet region.

The operating parameters recommended also offer contradictory recommendations, indicating that an engineering trade-off will be required. Schiaffino cautions against high machine frequencies, due to the implication of secondary flows, while Wisnewski recommends high frequencies to provide the best segregation performance. The current work should provide insight in this area. However, Wisnewski's work finds that high inlet flow rates provided the highest quality segregation, while Schiaffino found that inlet flow rates above the terminal velocity of the fine products, resulted in poorer segregation quality. This is best explained by the effects of the moving wall introduced in Wisnewski's work.

1.6 Organization

This research is part of the Comminution Program at MIT. The program has included work conducted on particle fracture and material transport. The work in material transport was necessarily simple in nature. The first experiments were conducted in constant area test sections, while the second set of experiments were conducted in a test section with a changing cross sectional area, as described above. This thesis describes the design and construction of the apparatus for the final experiments. This apparatus simulates the operating conditions that would be present in an actual comminution machine.

In chapter two, the functional requirements and machine design are discussed. The objectives the apparatus was to meet are stated. Design alternatives are discussed.

In chapter three, the apparatus' performance is discussed. Preliminary data is interpreted. A discussion of the limitations of the apparatus follows.

In chapter four, recommendations are made for experimental procedure and hardware completion. Included in this chapter is a set of sixteen suggested experiments that should be conducted.

Chapter 2

Design of An Apparatus for Fluidized Segregation of a Bidisperse Particulate Mixture in a Nonuniform Annular Geometry

The objective of this research program is to investigate the issues that are relevant to the design of a more efficient comminution device. In addition to this general understanding, we also hope to answer some more specific questions. While models were proposed and correlated with the experimental behavior observed in the previous studies, in this work, the regime is sufficiently complex that we primarily attempt to optimize operating parameters.

The questions we are interested in comprise two categories: unique fluid mechanics behavior and the impact of the new geometry and cyclical nature of the machine. First, how does the previous experimental work correlate with the behavior observed in the current experiment? The data from the previous work allow us to see what phenomena are unique to this annular geometry, and will assist us in gaining understanding of these unique phenomena.

The remaining questions relate specifically to the cyclical nature of the machine. Each of these questions was considered while designing the apparatus. Specifically, we are interested in the following:

- What is the impact of the cyclical nature upon segregation efficacy?
- Does the annular geometry inhibit segregation due to its lack of lateral constraint in the region local to the segregation jet?
- What is the relationship between angular speed, flow stability, and segregation speed and quality?
- Can effective segregation be achieved in one machine cycle? What is the minimum period?
- What are the fluid velocity requirements (as they relate to fluidization velocities of the particles)?

2.1 Apparatus Objectives

In order to investigate the proposed design concept and answer the questions above, the apparatus had particular performance requirements. These requirements became the objectives for the performance of the apparatus. The objectives can be divided into four areas: geometry, kinematics, fluid mechanics, and observation. The requirements for each of these areas is discussed below.

The proposed design concept's geometry is a nonuniform annular volume. The eccentricity of the inner cylinder should be adjustable. The size of the annulus was not

important, as the curvature of the geometry is only required so that the machine may be cyclical in operation. The height of the test section should allow significant bed expansion.

The concept machine's kinematics can be simulated in the apparatus. The test section is to be contained on three sides: the inner cylinder, the outer cylinder, and the floor of the section. The outer cylinder and the floor of the section should be static. The inner cylinder should revolve around its own axis such that the tangential relative velocity between the walls at the minimum gap is zero. The axis of the inner cylinder should revolve around the axis of the center cylinder. The inner cylinder can be thought of as rolling inside a cylinder of radius equal to the sum of the radius of the inner cylinder and the offset.

The test section should include a jet of the working fluid at a constant position relative to the gap minimum. The fluid velocity of the jet should be such that the coarse and fines can be fluidized. The jet area and phase, relative to the minimum gap width, should be adjustable.

The experiments in the apparatus must be observable. The minimum gap should be constantly observed, as well as fixed points in the test section. More specifically, the apparatus should facilitate luminance measurements.

2.2 Experimental Apparatus

In this section, the experimental apparatus, shown in Figure 2.1, will be presented, including the test section, power system, supporting structure, fluid system, and the observation system. Additionally, the parameters of the apparatus will be discussed and correlated to parameters used in previous experiments. Finally, some alternative concepts not employed will be discussed.

The apparatus described here simulates the kinematic relationships of the proposed design. However, crushing is not performed in the machine for several reasons. Primarily, the particles we would like to study for segregation must be uniform and regular; crushed particles are non-uniform and irregular in shape. Second, were we to perform crushing, the machine would most likely be fabricated from steel, which would preclude the ability to observe the behavior of the particles in the test section. However, the kinematic and geometric similarity, as well as the bidisperse particle mixture will exhibit behavior we anticipate to occur in the proposed design. Limitations of the data from this apparatus will be discussed in chapter three. The apparatus is presented schematically in Figure 2.2.

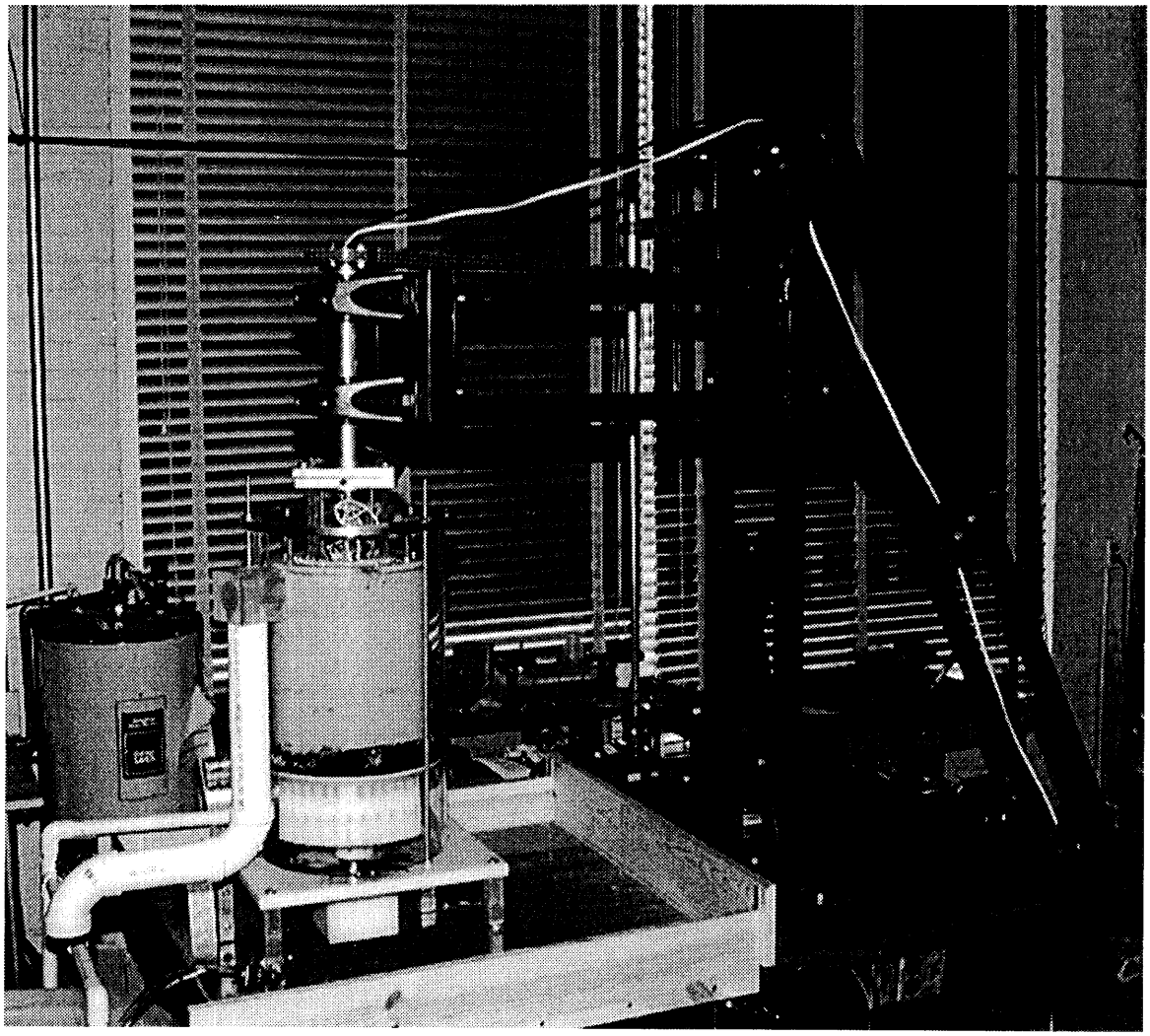

Figure 2.1. The apparatus.

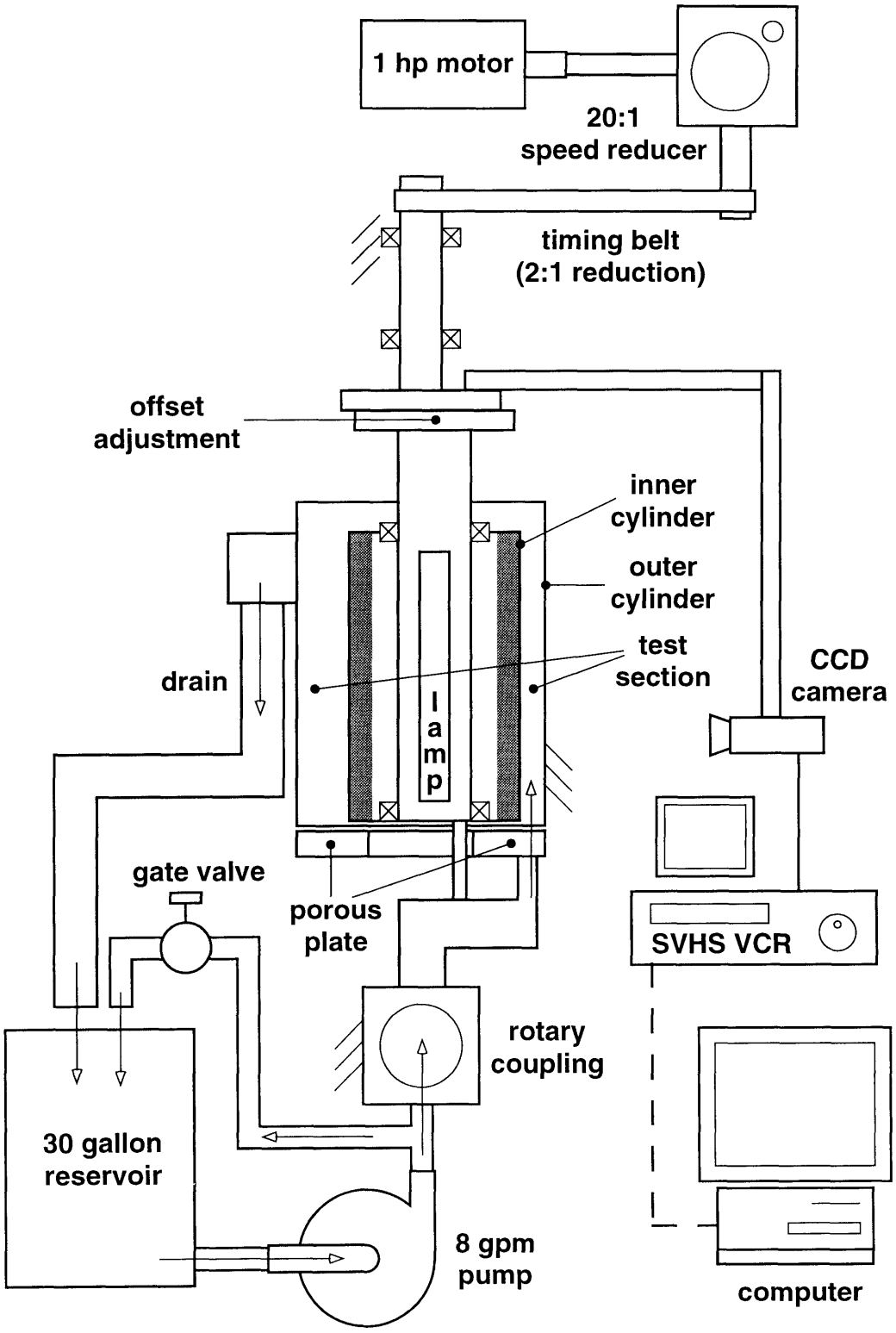

Figure 2.2. A schematic illustration of the apparatus.

2.2.1 Test Section Geometry & Kinematics

The design of the apparatus (see Figures 2.1 and 2.4) initially focused on the test section, since its characteristics were most important. The geometric and kinematic requirements for the test section were fixed by the concept we wished to explore. These requirements were: annular geometry, zero relative wall velocity at the minimum gap, adjustable eccentricity, and planetary motion. Additionally, the test section had to be transparent and backlit (from the center) to allow observation. It was also required that the upward water jet rotate with and maintain a constant position with respect to the minimum gap width. Requirements for observation included point of views synchronous with the minimum gap and fixed in space.

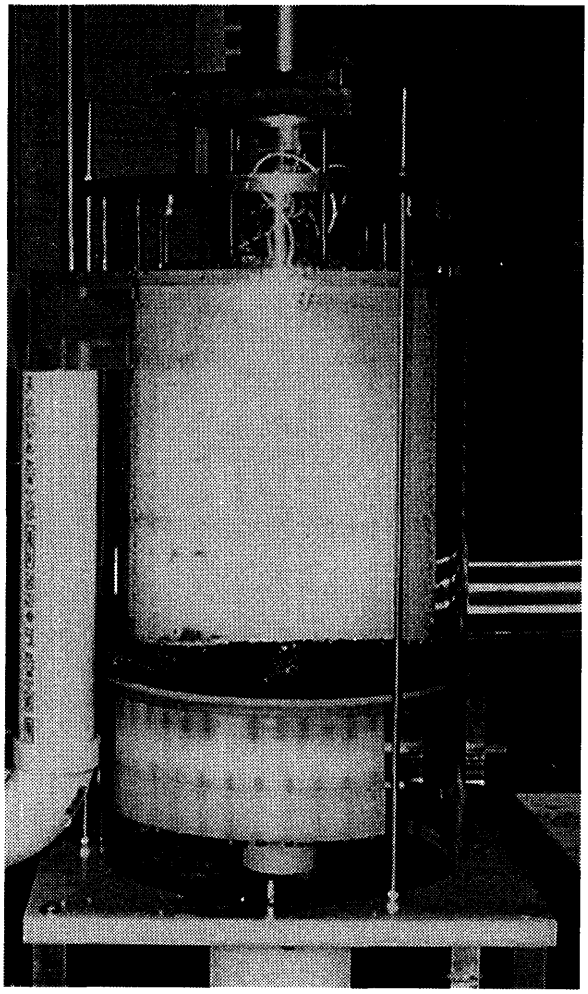

Figure 2.3. The test section of the apparatus.

The test section consists of the space between two cylinders. A cross section of the test section is presented in Figure 2.5; the cross section is presented labeled with part numbers in Appendix C. The centerlines of the cylinders are not necessarily collinear, although they may be; an adjustment provides the eccentricity that simulates the desired crushing geometry. Both cylinders are cast acrylic, with a wall thickness of one-quarter inch. Acrylic was chosen for its durability, transparency, and availability in the sizes and shapes

needed. The outer cylinder has an inner diameter of 11.50 inches, while the inner cylinder has an outer diameter of 10.00 inches. When the centerlines of the cylinders are collinear (no eccentricity), the test section is a uniform annular gap of 0.75 inches. The inner cylinder is 12 inches in height, and the effective height of the test section is approximately 10 inches. The eccentricity can range from zero inches (resulting in a uniform 0.75 inch annular volume) to 0.75 inches (resulting in a non-uniform annular gap that ranges in width from zero inches to 1.5 inches). A driveshaft supports an adjustable plate, which, in turn, supports the inner cylinder. The centerline of the driveshaft and the outer (twelve-inch) cylinder are always collinear. The cylinders are held in compression by tie rods, which eliminated the need for tapped holes in the walls of the cylinders.

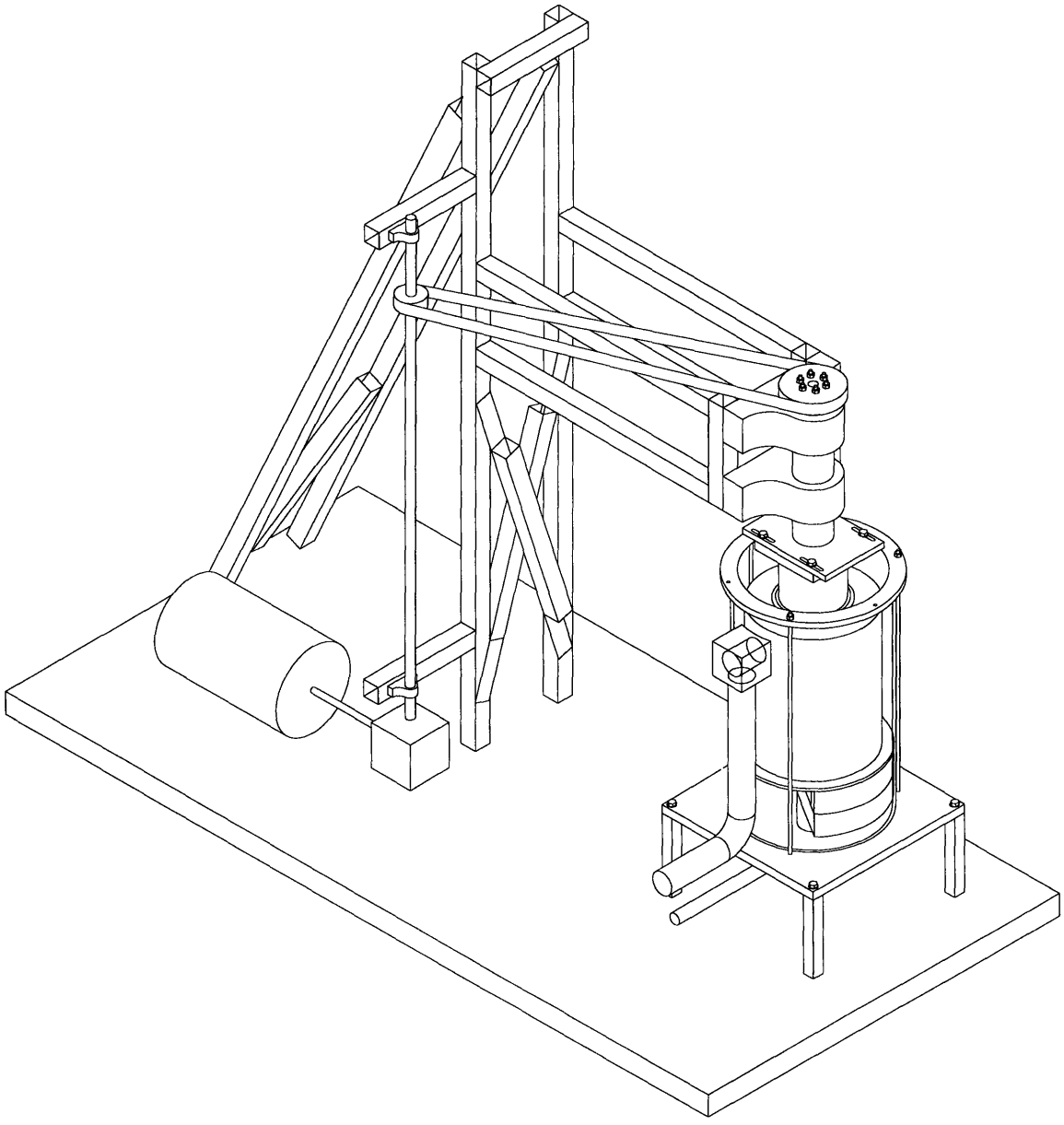

Figure 2.4. An isometric illustration of the apparatus.

The inner (ten-inch) cylinder of the test section rotates freely about an acrylic shaft that supports it. This supporting shaft's centerline can be offset (up to 0.75 inch) from the driveshaft's centerline, introducing the eccentricity/non-uniform gap. The offset is achieved by adjusting the relative position of the plate to which the supporting shaft is attached. The inner cylinder is free to rotate about the support shaft. In effect, the inner cylinder is rolling in an imaginary cylinder of radius r=5" + O_w, since its linear velocity where the gap is a minimum is zero. As long as the friction force (torque) between the cylinder surface and the bead mixture is greater that the friction force (torque) between the supporting shaft and the inner cylinder, the cylinder will rotate properly. This condition is imposed so that (in a crushing machine) loads are normal to the media and do not shear the bed.

The inner cylinder has endcaps fabricated from UHMW polyethylene. These endcaps provide bearing surfaces for the cylinder. In general, components that were not required to be transparent were fabricated in UHMW PE.

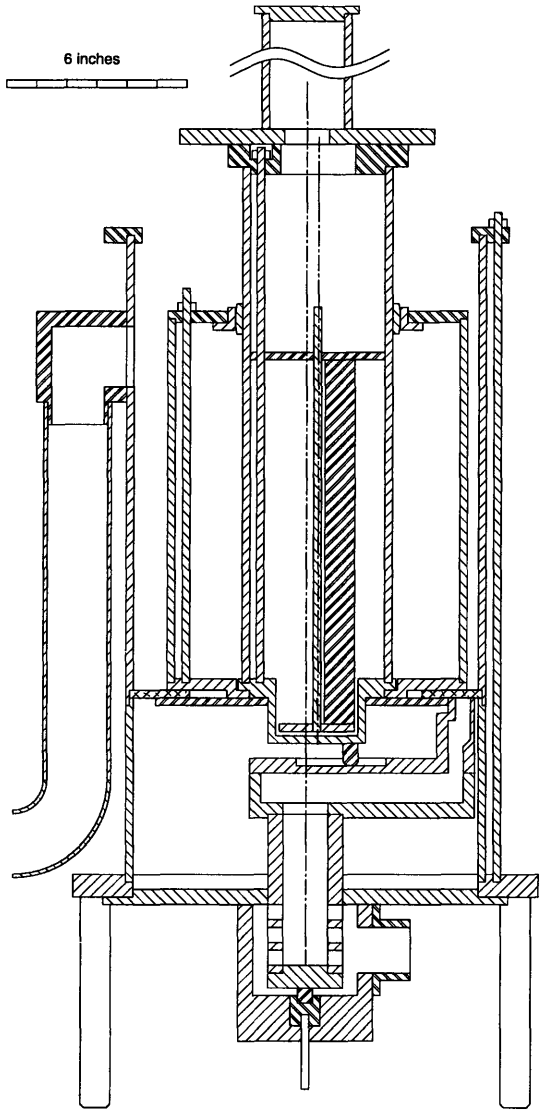

Figure 2.5. A cross section of the test section of the apparatus. A cross section with part numbers is presented in Appendix C.

The driveshaft is a three inch (outer-diameter), one-quarter inch wall aluminum tube. The ends of the tube were turned so that the bearings in the pillow blocks could be seated. A plate is attached to the bottom of the tube; the plate is located by a pilot on the plate on which the tubing is seated. Four slots in the plate allow the support cylinder's axis to be offset from that of the driveshaft. The plate at the top of the support cylinder features four tapped holes; with the bolts in place, but loosened, the radial offset can be adjusted. At the top of the driveshaft, an end cap is in place. Above the end cap, a timing pulley is secured by the tie rods that extend from the clamp plate through the end cap. The diameter of the tubing for the driveshaft was selected based on bending strength and room for tie rods.

The lower end cap of the support cylinder supplies both a horizontal and vertical bushing. A perforated retaining plate is attached to a step in the lower end cap that allows porous plate to be mechanically captured. This prevents the plate from deflecting under the load of the compressed bead mixture. The holes in the retaining plate allow any beads that get trapped between the porous plate and the inner cylinder to fall through to the lower reservoir, reducing the risk of binding. The retaining ring's geometry ensures that it does not interfere with the nozzle and is effective for all possible eccentricities.

The floor of the test section is a 0.25 inch thick sheet of porous polyethylene. The porous plate is captured between the top and bottom halves of the outer (12 inch) cylinder. The inner edge of the plate floats between the bottom of the inner cylinder and support shaft and a retainer that is bolted to the support shaft.

The test section also features an upward jet which is synchronized (in angular position) with the minimum gap, *i.e.* the jet's angular position is always the same relative to the location of the minimum width of the gap. The jet is discussed in section 2.2.4.

2.2.2 Power System

Power to drive the inner cylinder and the jet (described in 2.2.) is supplied by a one horsepower direct current motor (maximum speed: 1760 rpm). The motor is controlled through an infinitely variable controller. The output of the motor is transmitted to a 20:1 speed reducer, from which it is transferred to a 2.5 inch toothed pulley. A steel-cable reinforced timing belt is used transfer the power to a 5.0 inch toothed pulley connected to the drive shaft of the apparatus. The driveshaft is supported in two $2^{15}/_{16}$ pillow blocks. The pillow blocks are supported by a structure built from Unistrut flexible assembly channel. The bearing position was adjusted after the structure was built.

The rotation of the nozzle is also powered by the motor. A stainless steel pin attached to the bottom of the support cylinder slides in a radial slot in the top of the nozzle. This allows the tangential force for rotation to be transmitted to the nozzle regardless of the offset imposed.

2.2.3 Structure

A structure was required to support the bearings for the driveshaft and the transmission components. Unistrut flexible assembly channel was selected for the structure. Unistrut is an extruded steel U-channel that is available in many different forms. Different fixtures and fittings can be fastened together with Unistrut nuts and $^1/_2$-13 bolts. The structure is shown in Figures 2.1 and 2.4. The large cantilevered structure on which the bearings are mounted is necessary to provide clearance for the rotating camera arm. The apparatus is constructed on a wood workbench. Level adjustments were made between the pillow block subassembly and the structure.

2.2.4 Fluid System

The moving jet in the test section is produced by a rotating nozzle that is driven by the rotation of the support cylinder. The lower end cap of the support cylinder features a stainless steel pin which drives the nozzle synchronously with the minimum gap width. The nozzle features a groove that allows the pin to slide radially, so that nozzle is driven regardless of the eccentricity imposed upon the support cylinder. The nozzle, shown in Figure 2.6, consists of three parts: the top part of the nozzle features thirteen holes, each of which may be individually closed with a rubber stopper. By opening and closing particular holes, the jet arc length and phase can be controlled. The lower half of the nozzle simply provides a path from the tube to the top half of the nozzle. The tube connects the nozzle to the interior chamber of the rotary coupling, allowing the rotating nozzle to be supplied with fluid from a non-rotating source. The upper and lower pieces of the nozzle are held together with stainless steel screws placed every inch along the perimeter. A gasket prevents leaks at the interface. The tube is attached with four stainless steel screws; RTV silicone prevents leaks at the interface. The upper and lower pieces of the nozzle are UHMW PE. The tube is Delrin. The tube is supported by a stainless steel pin that rotates in a movable bushing and by lower lid of the test section (UHMW PE). The bushing's height can be adjusted by using a lead screw; this allows the height of the nozzle to be adjusted, so that it is adequately pressed against the porous plate.

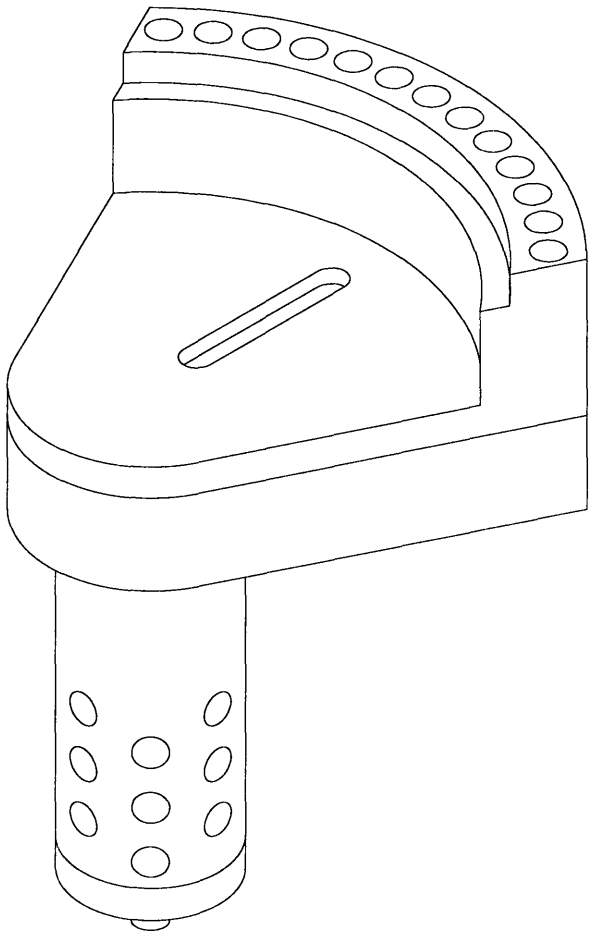

Figure 2.6. Isometric illustration of the nozzle employed in the apparatus.

To produce the rotating jet, a rotary coupling was required since the outlet was rotating, while the inlet was static. Fabricated rotary couplings were only suitable for very slow speeds and were unsuitable. The rotary coupling employed was designed and fabricated. It consists of a polyethylene chamber, a polyethylene plate, and a rotating tube which was rigidly connected to the nozzle assembly. The tube is perforated with twenty-four one-half inch holes on the area that is enclosed in the chamber. Fluid enters the chamber, flows through the holes on the rotating tube and finally through the nozzle and porous plate.

The fluid leaves the system through a two inch port in the wall of the outer cylinder located ten inches above the height of the test section floor. The fluid is returned to the reservoir which supplies the pump. The test section can be drained through a port in the base of the unit; a valve closes the port during experiments.

2.2.5 Observation

In addition to the kinematic and geometric requirements of the test section, it was also required that the experiments be observable. Instrumentation was a considerable challenge in this experiment. Observation of the minimum gap, as it traveled around the test section, was desired, which required the camera to rotate with minimum gap. Mounting the camera close to the driveshaft, to reduce the rotating mass, was considered, however, the mass of the mirrors and the required supporting structure would have been greater than that of the camera and it's structure. Due to the radius required by the focal length of the camera, it can only be mounted and used with the apparatus at slow angular speeds.

In order to acquire data, luminance measurements would be required, as were performed in previous experiments of this kind (Schiaffino, 1993; Wisnewski 1994). This required a light source at the center of the inner cylinder. The light also had to be as even as possible throughout the height of the test section. To provide illumination, three fluorescent lamps were mounted inside the support cylinder for the inner cylinder. The support cylinder extends below the surface of the surface of the porous plate, to ensure that lower region of the test section is illuminated as evenly as possible. The support cylinder is five inch diameter, one-quarter wall acrylic, which provided the desired stiffness for the anticipated loads. The inner cylinder was supported with bushings on the support cylinder. The inner cylinder was lined with a Roscolux diffusion gel to ensure that the light was even. Both the inner cylinder and the support cylinder were held in place with end caps and tie rods that held the members in compression. The tie rods induce artifacts in the observations, however, the artifacts should be readily detectable, and a significantly large area is available for observation.

A CCD camera (Techni-Quip Micro-Mac 8, with a 12.5 - 75 mm/f1.2 zoom lens), either fixed in space or rotating with the minimum gap width, records the images to SVHS videocassette. Power cables for the camera and the lamp, as well as a cable for the video signal, are routed through the driveshaft to prevent winding. Images are selected from the SVHS videotape (*e.g.*, every sixth frame) and imported into the digital image analysis system. This system consists of an Apple Power Macintosh 7100/66 AV, NIH Image 1.57, Adobe Premiere 4.0, and Adobe Photoshop 3.01. The Macintosh features a built-in digitization card, which allows a direct connection from a video source; in our case, this is the SVHS VCR. (The VCR features a digital frame memory, which allows high quality still images to be obtained.) Adobe Premiere is used to capture a series of stills. After a batch of images is acquired, they can be saved in one of many formats, including PICT and Adobe's Photoshop format; Premiere can write the files to the disk and automatically number them. NIH Image is then used to open each of the image files individually or as a batch. In Image,

measurements can be made to quantify the species concentration of particle sizes. Image also supports a macro language, which is useful in performing repetitive analyses. Additionally, NIH Image can compile multiple images into a "stack". The stack can then be animated or made into a composite.

2.2.6 Parameters

Since the goal of this research is to explore the operation space of fluidized comminution, it would be ideal to investigate every conceivable configuration. However, this is simply not feasible. The parameters that we have chosen to fix for this apparatus include the following: coarse particle size, fine particle size, outer cylinder size, inner cylinder size, and offset/compression ratio relationship (*i.e.*, compression ratio is dependent upon offset in the apparatus). These parameters, and their fixed values are presented in Table 2.1. The remaining parameters are fluid velocity, angular velocity, offset/compression ratio, jet arc length, and jet phase.

These parameters have analogs in Wisnewski's experimental apparatus. These relationships are presented in Table 2.2.

2.2.7 Alternatives Considered

The primary conceptual alternative considered for the apparatus consisted of actuating both the inner and outer cylinders. Since the relative motion of the components of the test section were defined, we had the option of which components to ground and which ones we should actuate. By rotating the inner and outer cylinders about their centerlines at the appropriate velocities, we could achieve the desired kinematics. Advantages of this configuration included the option of using a static camera to capture images of the minimum gap, and a static jet. However, this solution would involve large diameter (12") moving seals and might also induce centrifugal flows. This solution would also require both cylinders to be actuated. These additional complexities made this alternative unattractive.

Parameter	Value/Range
Fixed Parameters	
Coarse Particle Size	3.0 mm
Fine Particle Size	0.2 mm
Outer Cylinder Size	11.5 inches
Inner Cylinder Size	10.0 inches
Compression Ratio/ Offset Relationship	$R_c = \frac{O_w}{0.75\ inches} \times 100\%$
Variable Parameters	
Offset, O_w	0.0-0.75 inches
Angular Speed	0-44 rpm
Flow Rate	0-8 gpm
Jet Arc	7-90°
Jet Phase	-45-45°

Table 2.1. Parameters of the currents apparatus.

Moving Wall Experiment	Non-Uniform Annular Geometry
Coarse Particle Diameter	Coarse Particle Diameter
Fine Particle Diameter	Fine Particle Diameter
Bed Height	Bed Height
Wall Displacement	Offset
Wall Velocity	Angular Velocity
Flow Rate	Flow Rate
Wall or Flow Delay	Jet Phase

Table 2.2. Parameter analogs in the Moving Wall experimental apparatus.

Several different concepts for the moving jet system were considered. Concepts explored include a system of tubes all connected to a rotating valve. Difficulties with this concept included actuation; in order to ensure synchronicity, both the valve and the inner cylinder would have to be driven by the same shaft. Advantages of this concept included better mating with the porous plate, since this interface would be static. However, this concept was not as flexible as the implemented nozzle. Nozzle alterations are discussed in chapter four.

2.2.8 Sample Data

The following data sets (Figures 2.7 and 2.8) were obtained from the apparatus. The bed is approximately 3 cm tall (10 bead diameters) and is composed of 55% coarse, and 45% fines (by volume). The jet in these samples was produced by line pressure, with a flow rate of approximately four gpm; one hole in the nozzle was open. The annular volume is of uniform width (0.75 inches) and the inner cylinder and jet are not rotating. The media used in these experiments are 0.2 mm black glass beads (the fines) and 3.0 mm colorless glass beads (the coarse). The bed depth in these experiments was a uniform 0.75 inches. With the 8 gpm pump, deeper beds and wider jets can be supported.

In Figure 2.7, a series of eighteen images, spaced one second apart, is presented. This series of images illustrates the transient behavior that occurs as the jet flow begins. In Figure 2.8, eighteen images, spaced one-sixth of a second apart, are presented. These images occur between the first and fourth frames of Figure 2.7 and offer a detailed view of the events surrounding the breakthrough of the jet through the coarse matrix.

Initially, the jet forces the fines to percolate through the coarse particle matrix. Almost immediately, the peripheral flow agitates the fines in other regions of the test section, which flow to the area of the jet; this can be seen in frames 4, 5, and 6 of Figure 2.8. The peripheral flow is caused by water that does not pass directly through the porous plate from the jet and collects in the bottom reservoir. When the pressure in the bottom reservoir reaches the pressure required to pass through the porous plate, the peripheral flow begins. Due to the nozzle's width, there is no peripheral flow $\pm 45°$ of the jet. The height to which the fines from the region of the jet are fluidized is approximately equal to the height of the bed, as can be seen in frame 5 of Figure 2.8. While the jet did not fluidize the fines directly to the height of the drain, some of the fines were eventually ejected from the test section by the peripheral flow. A stronger jet would be able to directly fluidize the fines higher, which would aid in their removal from the crushing chamber.

As time passes, the width of the segregated area of the coarse matrix increases. The white area at the center of the bottom of the last 15 frames of Figure 2.7 is composed of coarse particles with all of the fines removed. The gray area above the initial bed height is composed of suspended fines. No coarse particles were fluidized.

A plug, as observed by Schiaffino with one dimensional flow, is not observed in this geometry. The plug most likely does not form due to the lack of lateral constraints for the flow. Instead of forcing a plug of particles upward, the flow diffuses and forces the fines to percolate through the coarse matrix. In practice, it will be necessary to fluidize the coarse particles to ensure that fines trapped in the matrix by intermediate-sized particles can be segregated. This condition will increase the height to which the coarse are fluidized, and thus, it will also increase the minimum height of the crushing chamber implemented in an actual machine.

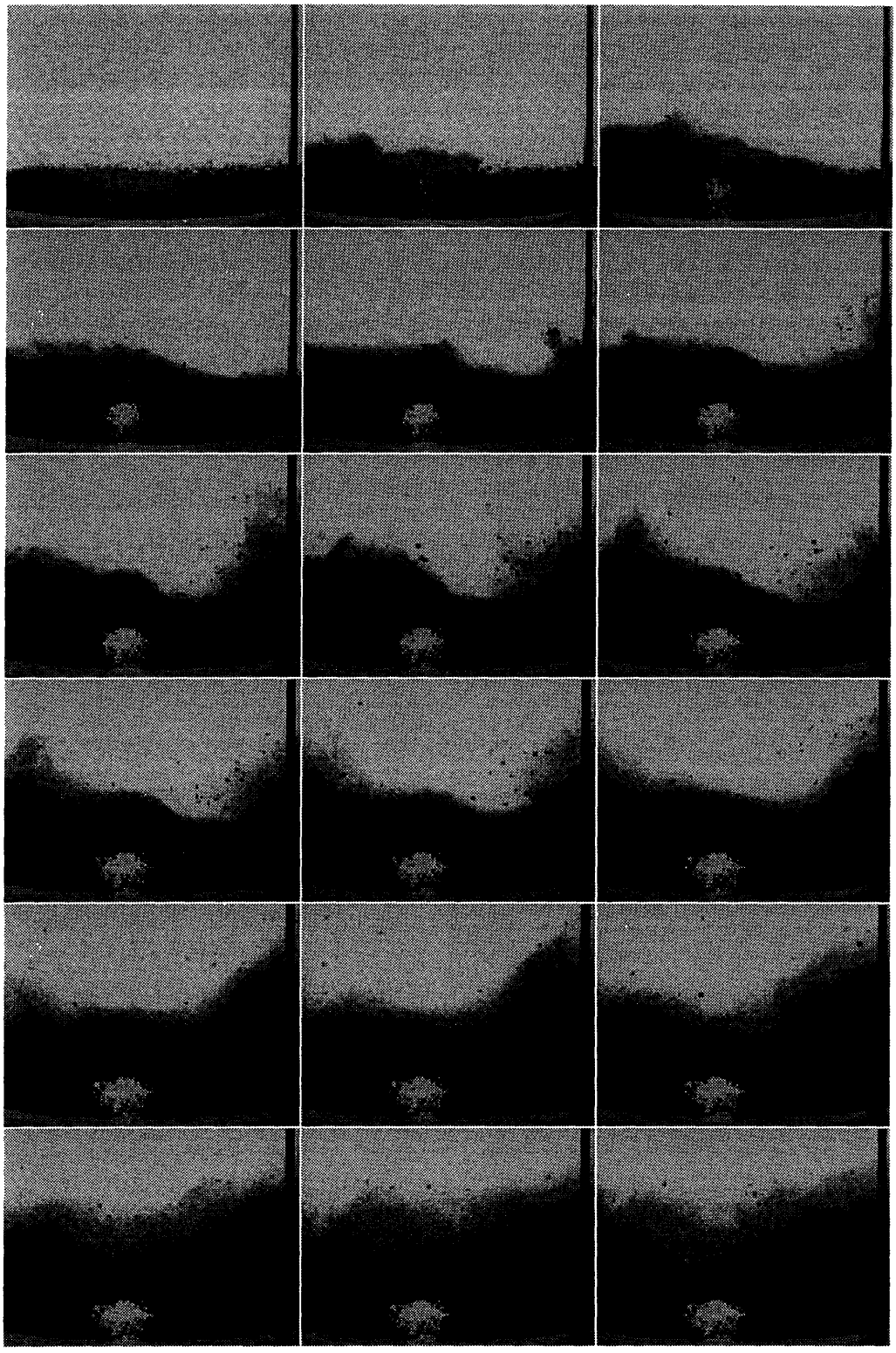

Figure 2.7. A sample image set. Images are one second apart from each other.

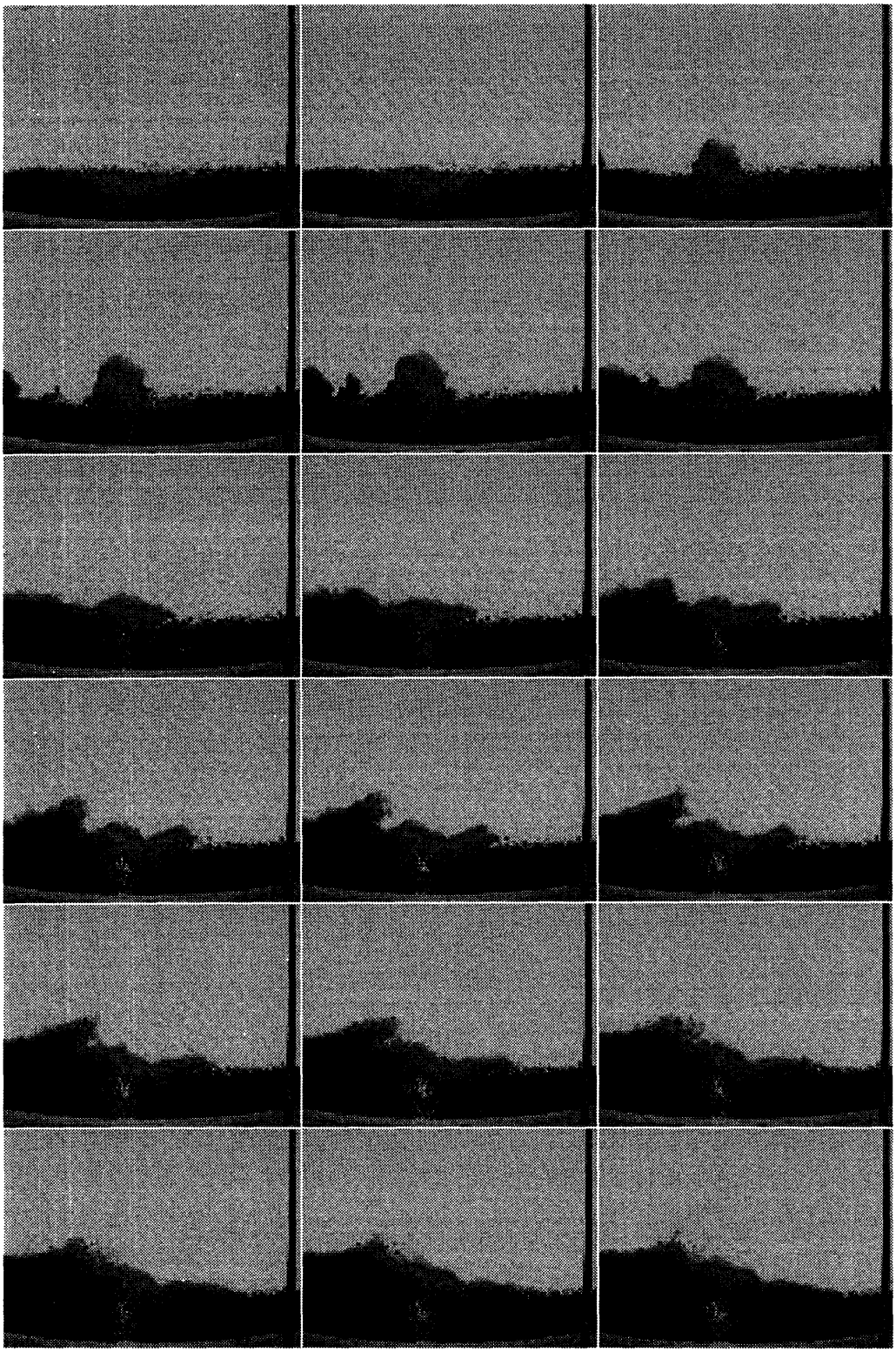

Figure 2.8. Images of the test section as the jet flow begins. These images are from the time period between the first and fourth images of Figure 2.7, and are one-sixth of a second apart.

Chapter 3

Discussion

While extensive experiments have not been performed with the apparatus, initial experiments offer insight into the performance of the apparatus and phenomena related to fluidized segregation. A number of idealizations were made in the development of the apparatus and the experiments designed (see section 4.2.2); these assumptions' implications should guide interpretation of results from the apparatus. Additionally, there are issues that have not been addressed as part of the research program that merit discussion. Finally, performance of the apparatus could be enhanced by some modifications, which are discussed here.

3.1 Preliminary Data Interpretation

Preliminary experiments were performed with a short bead bed and 4 gpm flow. Although these data are not conclusive, some recommendations can be made. From the performed experiments (images from these experiments can be seen in Figures 2.7 and 2.8) it can be observed that even though there is not a restricted pathway for the fluid, segregation still occurs in the region of the jet. One of the major questions this apparatus will answer is the effectiveness of fluidization as a segregation mechanism in an actual crushing geometry. The preliminary indication is that fluidization will be an effective segregation mechanism. Segregation in the coarse matrix was effective. Above the bed there was significant fine particle activity, caused by the peripheral flow in the chamber.

Previous work in this area has focused on the effectiveness of fluidized segregation in closed, one-dimensional volumes; *i.e.*, the entire area of the test section (covered by the bead bed) was fluidized and the fluid was forced to leave the test section through the "ceiling" of the section, an area equal to the floor. An important implication of this configuration is that the fluid velocity was nearly uniform throughout the section; the flow could not diffuse. In the annular geometry with a local jet, the flow can diffuse laterally, and consequently, the height to which particles are fluidized is not predetermined. Diffusion did occur in the preliminary experiment, however, the peripheral flow was sufficient to fluidize the fines through the coarse particle matrix. Additionally, the flow was sufficient to fluidize some of the fines out of the test section (*i.e.*, to a height of ten inches).

The peripheral flow in the test section can enhance overall segregation. The peripheral flow is the flow that is not directly from the jet. This observation implies that the jet arc length should be long (*i.e.*, jet arc should be large). While it may appear that this would imply a jet arc of 360°, this is not the case, since a fully fluidized bed would be difficult or impossible to "capture" and crush. Limitations imposed by crushing are discussed further in section 3.3.

3.2 Apparatus Idealizations *v.* Actual Practice

In designing this experimental apparatus, idealizations were made, primarily to simplify the observation of phenomena. The primary idealizations relate to the shape and size of the particles. Additionally, the size and construction of the apparatus also incorporate idealization that facilitate observation. Understanding these idealizations permits useful and worthwhile data to be obtained from the experiments performed.

The particle mixture for the experiments is bidisperse, consisting of particles of diameters 3.0 mm and 0.2 mm. This is a first order approximation of a mixture of crushed media. Once experiments have been conducted with the bidisperse mixture, further experiments could include multidisperse mixtures consisting of several different particle sizes. The shape of the particles to be used in the apparatus is spherical. Spherical particles are readily available and remove the many degrees of freedom associated with shape, ensuring that phenomena observed can be better understood. Certainly, the angular particles that result from industrial crushing will behave somewhat differently that the uniform spherical particles, however, Snow and Paulding note that angular and spherical particles are qualitatively similar in behavior. Further, Misra conducted fluidization experiments with granular particles (sand) as the media and found that the behavior observed was qualitatively similar to that of the spherical glass particles. Thus, while the flow rates, *etc.*, might vary for angular particle mixtures, if the spherical particles can be consistently fluidized, so can angular particles.

The scale of the machine will have performance implications. This experiment is designed to explore the use of fluidization. However, an industrial comminution machine must be economically viable; this indicates that a certain level of productivity is required. It may be the case that a machine must be much larger in order to produce enough product per hour. In this case, the important characteristics are the bed height, the bed depth, the compression ratio, and the rotational speed. The diameter of the chamber is inconsequential; we do not believe that the curvature of the test section has a significant impact upon fluidization performance. Alternatively, a number of machines could be operated in parallel to achieve the desired productivity, although such benefits would have to be weighed against the increased capital requirements of several machines.

3.3 Fluidization Time *v.* Settling Zone

Another important question arises when crushing is considered. If a wide jet arc is recommended, we must be certain that crushing can still occur. In order for crushing to occur, large particles must be captured between the two cylinders as the walls converge. Angular particles will be more easily captured that spherical particles; however, it will likely be difficult to capture particles if fluidization is occurring in the crushing region. This is one reason that a leading jet may not perform well in actual practice (crushing and segregating) but will perform well in segregation only experiments. A jet of velocity less than the terminal velocity of the coarse particles may be suitable in this region.

In the current apparatus, the flow in the region ±45° of the minimum gap is restricted by the jet nozzle, *i.e.*, there is not significant peripheral flow in this region. Flow patterns can be adjusted in the ±45° region by replacing the solid stoppers with stoppers with holes that allow a reduced flow. In this way, any desired flow can be achieved in this region.

3.4 Issues Not Addressed By This Apparatus

Since the objective of this apparatus was to investigate the efficacy of fluidization, it is not possible to extract machine design recommendations from experiments conducted with

this apparatus alone. Two major issues remain to be investigated in the design of a comminution machine such as the concept presented here. These issues are the dynamics of crushing and coarse material transport into the machine.

The dynamics of crushing can vary significantly, however in a machine such as the design concept, comminution would be performed by compression, as opposed to impact. Impact crushing may be possible, although the machine frequencies for such operation may be very high and affect the quality of segregation. Machine frequencies may be limited by the settling zone (the area required for the particles to settle so that they are ready for crushing) and by secondary flows, as high lateral fluid velocities are created by high frequency wall motion.

Additionally, the issue of material inflow has not be investigated as part of this research program. One transport that has been proposed is that of feeding the coarse particles into the bottom of the comminution device with the working fluid. Essential to this concept is a reduction in the mass flow rate of the working fluid in the comminution chamber and wherever segregation is desired. This implies that the area of the inlet (where the coarse mixture enters the machine) must be smaller than the area of fluidization so that the coarse are not expelled from the chamber. Such a flow must also be managed with respect to the jet.

One possible solution to the transport problem is the conical crushing geometry presented in Figure 1.3. In this geometry, a decreasing fluid velocity can be achieved simultaneously with a decreasing gap width. In this configuration, the area at the top of the machine must be greater than the area of the inlet. In this geometry, segregation must occur in an inclined chamber, which may or may not be as effective as segregation in a vertical chamber. Particles must also be captured before crushing can occur.

An alternative mechanism for material transport does not use fluidization for incoming material transport. Instead, the coarse mixture can be loaded into the chamber from the top of the machine. Any fines present will automatically be segregated out, and the coarse material will descend into the crushing zone. Comminution will then occur, generating more fines, until the coarse is exhausted. The coarse inflow could be discrete or continuous, depending on the processing rate of the machine. Although the top feeding concept is simpler than the bottom feeding concept, some difficult problems would still remain to be solved. In particular, the chamber must have a floor, but a jet (for segregation) must be able to pass through this floor, while the fines should not percolate through it. This is similar to the difficulties encountered in the design of this apparatus; a series of fixed jets may offer better performance in this regard.

Chapter 4

Conclusions

4.1 Summary

This research is part of the MIT comminution program. The activity holds as a goal to describe and develop the physical understanding necessary to design a new generation of comminution machines with increased energy efficiency. The design considers material transport and material fracture as important simultaneous issues.

Previous research has provided the necessary information on the behavior of particle beds under compressive loads. Crushing efficiency is optimized if the fine particles created with the comminution action are continuously removed and if crushing occurs during each stroke on a cleared bed. In order to maintain an elevated product output it is also desired that the size-dependent segregation process be fast. Previous work in the area of fluidized segregation has explored the efficacy of fluidization in a constant area and expanding area vertical test sections, both as approximations of the annular geometry of the current apparatus. The current work focuses upon the design of an apparatus to simulate the geometry and kinematics of the new comminution machine concept, while facilitating quantifiable observations of particle behavior.

An apparatus for determining the efficacy of fluidized segregation in a new comminution device has been designed and constructed. Initial experiments showed that fluidized segregation can occur in the annular geometry.

4.2 Future Work

4.2.1 Hardware Completion

Currently, experiments can only be conducted with line pressure and flow rates (approximately 4 gpm). In order to provide more flexibility (*e.g.*, more holes open in nozzle) a pump should be used. A Teel 8 gpm/60 psi pump is currently connected to the apparatus. A bypass valve permits control of the flow rate to the experiment. In order to make the pump operational, the power supply cord to the pump should be rewired to permit connections with standard 220 V outlets. Additionally, a feed through switch should be placed in line, so that the pump can be easily switched on and off.

An additional, but optional, modification involves the jet system. Currently, the peripheral flow is not easily controlled. The porous plate currently installed in the apparatus was perforated to reduce the obstruction it presented to the jet. The perforations consist of approximately 1800 holes (10 radial perforations every two degrees). One alternative is to replace the perforated porous plate with an unmodified, non-perforated one. A second alternative would be to fabricate a new nozzle.

The new nozzle would operate in a similar fashion to the current nozzle in that it would rotate with the minimum gap width. However, while the current nozzle covers 90° of arc, the new nozzle would cover 360° of arc, allowing the flow to be well-controlled in all

regions of the test section. An additional pin can be added to the end cap of the support tube (part 1) directly opposite the current pin. An isometric view of a possible nozzle is shown in Figure 4.1.

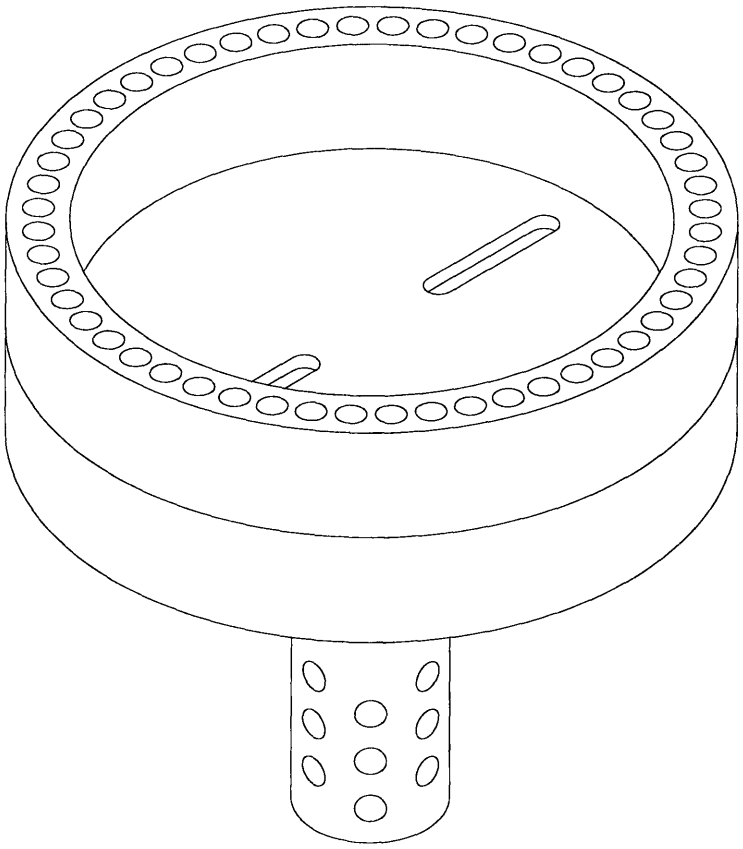

Figure 4.1. An isometric illustration of a new nozzle design.

4.2.2 Experimentation Recommendations

It would be nearly impossible, and very time consuming, to conduct every possible experiment with the apparatus. Furthermore, the immense amount of data produced would require large amounts of time for analysis. In order to make the most efficient use of experiments run, I recommend using Robust Design methods (also known as Taguchi Methods), adapted from *Quality Engineering Using Robust Design* (Phadke, 1989). This technique permits efficient determination of the effects of several parameters. After these experiments are conducted, a second round of experiments could be configured to investigate interesting configurations in more detail.

To determine which experiments should be conducted, we must first determine how many orthogonal parameters we have, and at how many levels we need to investigate each of them. Since there are five parameters we are interested in studying, we must find an orthogonal array that will accommodate five variables, with three or four values for each one. Either three or four levels will be sufficient for the initial experiments, and we let the suitability of an array determine the number of levels we choose. The parameters are presented in Table 4.1 below; the variable parameters are those in which we are interested.

Note that the superficial fluid velocity encountered in the test section is dependent upon the jet arc length and the flow rate. Thus, the flow rate, and not the superficial fluid velocity is selected as a control factor.

Parameter	Value/Range
Fixed Parameters	
Coarse Particle Size	3.0 mm
Fine Particle Size	0.2 mm
Outer Cylinder Size	11.5 inches
Inner Cylinder Size	10.0 inches
Compression Ratio/Offset Relationship	$R_c = \frac{O_w}{0.75\ inches} \times 100\%$
Variable Parameters	
Offset, O_w	0.0 - 0.75 inches
Angular Speed	0 - 44 rpm
Flow Rate	0 - 8 gpm
Jet Arc	7 - 90°
Jet Phase	-45 - +45°

Table 4.1. Parameters and their possible values for the current apparatus.

Upon examination of a table of standard orthogonal arrays, we find that an L'_{16} array can accommodate five variables with four levels each. After selecting an orthogonal array, we must set four levels for each of the parameters to be investigated. Experiments will be conducted using these values for each of the parameters.

	Factors				
	1	*2*	*3*	*4*	*5*
Level Number	*Offset (inches)*	*Flow Rate (gpm)*	*Jet Arc Length (°)*	*Jet Phase (°)*	*Angular Velocity (rpm)*
1	0.00	4	7	-30°	0
2	0.18	5.33	21	15°	1
3	0.38	6.66	35	30°	5
4	0.58	8	49	45°	10

Table 4.2. Parameter values for the recommended experiments.

The experiments to be conducted are then given by the L'_{16} matrix below. The numbers in the table indicate the level of the factor (parameter) indicated by the heading in the column.

Experiment Number	*1 Offset*	*2 Flow Rate*	*3 Jet Arc Length*	*4 Jet Phase*	*5 Angular Velocity*
1	1	1	1	1	1
2	1	2	2	2	2
3	1	3	3	3	3
4	1	4	4	4	4
5	2	1	2	3	4
6	2	2	1	4	3
7	2	3	4	1	2
8	2	4	3	2	1
9	3	1	3	4	2
10	3	2	4	3	1
11	3	3	1	2	4
12	3	4	2	1	3
13	4	1	4	2	3
14	4	2	3	1	4
15	4	3	2	4	1
16	4	4	1	3	2

Table 4.3. Orthogonal array for experiments to be conducted. The number in each cell represents the level of the parameter indicated in the column heading that should be used. The levels and their values are presented in Table 4.2.

Evaluating different configurations requires the selection of a metric. What determines "good performance"? Segregation quality is an obvious metric, and is also quite measurable using the luminance measuring system; segregation quality can simply be defined as the luminance transmission measurement. Thus, segregation quality could be measured by simply measuring the luminance in a prescribed region (or regions) of the test section. In fact, we are actually measuring the fines remaining after segregation. Another possible metric is segregation time, which can be defined as the time required to reach a certain level of segregation in a prescribed region, although this is a more difficult metric to analyze. It is advisable to take segregation quality measurements in several places and then to find the mean and the standard deviation for each experiment. This information can be used to determine the signal to noise ratio, defined below.

$$S/N\ Ratio = \eta = -10 \log_{10}\left(\frac{1}{n}\sum_{i=1}^{n} y_i^2\right) \tag{4.1}$$

The negative sign results because segregation quality (*i.e.*, amount of fines remaining), as we have defined it, is a smaller-is-better metric. The segregation for a particular experiment in a particular region is represented by y_i, and can be defined as the luminance value measured. The expression enclosed in the parentheses is termed the mean square quality characteristic. It is desirable to maximize the S/N ratio; this simply says that we would like achieve the greatest mean segregation.

It is also important to note the height to which the fines can be fluidized, as this will be important in determining the height required in an actual machine. The flow must be capable of transporting the fines out of the machine.

The most significant noise factor is likely to be the bead mixture composition. Every effort should be made to maintain the 55:45 coarse/fines concentration in the experiment. Of course, it is more important that the experiments be conducted with similar concentrations than the particular concentration at which they are conducted.

Interactions between control factors cannot be estimated from these experiments. In order to estimate interactions with the L'_{16} matrix, the factors for which interactions are to be investigated must be placed in the first two columns, while the remaining three columns are empty. For further analysis techniques, consult *Quality Engineering Using Robust Design* (Phadke, 1989).

Appendix A

Assembly & Disassembly Instructions

A.1 Disassembly

To disassemble the device for maintenance, perform the following operations:

1. Ensure that the machine is drained and that all power connections have been unplugged. Remove the camera if it is mounted. Disconnect the pump from the inlet by loosening the hose clamp over the two inch inlet and sliding the reducer off the inlet.
2. Loosen and remove the bolts on top of the upper tie rod brackets.
3. Loosen and remove the bolts securing the angle brackets on the legs to the table.
4. Remove the tie rods from the base assembly.
5. Twist the upper outer tubing off the base assembly; an assistant or hooks and cable will be required to support the upper outer tubing.
6. Remove the base unit. This is easiest if the nozzle is directly opposite the user and the edge of the base unit closest to the user is lifted up. The base unit can then be moved from under the lamp assembly.
7. The upper outer tubing can now be removed.
8. The four bolts securing the lamp assembly to the upper clamp plate (part 11) can be removed so that the lamp will rest on the work surface.
9. Place the lamp assembly on its side while ensuring it will not roll.
10. Remove the porous plate retainer (part 4) by unscrewing the twelve screws.
11. Remove the porous plate.
12. Slide the lamp out of the inner cylinder assembly.
13. The lamp should be inspected for seal damage and wear between the lower inner end cap (part 1) and the five inch diameter acrylic tubing (part 5). It should be tested by submerging it in twelve inches of water. Any repairs should be made with marine quality sealant.
14. The nozzle can be lifted out of the base assembly. The upper half of the nozzle can be removed by removing all of the screws on the top and bottom of the nozzle. Stoppers in the nozzle can be removed with a screwdriver and needlenose pliers.

A.2 Assembly

To assemble the device after maintenance, perform the following operations:

1. Ensure that the nozzle is assembled and in place in the base assembly. Use caution when installing the screws to reassemble the nozzle to avoid damage to the gasket.
2. Place the assembled inner cylinder (ten inch diameter) over the lamp assembly.

3. Place the upper tie rod bracket and the upper outer tubing over the lamp assembly.
4. Position the porous plate and the porous plate retainer. Install screws.
5. An assistant or hooks and cables should hold the upper outer tubing and upper tie rod bracket in position. This will allow the user to have both hands free for the remaining steps. If an assistant is available, he or she can simply hold these parts in place for the next step.
6. Secure the lamp assembly (five inch diameter acrylic tubing) to the upper clamp plate (part 11) with four bolts.
7. Position the base unit. It will have to be tilted away from the user and slid under the lamp assembly. Pay attention to the orientation of the pin on the lower inner end cap; it should be directly opposite the user, as should the nozzle.
8. Install the eight nuts and bolts to secure the angle brackets to the bench, but do not tighten them.
9. Locate the base unit by aligning the porous plate and the top edge of the lower outer tubing. Measure the distance between the edge of the porous plate and the inner cylinder in four places, 90° apart. These measurements should be the same. Tighten the eight nuts and bolts to secure the base unit.
10. Lower the upper outer tubing and position it over the lower outer tubing and the porous plate. A slight tap with a mallet may be required to seat the upper tubing.
11. Install the tie rods.
12. Connect power supplies; ensure that a GFCI is in place between the power source and the lamp.

Appendix B

Resources

NIH Image is a public domain software package for scientific image analysis. The application (current version: 1.58) is available for both the Macintosh and Power Macintosh platforms. The application and complete documentation, as well as plug-in modules and complete source code, are available via anonymous ftp from the following site:

ftp://zippy.nimh.nih.gov/pub/nih-image/

Capra Optical (CCD Camera Vendor)
13 Mercer Road
Natick, MA 01760-2414
508.650.9700

Jaygo, Incorporated (Glass Media Vendor)
675 Rahway Avenue
Union, NJ 07083
908.688.3600

Porex Technologies (Porous Plate Vendor)
500 Bohannon Road
Fairburn, GA 30123
800.241.0195
404.964.1421

Ramco Machine (Machinist)
416 Cabot Street
Beverly, MA 01915-3152
508.921.4600

Unistrut Corporation (Flexible Assembly Structures)
35660 Clinton Street
Wayne, MI 48184
800.521.7730

Appendix C

Engineering Drawings

Engineering drawings are provided for all custom fabricated parts. A cross section in which each part is labeled with its part number is presented in Figure C.1.

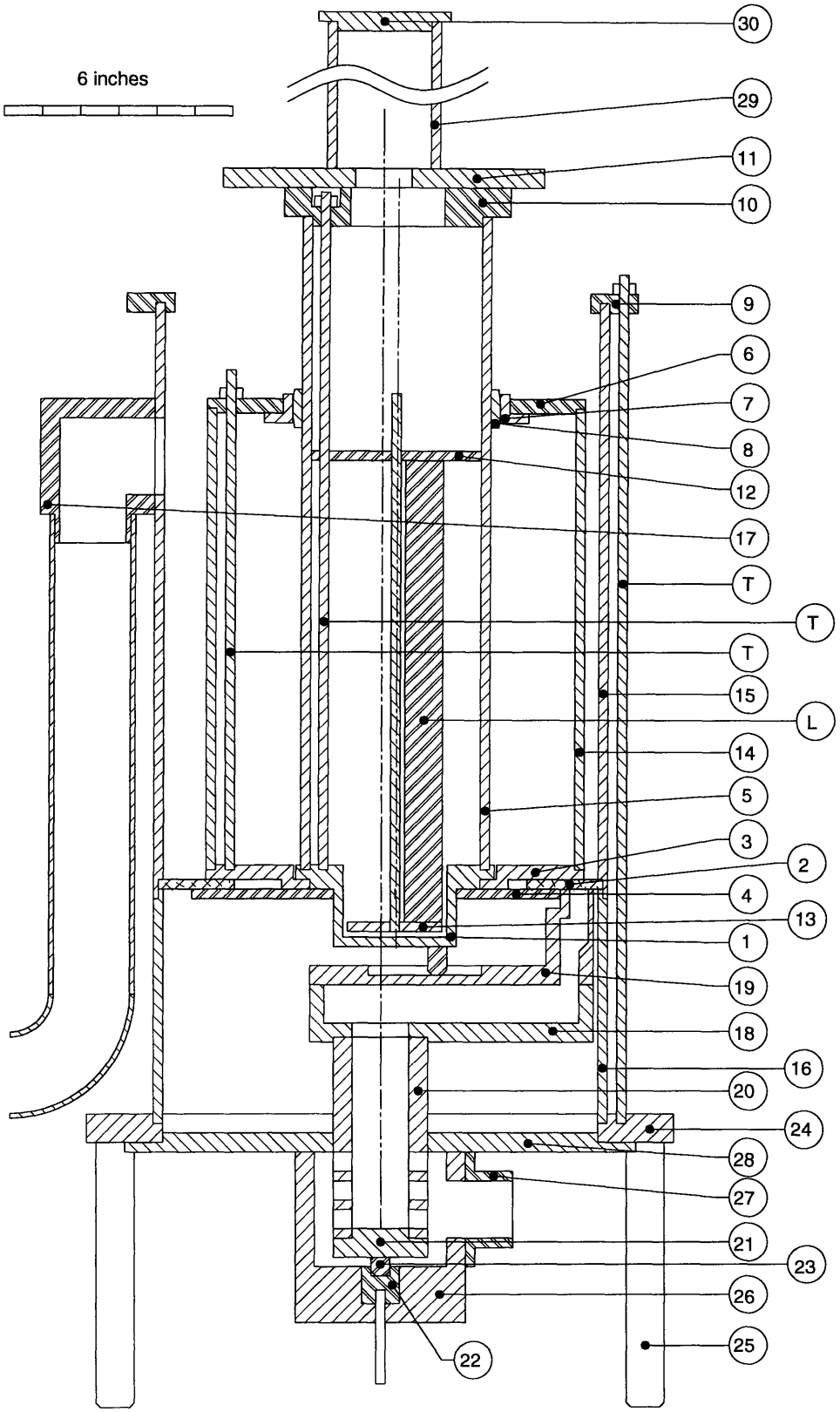

Figure C.1. A cross section of the test section; part numbers are indicated for each part. T denotes a tie rod; L denotes a fluorescent lamp tube.

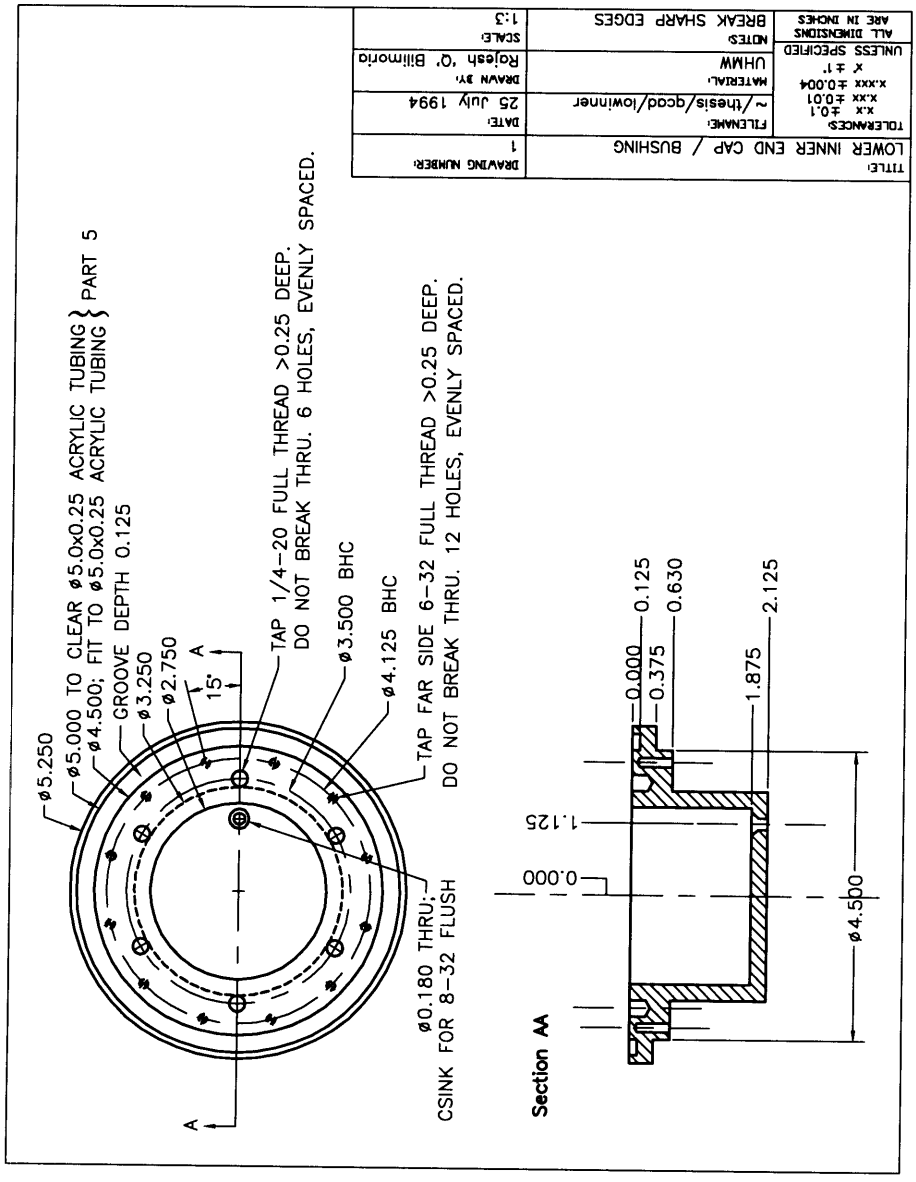
ø5.250
ø5.000 TO CLEAR ø5.0x0.25 ACRYLIC TUBING } PART 5
ø4.500; FIT TO ø5.0x0.25 ACRYLIC TUBING }
GROOVE DEPTH 0.125
ø3.250
ø2.750
15°
A
TAP 1/4-20 FULL THREAD >0.25 DEEP.
DO NOT BREAK THRU. 6 HOLES, EVENLY SPACED.
ø3.500 BHC
ø4.125 BHC
TAP FAR SIDE 6-32 FULL THREAD >0.25 DEEP.
DO NOT BREAK THRU. 12 HOLES, EVENLY SPACED.
ø0.180 THRU;
CSINK FOR 8-32 FLUSH
A
Section AA
0.000
0.125
0.375
0.630
1.875
2.125
1.125
0.000
ø4.500
TITLE: LOWER INNER END CAP / BUSHING
DRAWING NUMBER: 1
DATE: 25 July 1994
DRAWN BY: Rajesh 'Q' Billimoria
MATERIAL: UHMW
FILENAME: ~/thesis/qcad/lowinner
NOTES: BREAK SHARP EDGES
SCALE: 1:3
TOLERANCES: UNLESS SPECIFIED x.x ±0.1 x.xx ±0.01 x.xxx ±0.004 x' ±1' ALL DIMENSIONS ARE IN INCHES

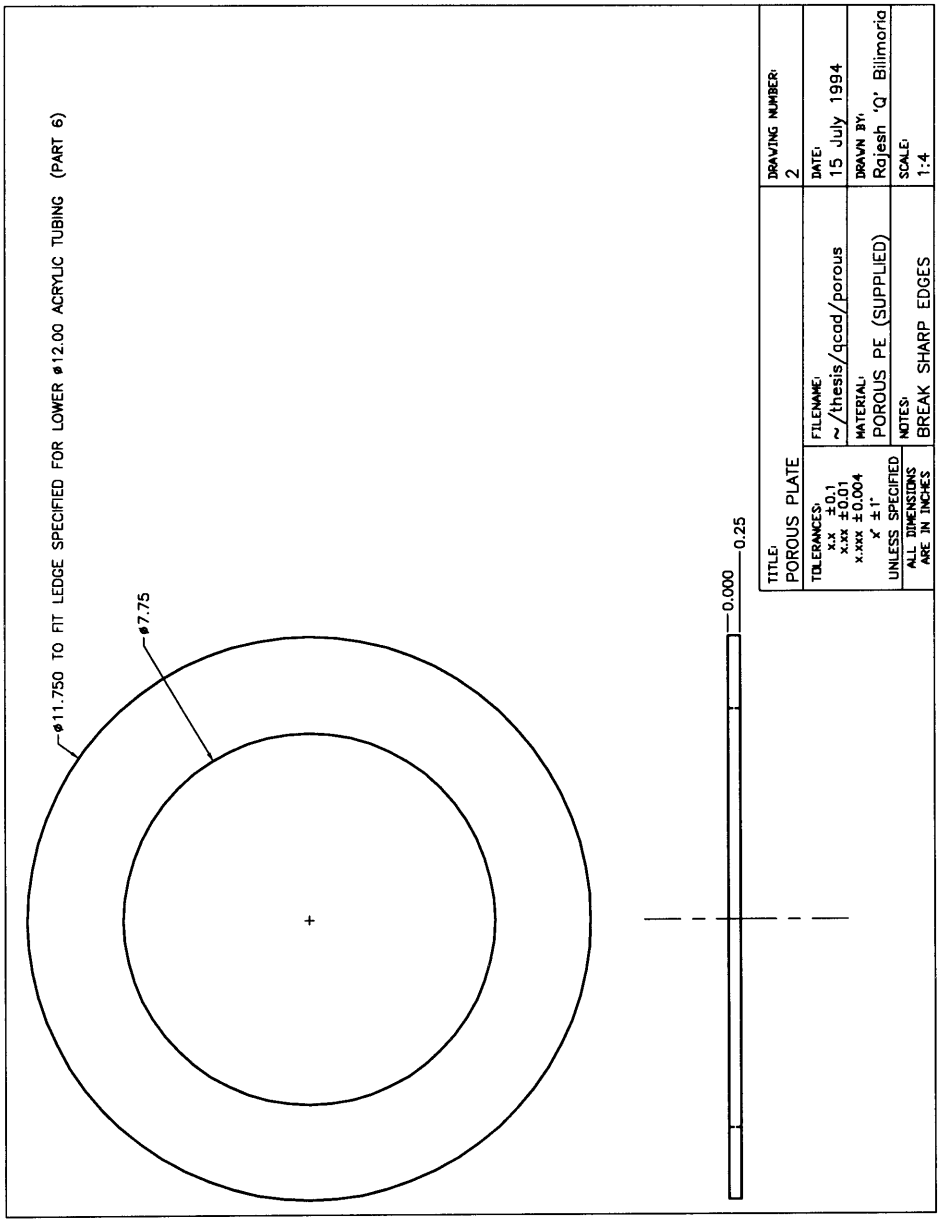
ø11.750 TO FIT LEDGE SPECIFIED FOR LOWER ø12.00 ACRYLIC TUBING (PART 6)
ø7.75
0.000
0.25
TITLE:
POROUS PLATE
TOLERANCES:
x.x ±0.1
x.xx ±0.01
x.xxx ±0.004
x' ±1'
UNLESS SPECIFIED
ALL DIMENSIONS ARE IN INCHES
FILENAME:
~/thesis/qcad/porous
MATERIAL:
POROUS PE (SUPPLIED)
NOTES:
BREAK SHARP EDGES
DRAWING NUMBER:
2
DATE:
15 July 1994
DRAWN BY:
Rajesh 'Q' Bilimoria
SCALE:
1:4

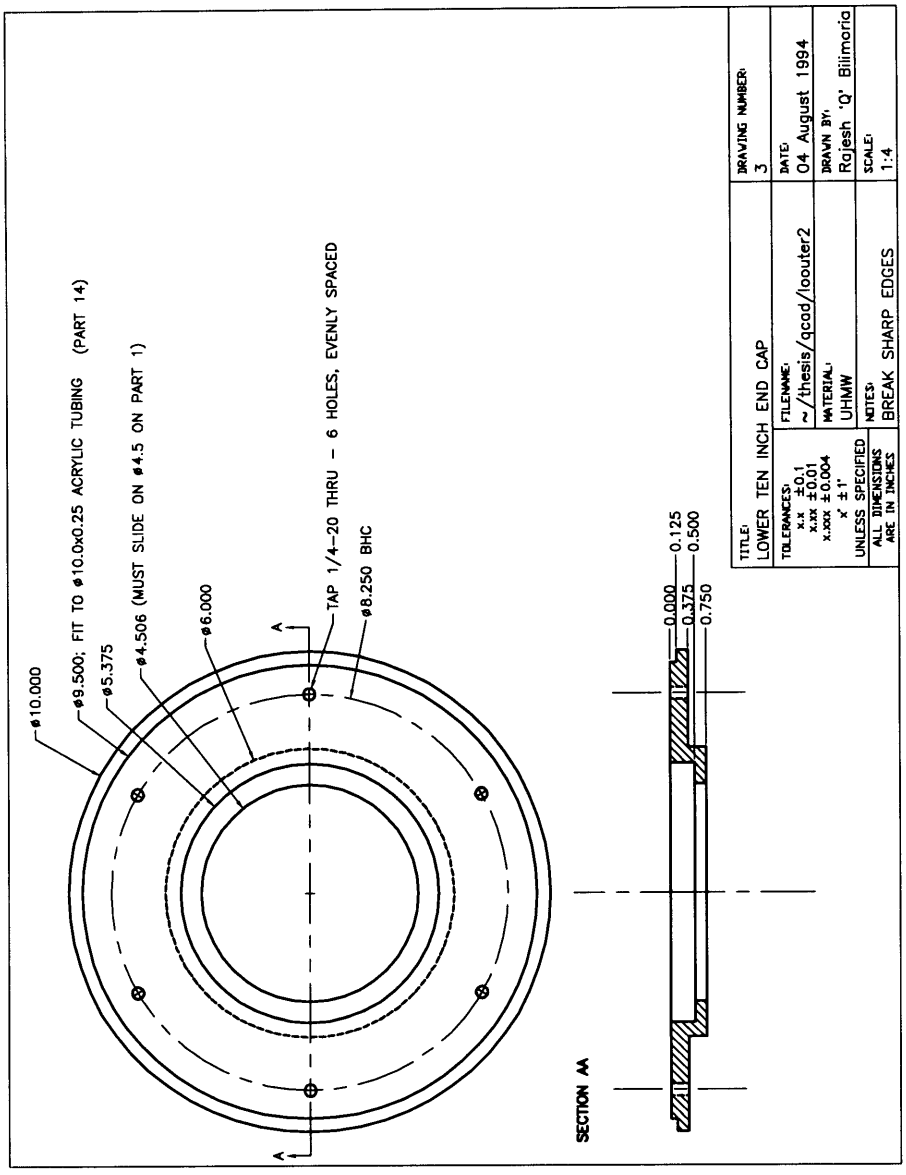
ø10.000
ø9.500; FIT TO ø10.0x0.25 ACRYLIC TUBING (PART 14)
ø5.375
ø4.506 (MUST SLIDE ON ø4.5 ON PART 1)
ø6.000
A
TAP 1/4-20 THRU - 6 HOLES, EVENLY SPACED
ø8.250 BHC
A
SECTION AA
0.000
0.125
0.375
0.500
0.750
TITLE:
LOWER TEN INCH END CAP
DRAWING NUMBER:
3
TOLERANCES:
x.x ±0.1
x.xx ±0.01
x.xxx ±0.004
x' ±1'
UNLESS SPECIFIED
ALL DIMENSIONS ARE IN INCHES
FILENAME:
~/thesis/qcad/louter2
MATERIAL:
UHMW
NOTES:
BREAK SHARP EDGES
DATE:
04 August 1994
DRAWN BY:
Rajesh 'Q' Bilimoria
SCALE:
1:4

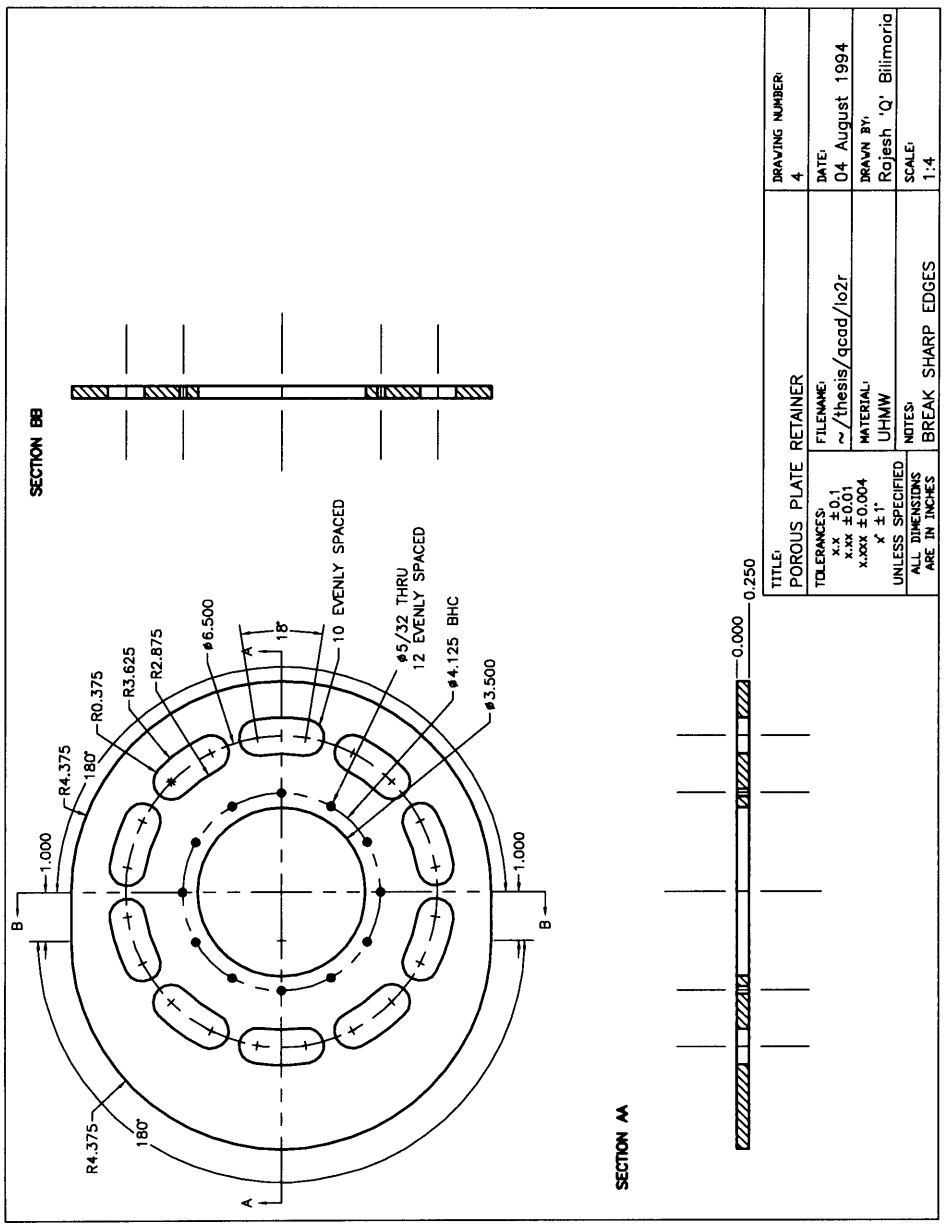
SECTION BB
SECTION AA
R4.375
180°
R0.375
R3.625
R2.875
ø6.500
18°
10 EVENLY SPACED
ø5/32 THRU
12 EVENLY SPACED
ø4.125 BHC
ø3.500
1.000
0.250
0.000
A
B
TITLE: POROUS PLATE RETAINER
DRAWING NUMBER: 4
TOLERANCES: x.x ±0.1, x.xx ±0.01, x.xxx ±0.004, x ±1°
FILENAME: ~/thesis/qcad/lo2r
DATE: 04 August 1994
MATERIAL: UHMW
DRAWN BY: Rajesh 'Q' Bilimoria
UNLESS SPECIFIED: ALL DIMENSIONS ARE IN INCHES
NOTES: BREAK SHARP EDGES
SCALE: 1:4

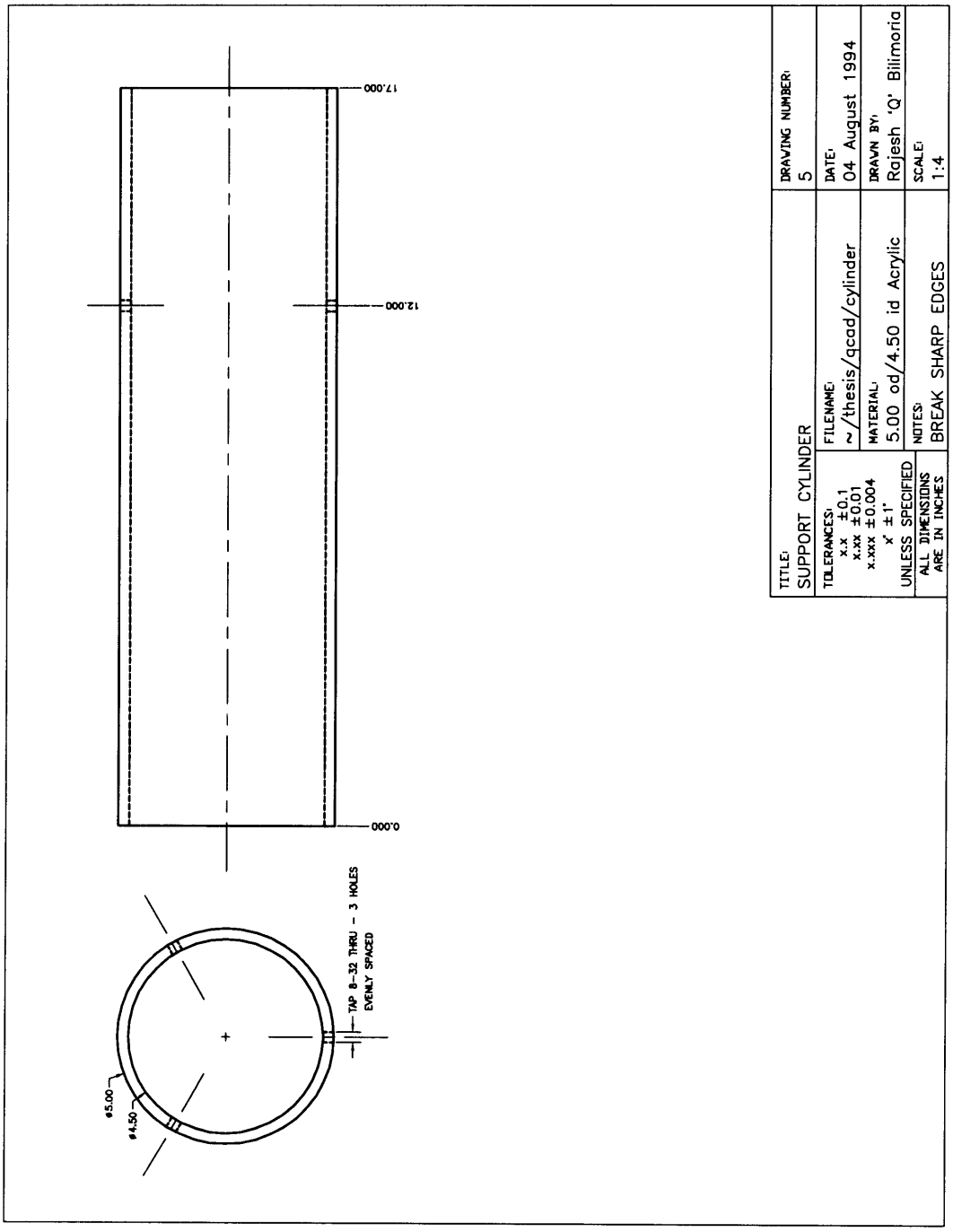
17.000
12.000
0.000
TAP 8-32 THRU - 3 HOLES
EVENLY SPACED
ø5.00
ø4.50
TITLE:
SUPPORT CYLINDER
DRAWING NUMBER:
5
TOLERANCES:
x.x ±0.1
x.xx ±0.01
x.xxx ±0.004
x' ±1'
UNLESS SPECIFIED
ALL DIMENSIONS
ARE IN INCHES
FILENAME:
~/thesis/qcad/cylinder
MATERIAL:
5.00 od/4.50 id Acrylic
NOTES:
BREAK SHARP EDGES
DATE:
04 August 1994
DRAWN BY:
Rajesh 'Q' Bilimoria
SCALE:
1:4

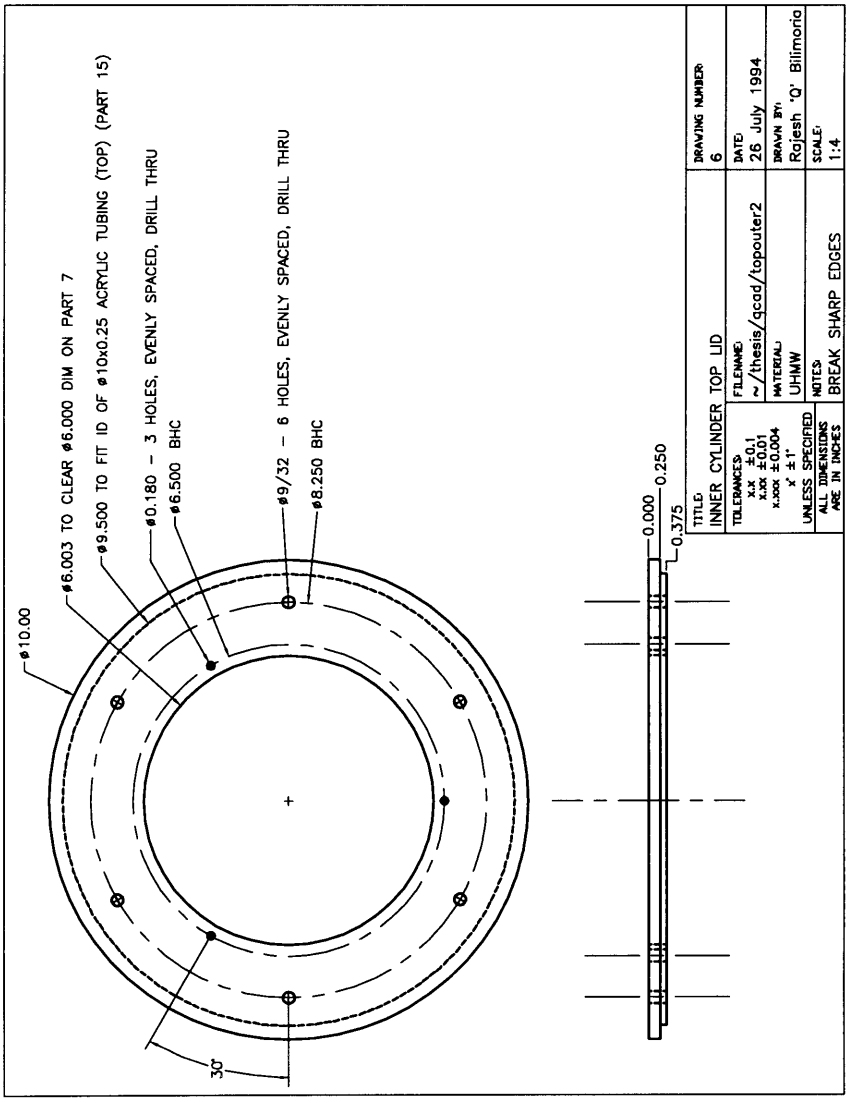
ø10.00
ø6.003 TO CLEAR ø6.000 DIM ON PART 7
ø9.500 TO FIT ID OF ø10x0.25 ACRYLIC TUBING (TOP) (PART 15)
ø0.180 - 3 HOLES, EVENLY SPACED, DRILL THRU
ø6.500 BHC
ø9/32 - 6 HOLES, EVENLY SPACED, DRILL THRU
ø8.250 BHC
30°
0.000
0.250
0.375
TITLE:
INNER CYLINDER TOP LID
DRAWING NUMBER:
6
TOLERANCES:
x.x ±0.1
x.xx ±0.01
x.xxx ±0.004
x° ±1°
UNLESS SPECIFIED
ALL DIMENSIONS
ARE IN INCHES
FILENAME:
~/thesis/gcad/topouter2
MATERIAL:
UHMW
NOTES:
BREAK SHARP EDGES
DATE:
26 July 1994
DRAWN BY:
Rajesh 'Q' Bilimoria
SCALE:
1:4

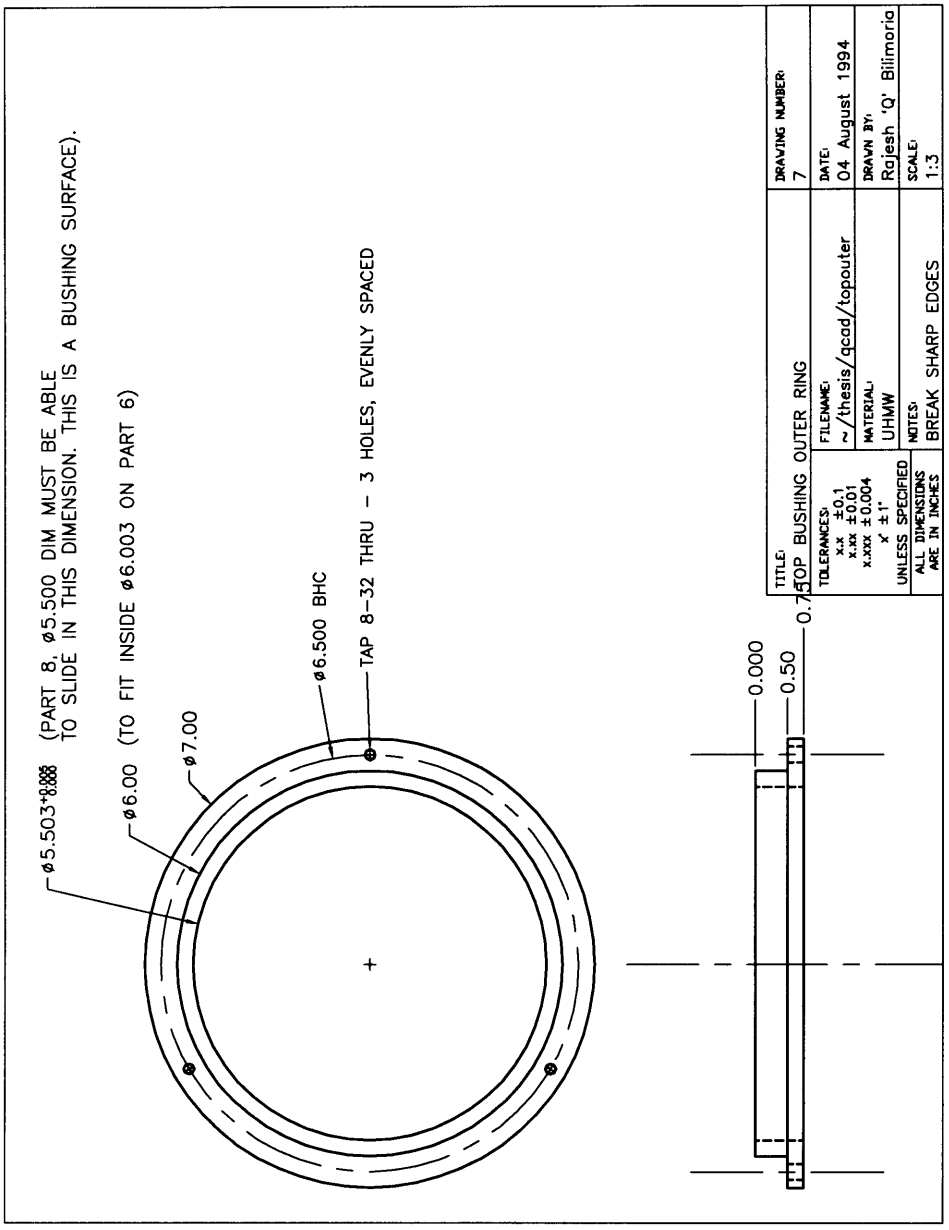
ø5.503+0.000 -0.000 (PART 8, ø5.500 DIM MUST BE ABLE TO SLIDE IN THIS DIMENSION. THIS IS A BUSHING SURFACE).
ø6.00 (TO FIT INSIDE ø6.003 ON PART 6)
ø7.00
ø6.500 BHC
TAP 8-32 THRU - 3 HOLES, EVENLY SPACED
0.000
0.50
0.75
TITLE: TOP BUSHING OUTER RING
DRAWING NUMBER: 7
TOLERANCES: x.x ±0.1 x.xx ±0.01 x.xxx ±0.004 x' ±1'
FILENAME: ~/thesis/qcad/topouter
DATE: 04 August 1994
MATERIAL: UHMW
DRAWN BY: Rajesh 'Q' Bilimoria
UNLESS SPECIFIED ALL DIMENSIONS ARE IN INCHES
NOTES: BREAK SHARP EDGES
SCALE: 1:3

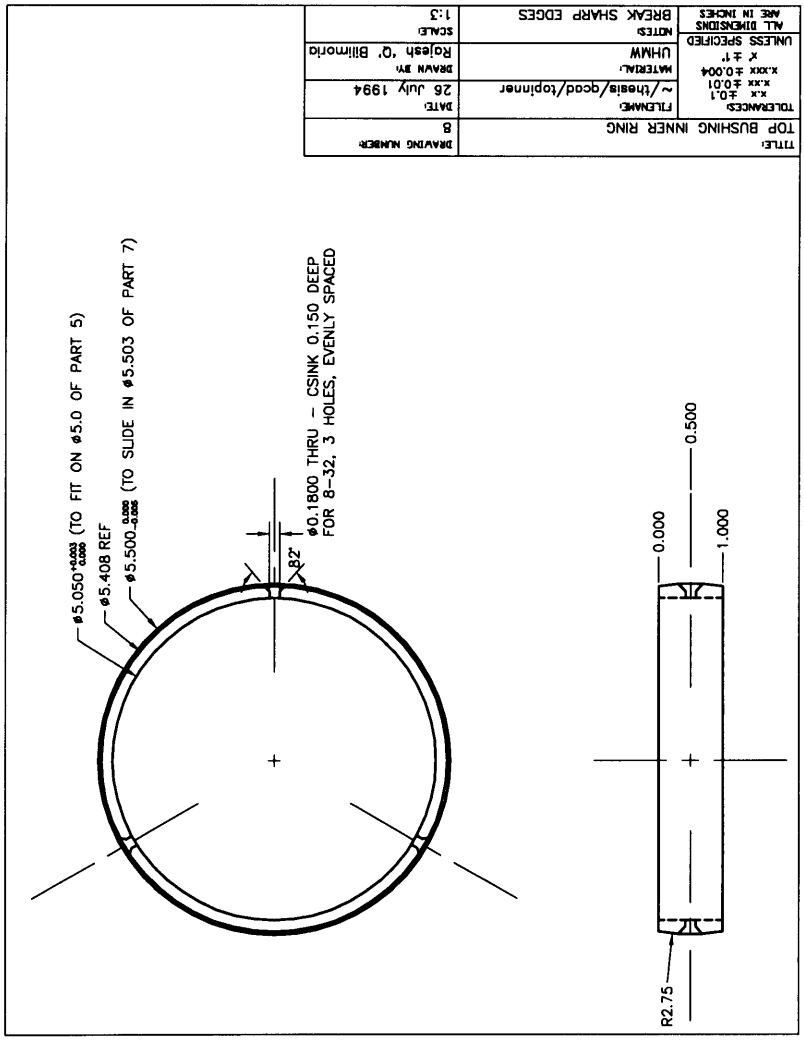
TOP BUSHING INNER RING
8
~/thesis/qcad/topinner
26 July 1994
Rajesh 'Q' Bilimoria
UHMW
BREAK SHARP EDGES
1:3
ALL DIMENSIONS ARE IN INCHES
UNLESS SPECIFIED
x ±1°
x.xxx ±0.004
x.xx ±0.01
x.x ±0.1
ø5.050 +0.003 -0.000 (TO FIT ON ø5.0 OF PART 5)
ø5.408 REF
ø5.500 -0.000 -0.005 (TO SLIDE IN ø5.503 OF PART 7)
ø0.1800 THRU - CSINK 0.150 DEEP
FOR 8-32, 3 HOLES, EVENLY SPACED
82°
0.000
0.500
1.000
R2.75

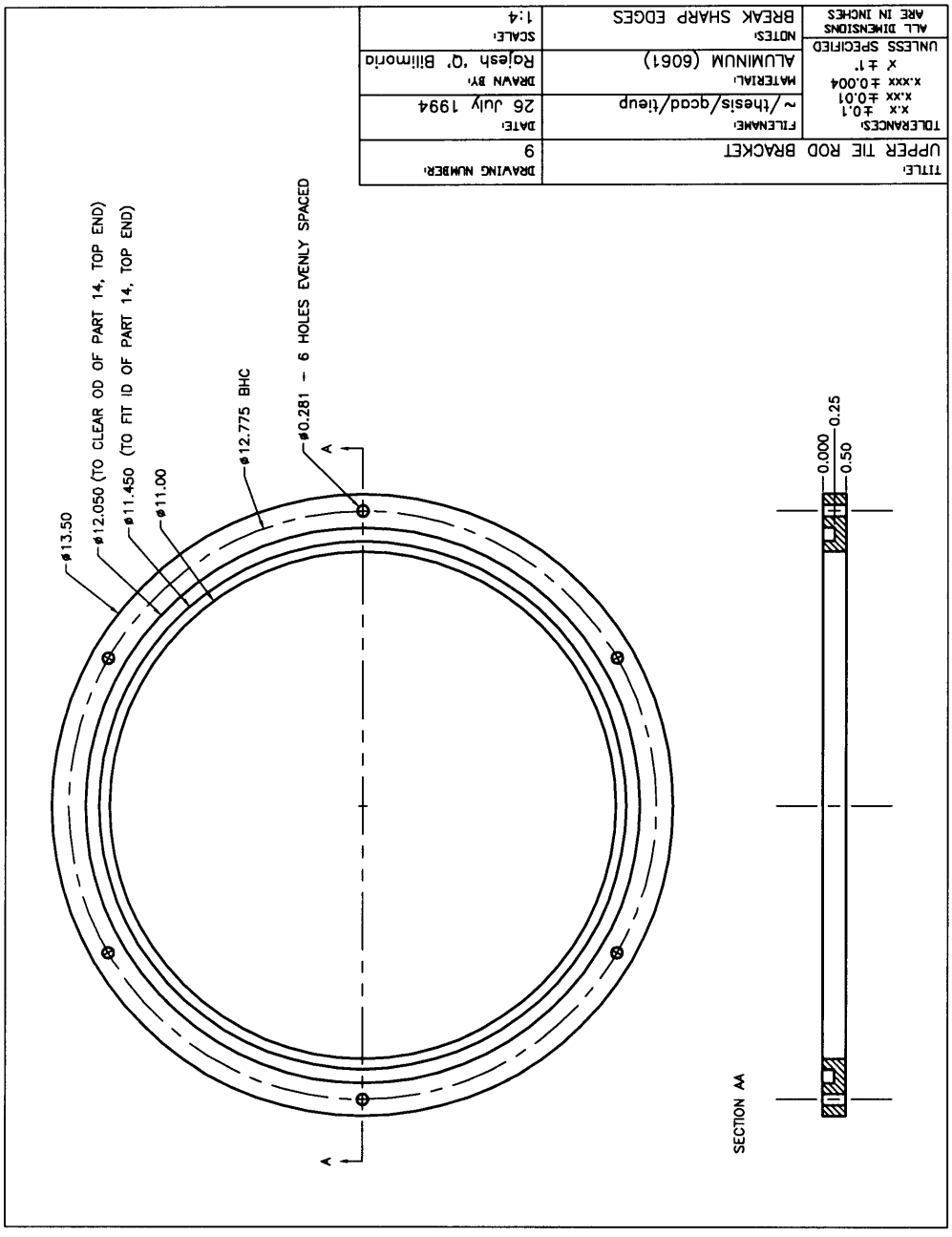
TOLERANCES:
x.x ±0.1
x.xx ±0.01
x.xxx ±0.004
UNLESS SPECIFIED
X' ±1'
ALL DIMENSIONS
ARE IN INCHES
TITLE:
UPPER TIE ROD BRACKET
FILENAME:
~/thesis/qcad/tierp
DATE:
26 July 1994
DRAWN BY:
Rajesh 'Q' Billimoria
DRAWING NUMBER:
9
MATERIAL:
ALUMINUM (6061)
NOTES:
BREAK SHARP EDGES
SCALE:
1:4
ø13.50
ø12.050 (TO CLEAR OD OF PART 14, TOP END)
ø11.450 (TO FIT ID OF PART 14, TOP END)
ø11.00
ø12.775 BHC
ø0.281 - 6 HOLES EVENLY SPACED
A
A
SECTION AA
0.000
0.25
0.50

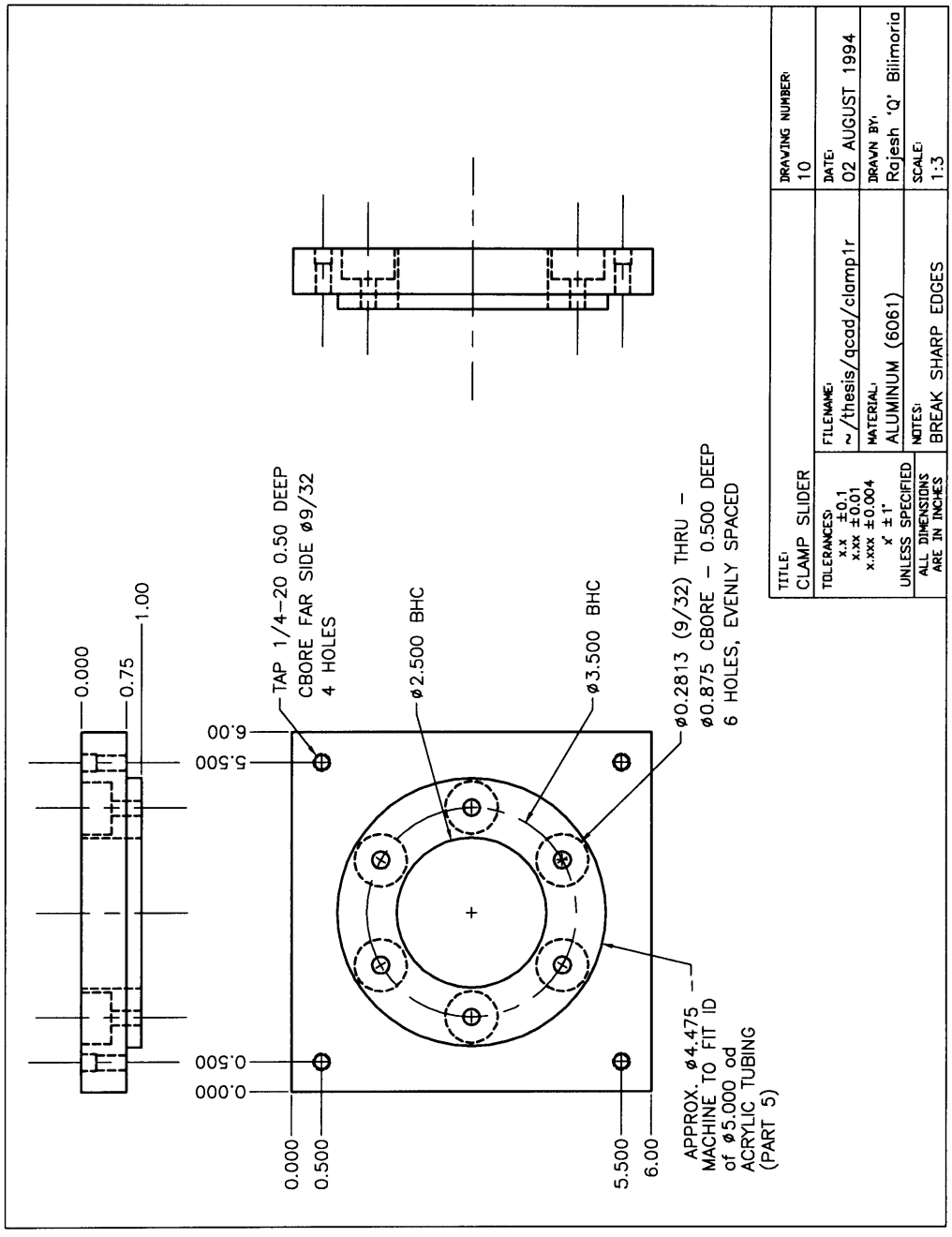
0.000
0.75
1.00
TAP 1/4-20 0.50 DEEP
CBORE FAR SIDE ø9/32
4 HOLES
ø2.500 BHC
ø3.500 BHC
ø0.2813 (9/32) THRU -
ø0.875 CBORE - 0.500 DEEP
6 HOLES, EVENLY SPACED
6.00
5.500
0.500
0.000
0.000
0.500
5.500
6.00
APPROX. ø4.475
MACHINE TO FIT ID
of ø5.000 od
ACRYLIC TUBING
(PART 5)
TITLE:
CLAMP SLIDER
TOLERANCES:
x.x ±0.1
x.xx ±0.01
x.xxx ±0.004
x' ±1'
UNLESS SPECIFIED
ALL DIMENSIONS
ARE IN INCHES
FILENAME:
~/thesis/qcad/clamp1r
MATERIAL:
ALUMINUM (6061)
NOTES:
BREAK SHARP EDGES
DRAWING NUMBER:
10
DATE:
02 AUGUST 1994
DRAWN BY:
Rajesh 'Q' Bilimoria
SCALE:
1:3

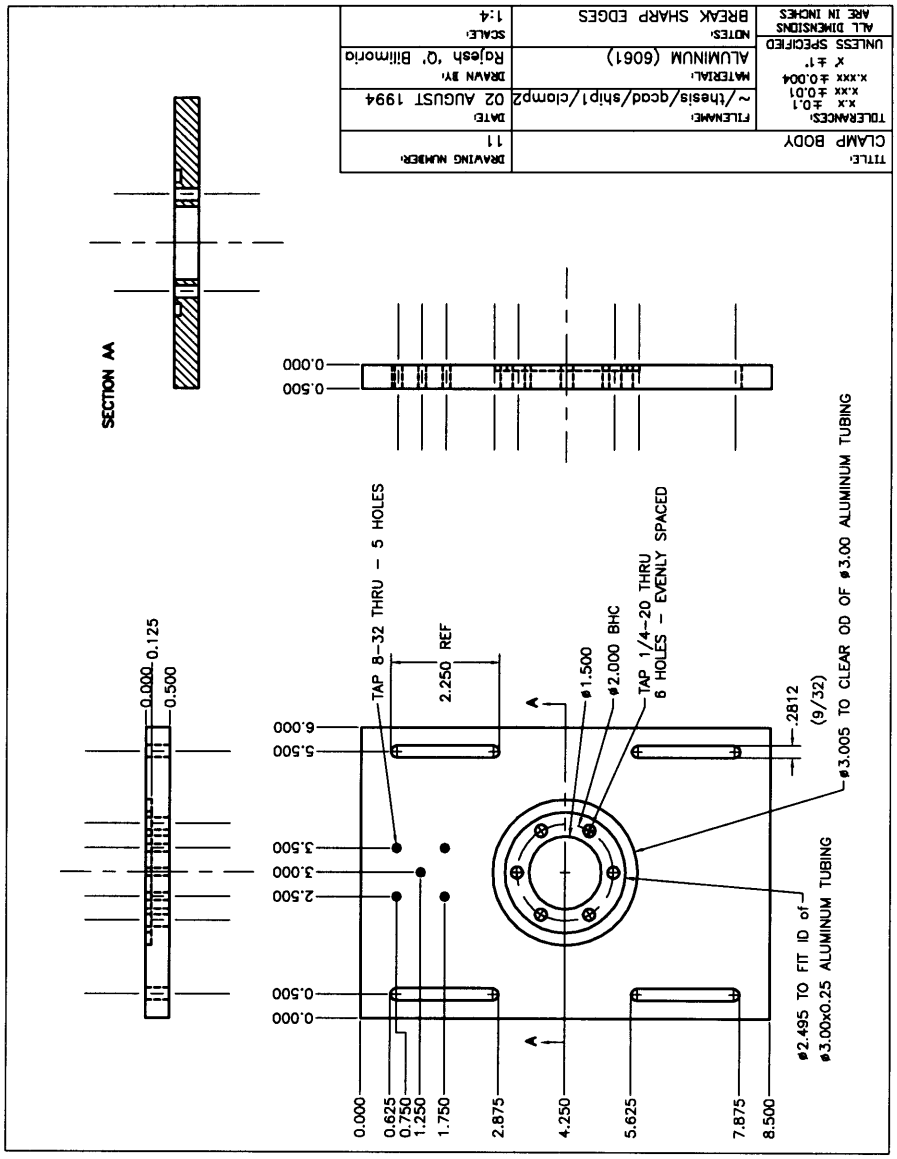
TITLE: CLAMP BODY
DRAWING NUMBER: 11
FILENAME: ~/thesis/qcad/ship1/clomp2
DATE: 02 AUGUST 1994
MATERIAL: ALUMINUM (6061)
DRAWN BY: Rajesh 'Q' Billimoria
NOTES: BREAK SHARP EDGES
SCALE: 1:4
TOLERANCES: x.x ±0.1 x.xx ±0.01 x.xxx ±0.004 UNLESS SPECIFIED X ±1° ALL DIMENSIONS ARE IN INCHES
SECTION AA
0.000
0.500
0.000
0.125
0.500
TAP 8-32 THRU - 5 HOLES
2.250 REF
ø1.500
ø2.000 BHC
TAP 1/4-20 THRU 6 HOLES - EVENLY SPACED
.2812 (9/32)
ø3.005 TO CLEAR OD OF ø3.00 ALUMINUM TUBING
ø2.495 TO FIT ID of ø3.00x0.25 ALUMINUM TUBING
6.000
5.500
3.500
3.000
2.500
0.500
0.000
0.000
0.625
0.750
1.250
1.750
2.875
4.250
5.625
7.875
8.500

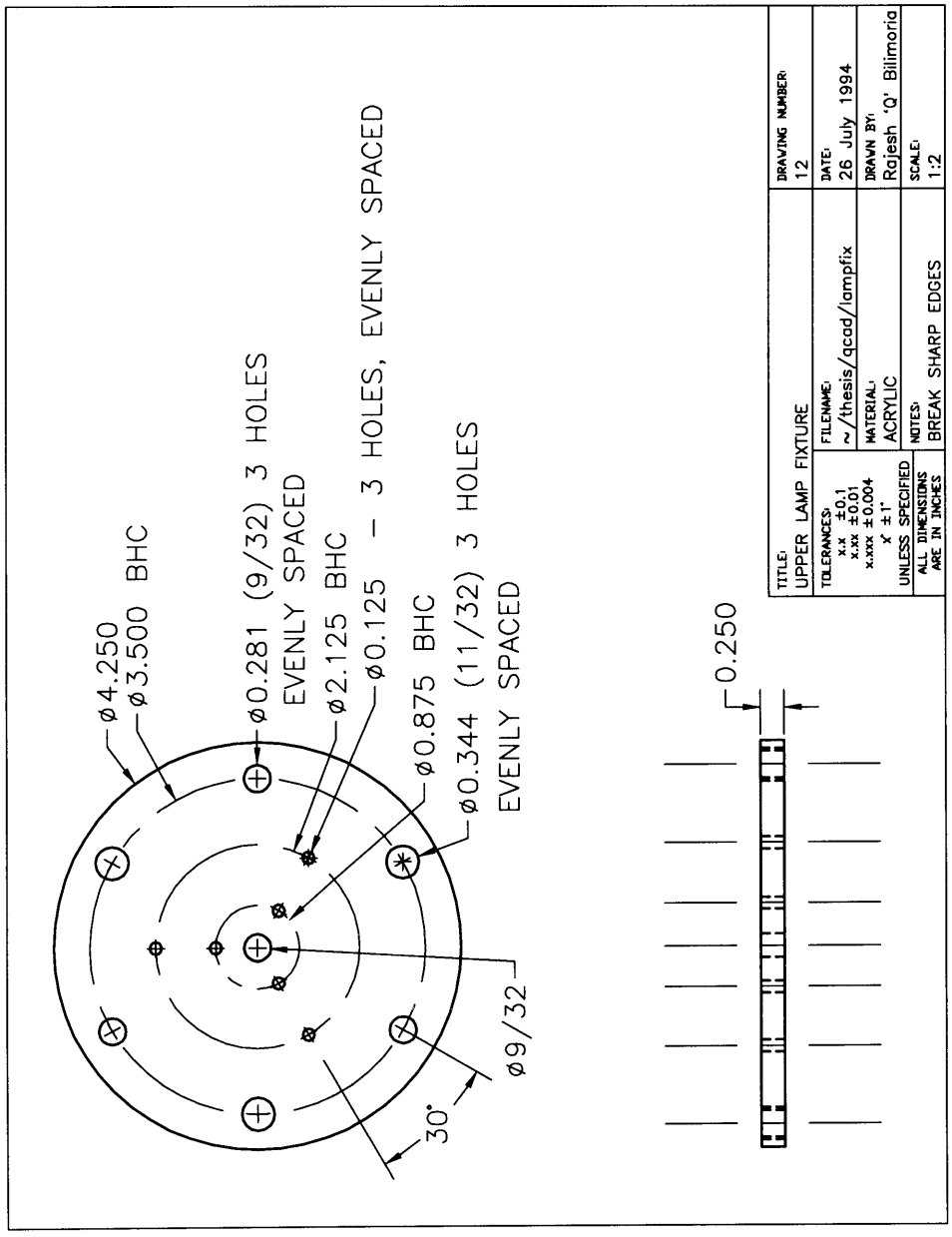
ø4.250
ø3.500 BHC
ø0.281 (9/32) 3 HOLES
EVENLY SPACED
ø2.125 BHC
ø0.125 - 3 HOLES, EVENLY SPACED
ø0.875 BHC
ø0.344 (11/32) 3 HOLES
EVENLY SPACED
ø9/32
30°
0.250
TITLE:
UPPER LAMP FIXTURE
DRAWING NUMBER:
12
TOLERANCES:
x.x ±0.1
x.xx ±0.01
x.xxx ±0.004
x' ±1'
FILENAME:
~/thesis/qcad/lampfix
DATE:
26 July 1994
MATERIAL:
ACRYLIC
DRAWN BY:
Rajesh 'Q' Bilimoria
UNLESS SPECIFIED
ALL DIMENSIONS
ARE IN INCHES
NOTES:
BREAK SHARP EDGES
SCALE:
1:2

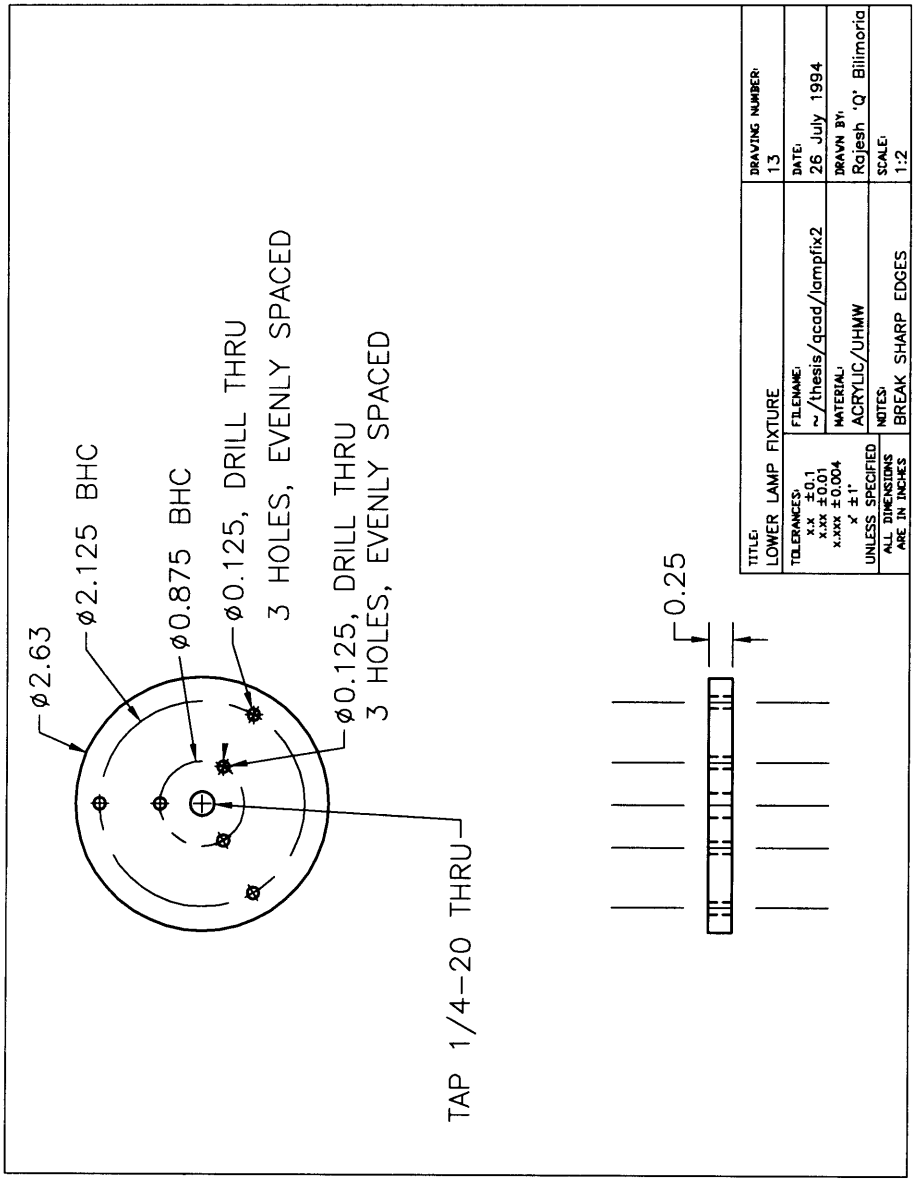
ø2.63
ø2.125 BHC
ø0.875 BHC
ø0.125, DRILL THRU
3 HOLES, EVENLY SPACED
ø0.125, DRILL THRU
3 HOLES, EVENLY SPACED
TAP 1/4-20 THRU
0.25
TITLE:
LOWER LAMP FIXTURE
TOLERANCES:
x.x ±0.1
x.xx ±0.01
x.xxx ±0.004
x' ±1'
UNLESS SPECIFIED
ALL DIMENSIONS
ARE IN INCHES
FILENAME:
~/thesis/qcad/lampfix2
MATERIAL:
ACRYLIC/UHMW
NOTES:
BREAK SHARP EDGES
DRAWING NUMBER:
13
DATE:
26 July 1994
DRAWN BY:
Rajesh 'Q' Bilimoria
SCALE:
1:2

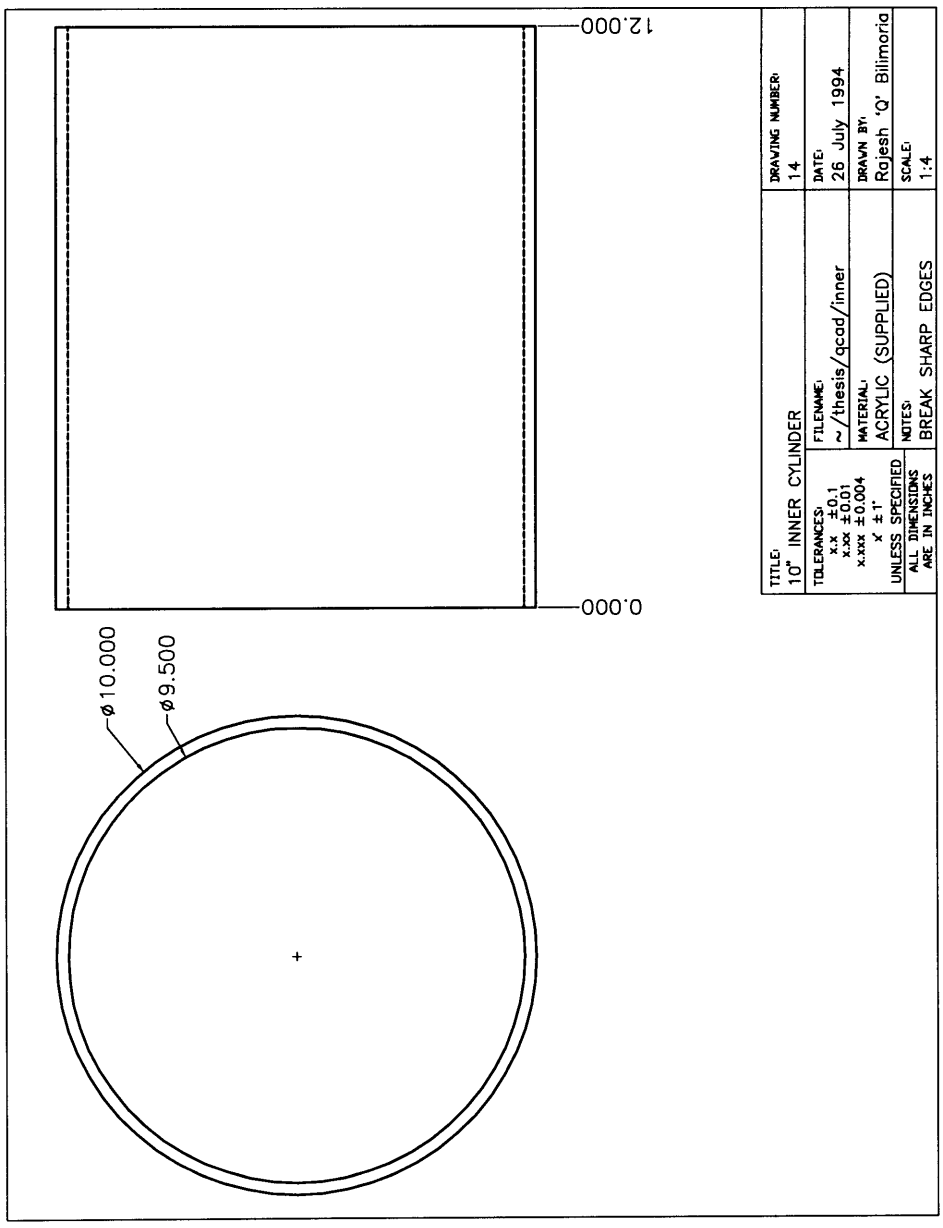
12.000
0.000
ø10.000
ø9.500
TITLE:
10" INNER CYLINDER
TOLERANCES:
x.x ±0.1
x.xx ±0.01
x.xxx ±0.004
x ±1°
UNLESS SPECIFIED
ALL DIMENSIONS
ARE IN INCHES
FILENAME:
~/thesis/qcad/inner
MATERIAL:
ACRYLIC (SUPPLIED)
NOTES:
BREAK SHARP EDGES
DRAWING NUMBER:
14
DATE:
26 July 1994
DRAWN BY:
Rajesh 'Q' Bilimoria
SCALE:
1:4

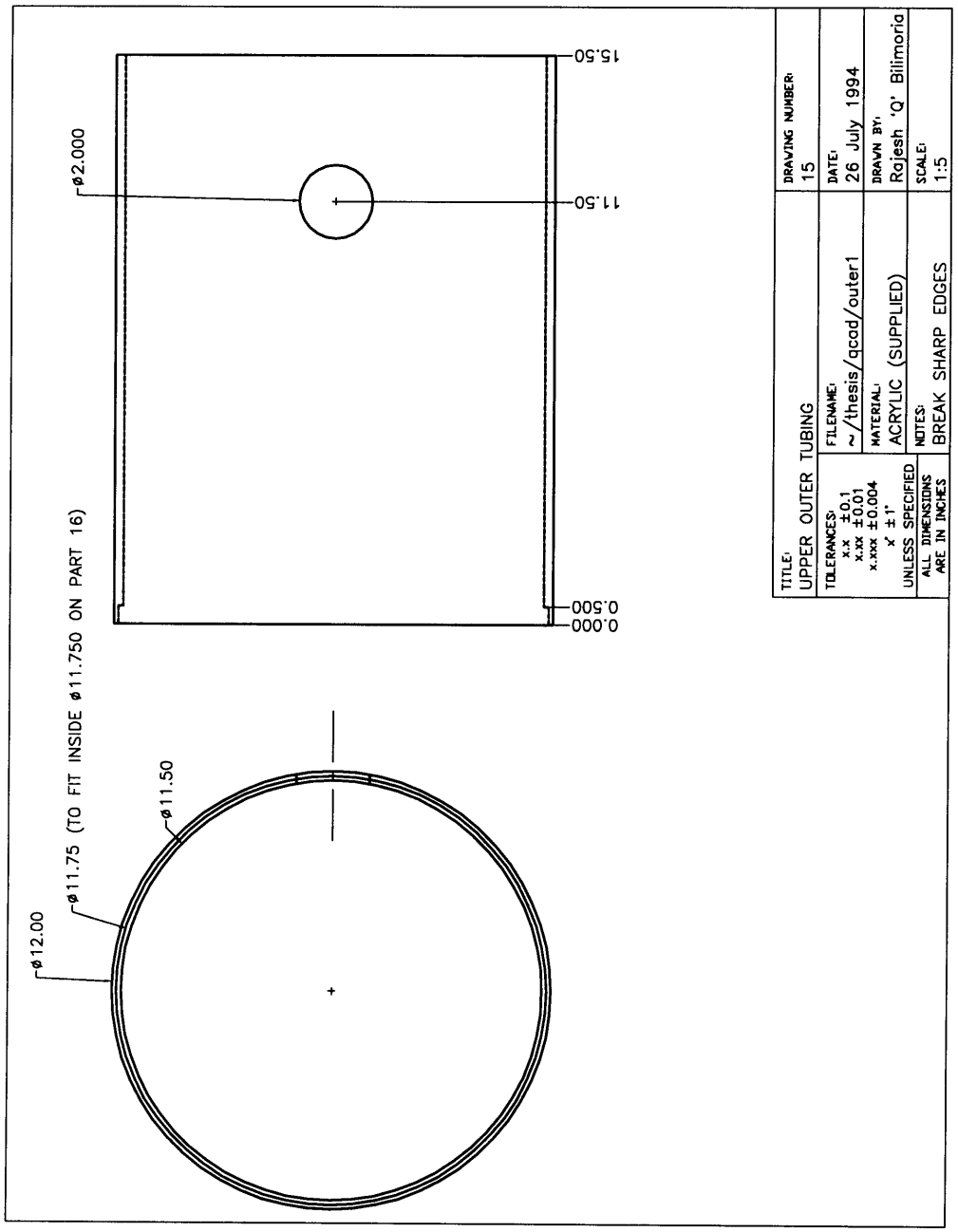
ø12.00
ø11.75 (TO FIT INSIDE ø11.750 ON PART 16)
ø11.50
ø2.000
15.50
11.50
0.500
0.000
TITLE:
UPPER OUTER TUBING
DRAWING NUMBER:
15
TOLERANCES:
x.x ±0.1
x.xx ±0.01
x.xxx ±0.004
x° ±1°
UNLESS SPECIFIED
ALL DIMENSIONS ARE IN INCHES
FILENAME:
~/thesis/qcad/outer1
MATERIAL:
ACRYLIC (SUPPLIED)
NOTES:
BREAK SHARP EDGES
DATE:
26 July 1994
DRAWN BY:
Rajesh 'Q' Bilimoria
SCALE:
1:5

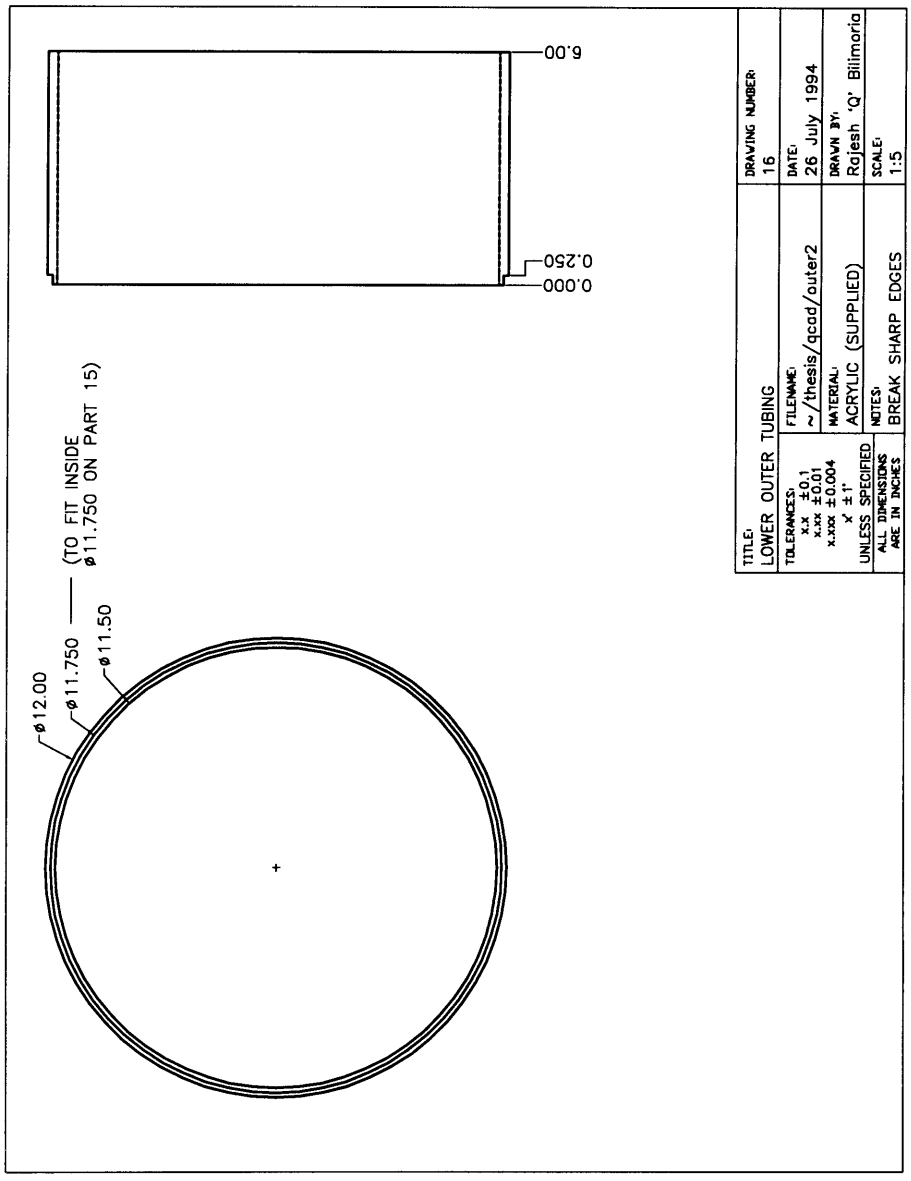
6.00
0.250
0.000
ø12.00
ø11.750
ø11.50
(TO FIT INSIDE
ø11.750 ON PART 15)
TITLE:
LOWER OUTER TUBING
DRAWING NUMBER:
16
TOLERANCES:
x.x ±0.1
x.xx ±0.01
x.xxx ±0.004
x' ±1'
UNLESS SPECIFIED
ALL DIMENSIONS
ARE IN INCHES
FILENAME:
~/thesis/qcad/outer2
DATE:
26 July 1994
MATERIAL:
ACRYLIC (SUPPLIED)
DRAWN BY:
Rajesh 'Q' Bilimoria
NOTES:
BREAK SHARP EDGES
SCALE:
1:5

TITLE:
DRAIN 'L'
DRAWING NUMBER:
17
DATE:
2 AUGUST 1994
DRAWN BY:
Rajesh 'Q' Billimoria
SCALE:
1:3
FILENAME:
~/thesis/qcad/drain
MATERIAL:
ACRYLIC
NOTES:
BREAK SHARP EDGES
TOLERANCES:
x.x ±0.1
x.xx ±0.01
x.xxx ±0.004
∠' ±1°
UNLESS SPECIFIED
ALL DIMENSIONS
ARE IN INCHES
NOTE:
INTERSECTING HOLES FOR FLUID FLOW.
INTERSECTION DETAILS ARE NOT CRITICAL.
ø2.00
3.00
1.50
0.000
3.75
3.00
1.50
0.000
ø2.00
ø1.75
R6.000
3.00
1.375
0.50
0.000
3.00
2.50
1.50
0.50
0.000

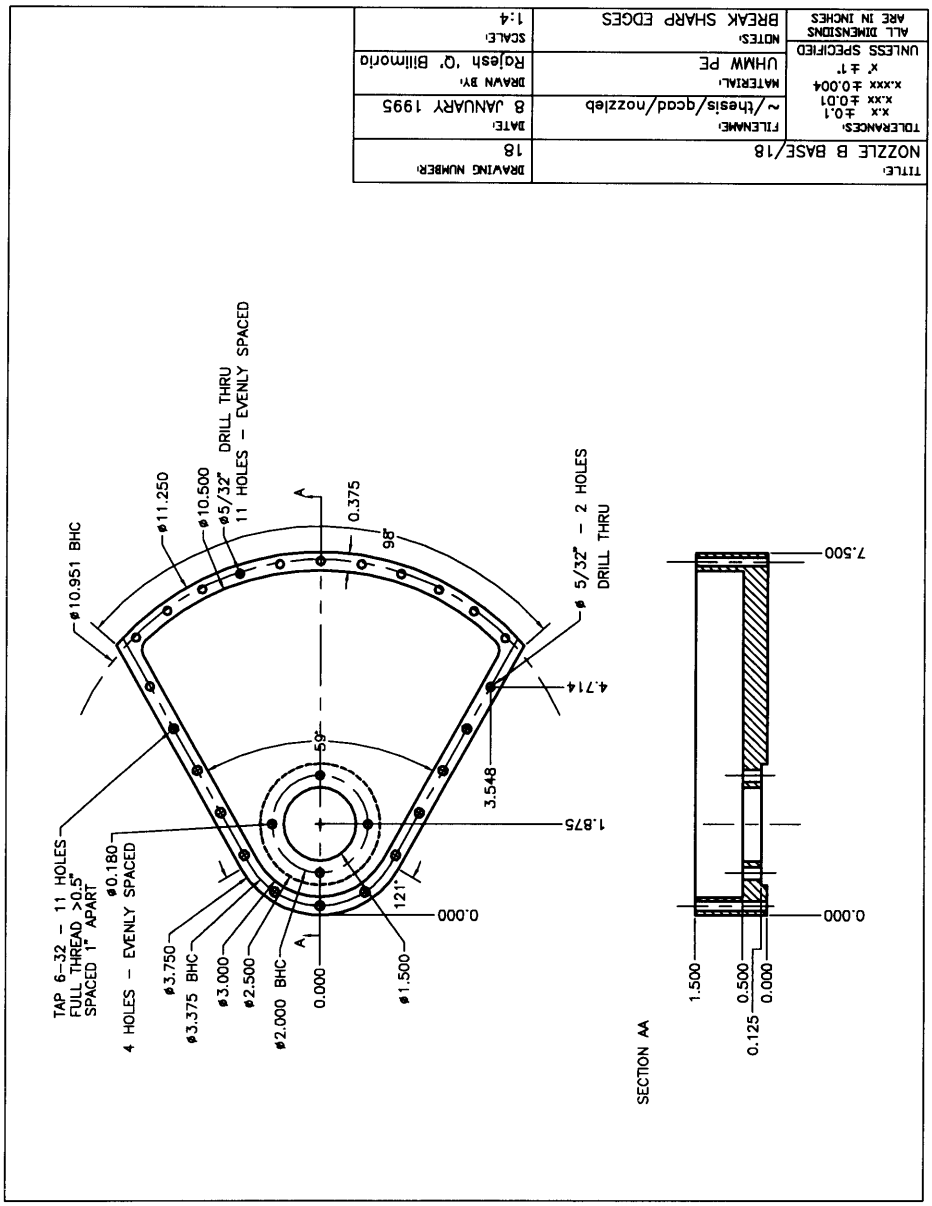
TITLE: NOZZLE B BASE/18
DRAWING NUMBER: 18
FILENAME: ~/thesis/qcad/nozzleb
DATE: 8 JANUARY 1995
MATERIAL: UHMW PE
DRAWN BY: Rajesh 'Q' Billimoria
NOTES: BREAK SHARP EDGES
SCALE: 1:4
TOLERANCES: x.x ±0.1 x.xx ±0.01 x.xxx ±0.004 x' ±1'
UNLESS SPECIFIED
ALL DIMENSIONS ARE IN INCHES
ø10.951 BHC
ø11.250
ø10.500
ø5/32" DRILL THRU 11 HOLES - EVENLY SPACED
0.375
98°
ø 5/32" - 2 HOLES DRILL THRU
4.714
3.548
1.875
0.000
1.500
121°
59°
TAP 6-32 - 11 HOLES FULL THREAD >0.5" SPACED 1" APART
4 HOLES - EVENLY SPACED ø0.180
ø3.750
ø3.375 BHC
ø3.000
ø2.500
ø2.000 BHC
0.000
A
A
SECTION AA
7.500
0.000
1.500
0.500
0.125
0.000

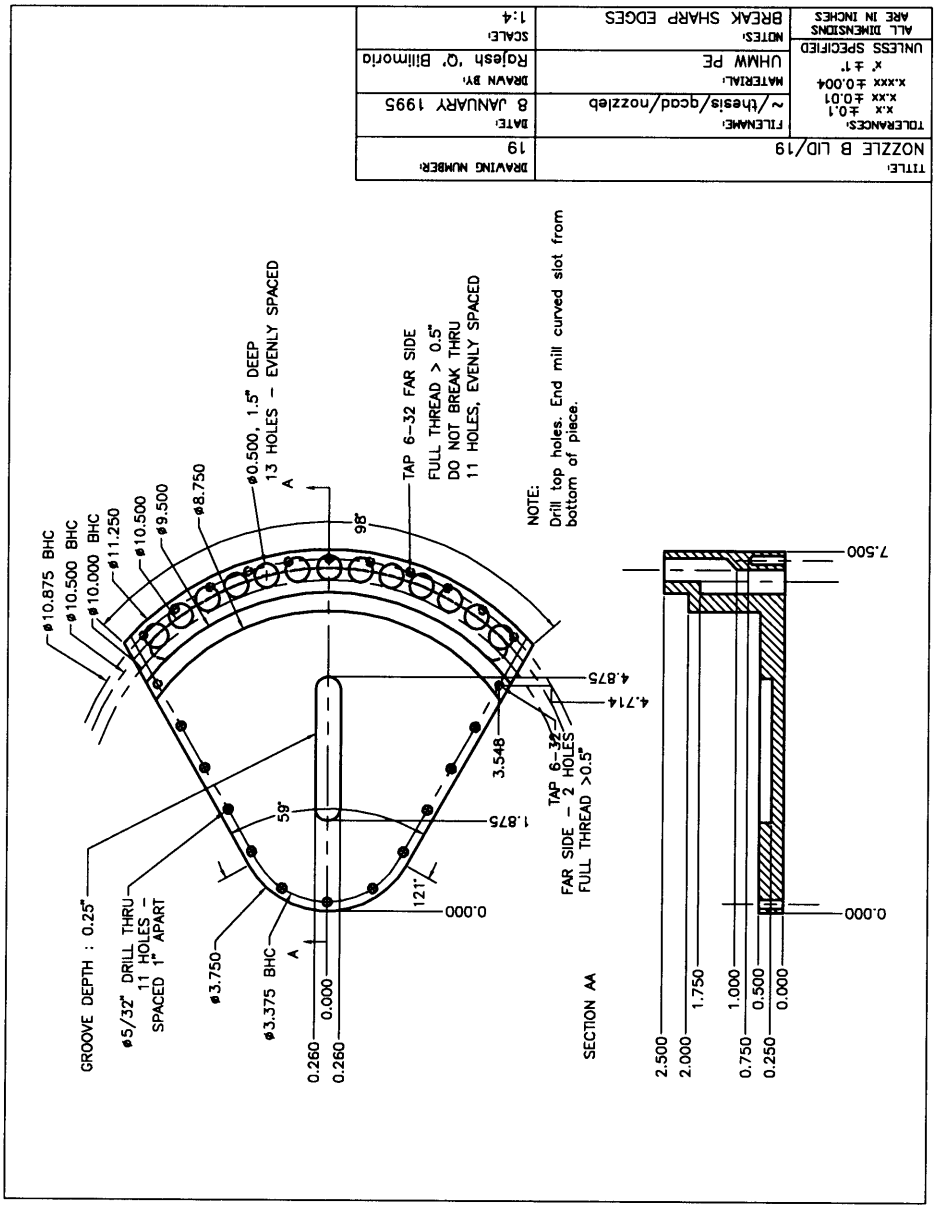
TITLE: NOZZLE B LID/19
DRAWING NUMBER: 19
FILENAME: ~/thesis/qcad/nozzleb
DATE: 8 JANUARY 1995
MATERIAL: UHMW PE
DRAWN BY: Rajesh 'Q' Billimoria
NOTES: BREAK SHARP EDGES
SCALE: 1:4
TOLERANCES: x.x ±0.1, x.xx ±0.01, x.xxx ±0.004
UNLESS SPECIFIED x' ±1'
ALL DIMENSIONS ARE IN INCHES
NOTE: Drill top holes. End mill curved slot from bottom of piece.
ø10.875 BHC
ø10.500 BHC
ø10.000 BHC
ø11.250
ø10.500
ø9.500
ø8.750
ø0.500, 1.5" DEEP 13 HOLES – EVENLY SPACED A
TAP 6–32 FAR SIDE FULL THREAD > 0.5" DO NOT BREAK THRU 11 HOLES, EVENLY SPACED
98°
4.875
4.714
3.548
1.875
58°
121°
0.000
TAP 6–32 FAR SIDE – 2 HOLES FULL THREAD >0.5"
GROOVE DEPTH : 0.25"
ø5/32" DRILL THRU 11 HOLES – SPACED 1" APART
ø3.750
ø3.375 BHC
A
0.260
0.000
0.260
SECTION AA
7.500
0.000
2.500
2.000
1.750
1.000
0.750
0.500
0.250
0.000

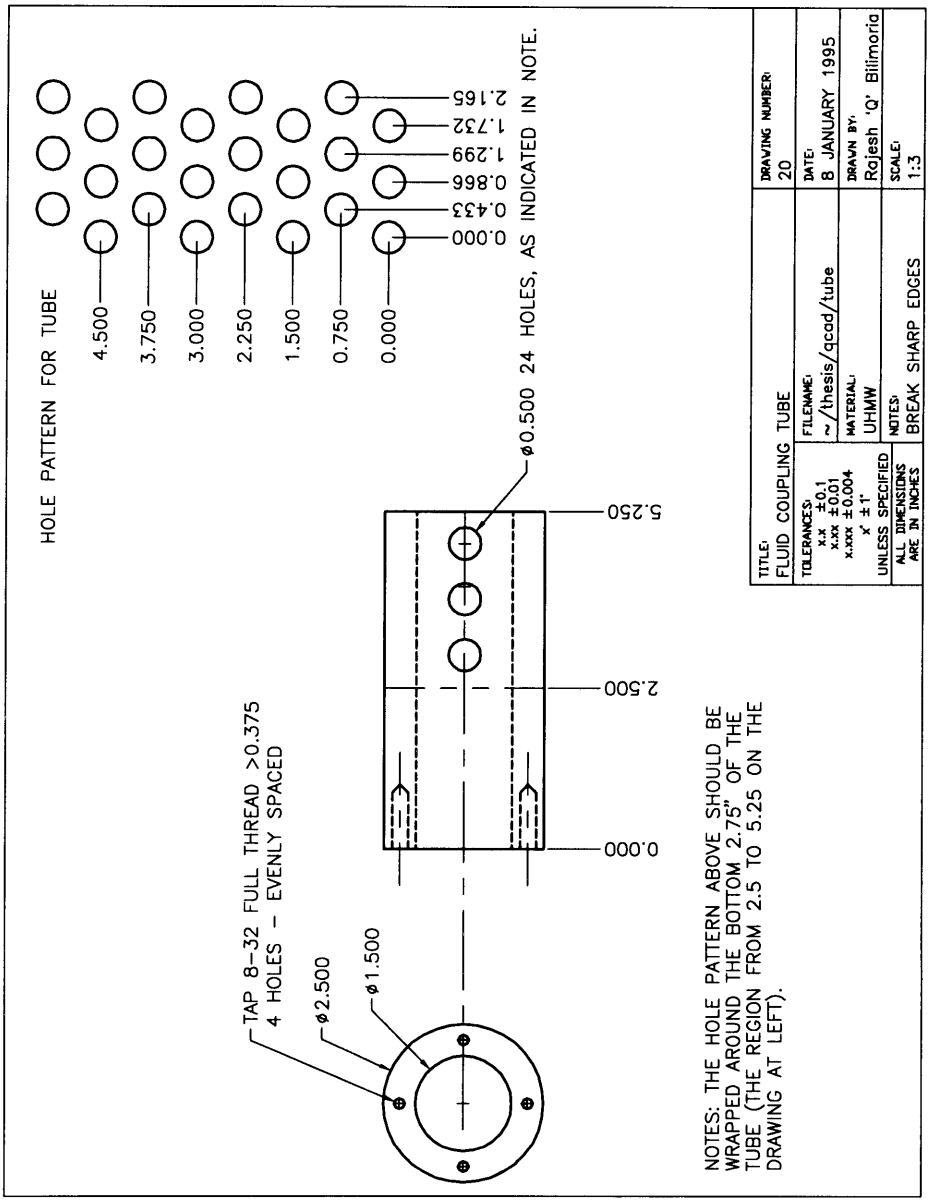
HOLE PATTERN FOR TUBE
4.500
3.750
3.000
2.250
1.500
0.750
0.000
2.165
1.732
1.299
0.866
0.433
0.000
ø0.500 24 HOLES, AS INDICATED IN NOTE.
5.250
2.500
0.000
TAP 8-32 FULL THREAD >0.375
4 HOLES - EVENLY SPACED
ø2.500
ø1.500
NOTES: THE HOLE PATTERN ABOVE SHOULD BE WRAPPED AROUND THE BOTTOM 2.75" OF THE TUBE (THE REGION FROM 2.5 TO 5.25 ON THE DRAWING AT LEFT).
TITLE: FLUID COUPLING TUBE
DRAWING NUMBER: 20
TOLERANCES: X.X ±0.1 X.XX ±0.01 X.XXX ±0.004 X° ±1° UNLESS SPECIFIED
FILENAME: ~/thesis/qcad/tube
DATE: 8 JANUARY 1995
MATERIAL: UHMW
DRAWN BY: Rajesh 'Q' Bilimoria
ALL DIMENSIONS ARE IN INCHES
NOTES: BREAK SHARP EDGES
SCALE: 1:3

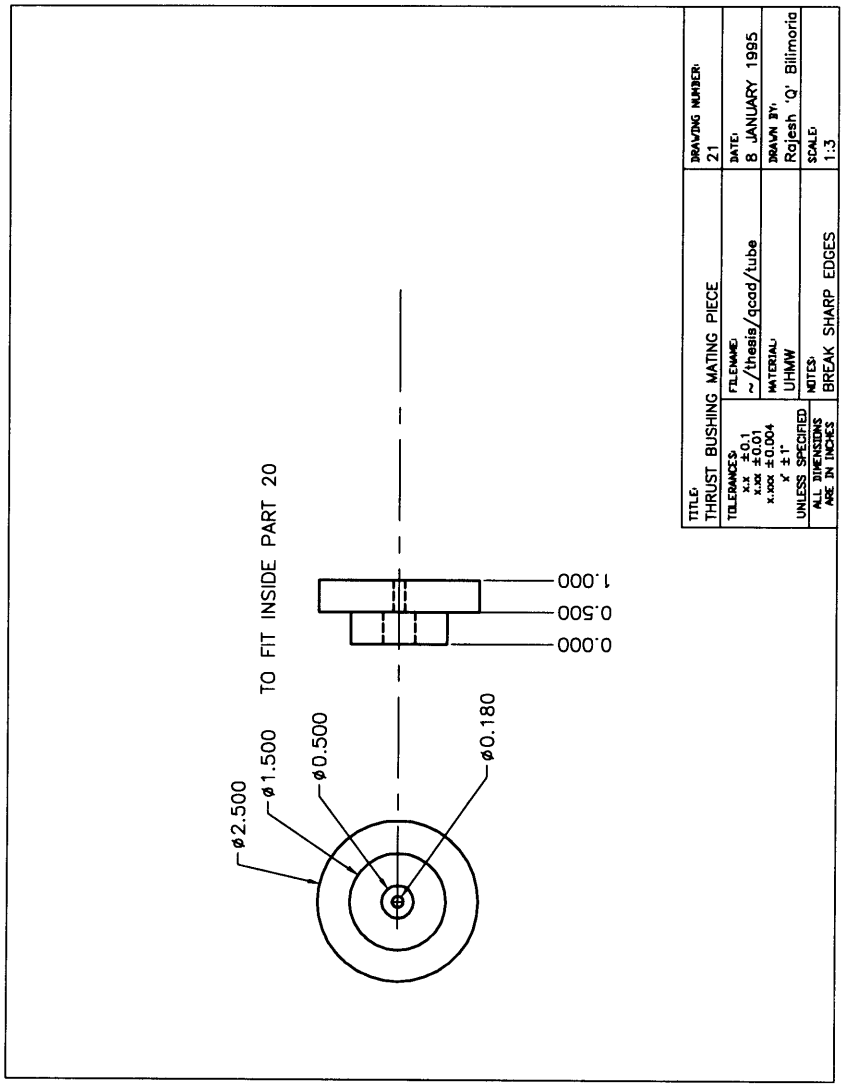
TITLE:
THRUST BUSHING MATING PIECE
TOLERANCES:
x.x ±0.1
x.xx ±0.01
x.xxx ±0.004
x' ±1'
UNLESS SPECIFIED
ALL DIMENSIONS ARE IN INCHES
FILENAME:
~/thesis/qcad/tube
MATERIAL:
UHMW
NOTES:
BREAK SHARP EDGES
DRAWING NUMBER:
21
DATE:
8 JANUARY 1995
DRAWN BY:
Rajesh 'Q' Bilimoria
SCALE:
1:3
TO FIT INSIDE PART 20
ø2.500
ø1.500
ø0.500
ø0.180
1.000
0.500
0.000

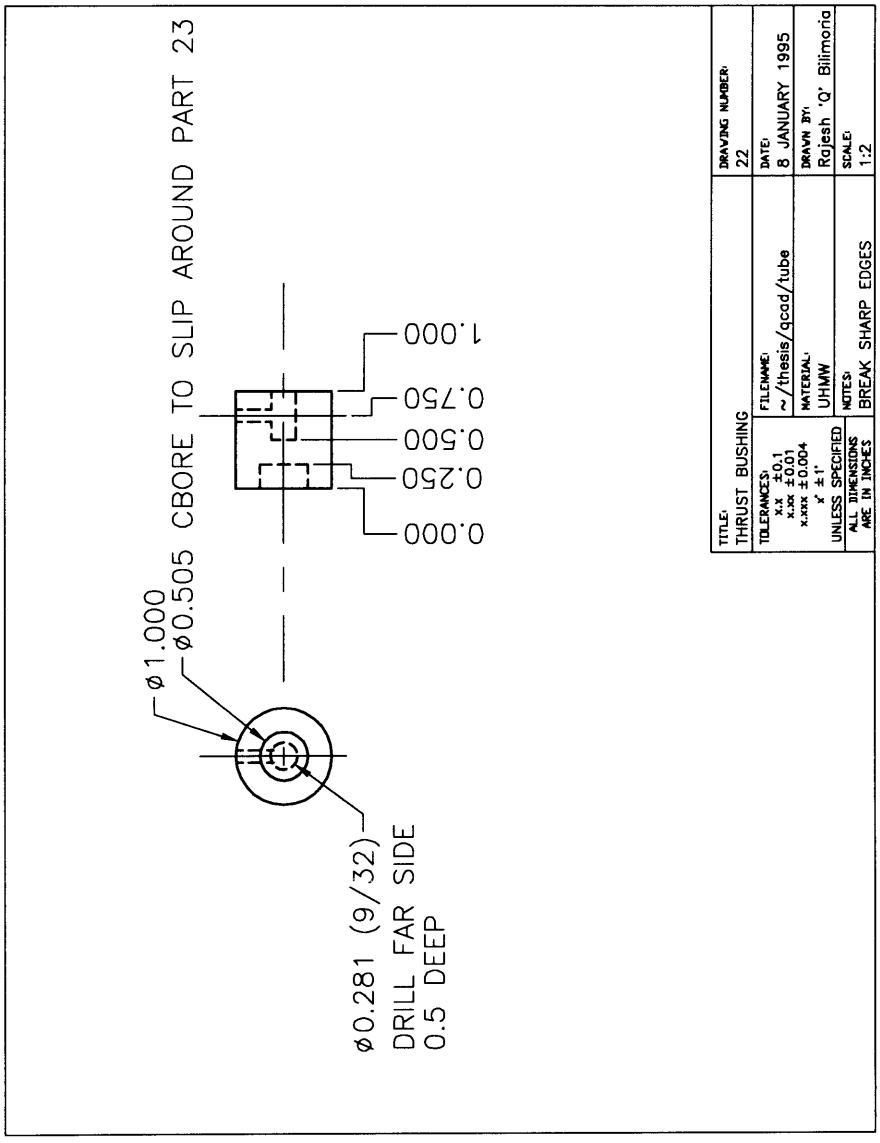
ø1.000
ø0.505 CBORE TO SLIP AROUND PART 23
1.000
0.750
0.500
0.250
0.000
ø0.281 (9/32)
DRILL FAR SIDE
0.5 DEEP
TITLE:
THRUST BUSHING
DRAWING NUMBER:
22
TOLERANCES:
X.X ±0.1
X.XX ±0.01
X.XXX ±0.004
X' ±1'
UNLESS SPECIFIED
FILENAME:
~/thesis/qcad/tube
DATE:
8 JANUARY 1995
MATERIAL:
UHMW
DRAWN BY:
Rajesh 'Q' Bilimoria
ALL DIMENSIONS ARE IN INCHES
NOTES:
BREAK SHARP EDGES
SCALE:
1:2

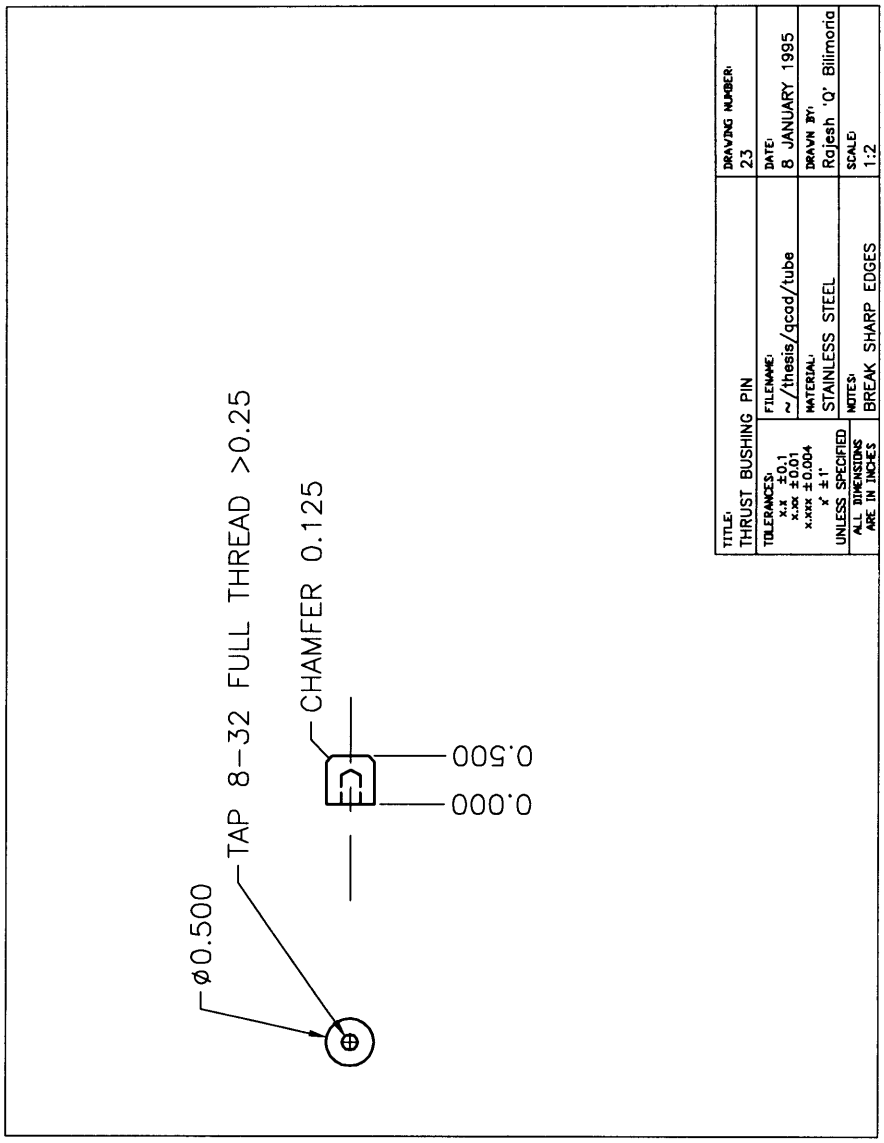
ø0.500
TAP 8-32 FULL THREAD >0.25
CHAMFER 0.125
0.500
0.000
TITLE:
THRUST BUSHING PIN
DRAWING NUMBER:
23
TOLERANCES:
X.X ±0.1
X.XX ±0.01
X.XXX ±0.004
X° ±1°
UNLESS SPECIFIED
ALL DIMENSIONS ARE IN INCHES
FILENAME:
~/thesis/qcad/tube
DATE:
8 JANUARY 1995
MATERIAL:
STAINLESS STEEL
DRAWN BY:
Rajesh 'Q' Bilimoria
NOTES:
BREAK SHARP EDGES
SCALE:
1:2

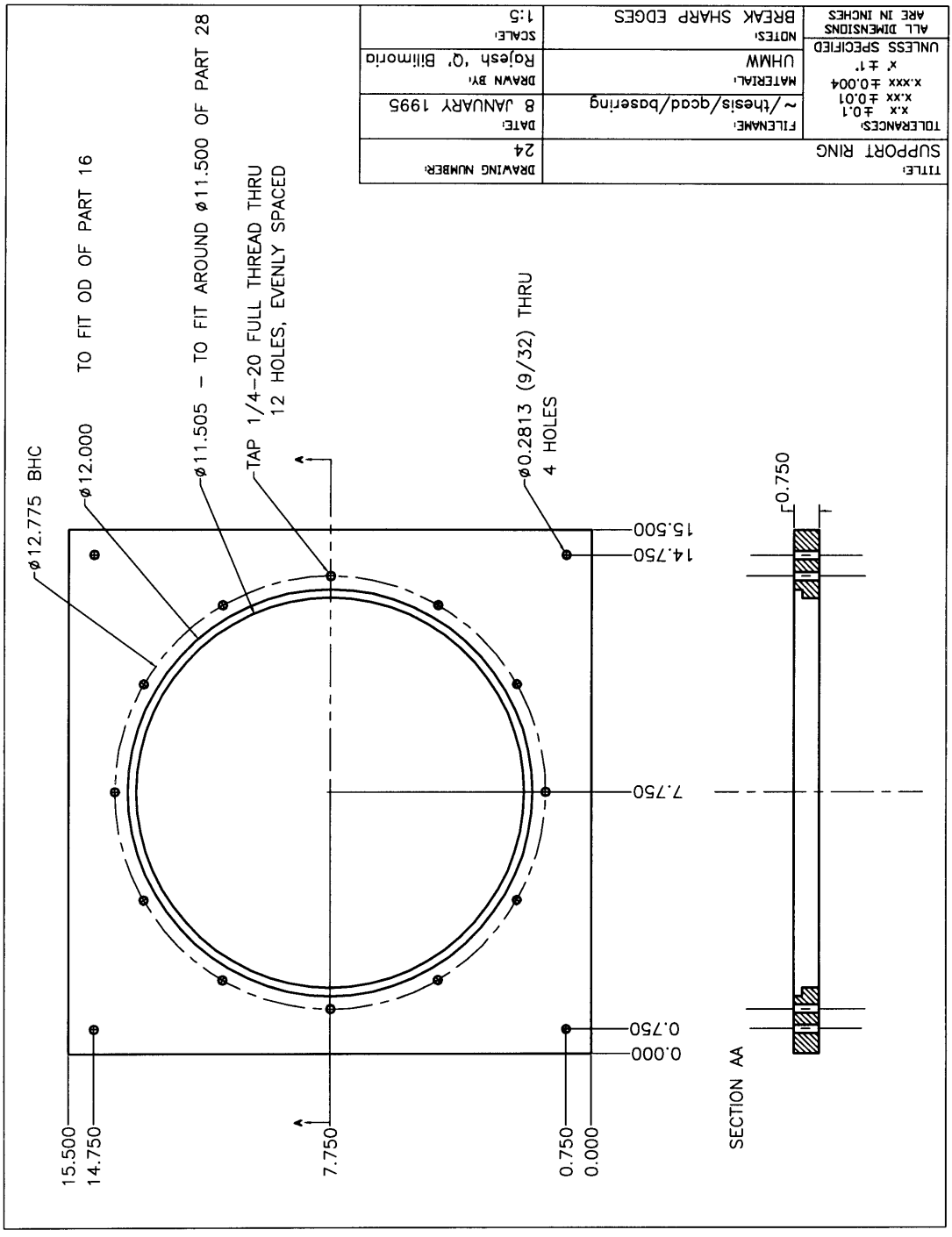
ø12.775 BHC
ø12.000 TO FIT OD OF PART 16
ø11.505 – TO FIT AROUND ø11.500 OF PART 28
TAP 1/4–20 FULL THREAD THRU
12 HOLES, EVENLY SPACED
ø0.2813 (9/32) THRU
4 HOLES
15.500
14.750
7.750
0.750
0.000
0.750
SECTION AA
TITLE: SUPPORT RING
DRAWING NUMBER: 24
DATE: 8 JANUARY 1995
DRAWN BY: Rojesh 'Q' Bilimoria
SCALE: 1:5
NOTES: BREAK SHARP EDGES
FILENAME: ~/thesis/qcad/bsering
MATERIAL: UHMW
TOLERANCES: x.x ±0.1, x.xx ±0.01, x.xxx ±0.004, x' ±1°
UNLESS SPECIFIED
ALL DIMENSIONS ARE IN INCHES

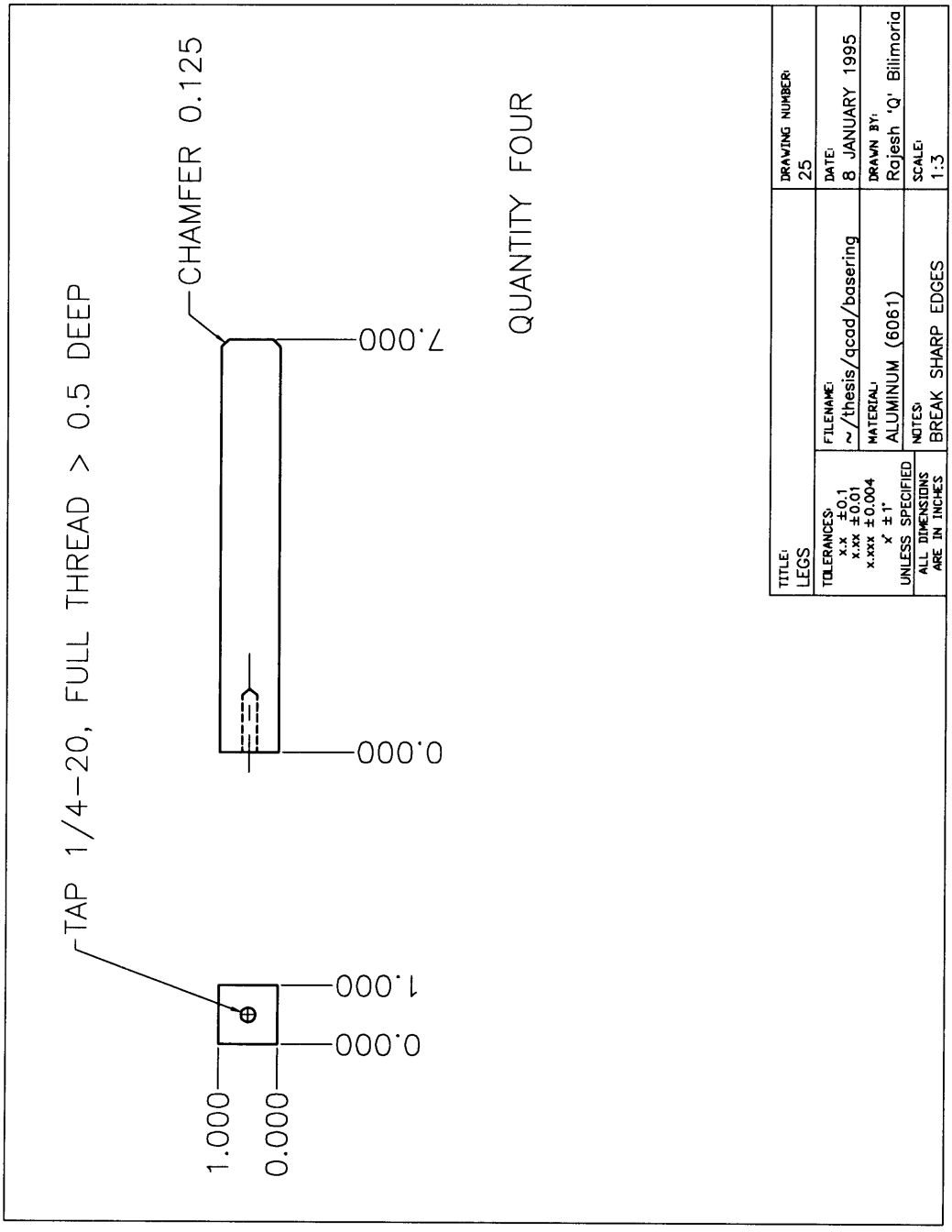
TAP 1/4-20, FULL THREAD > 0.5 DEEP
CHAMFER 0.125
7.000
0.000
QUANTITY FOUR
1.000
0.000
1.000
0.000
TITLE:
LEGS
DRAWING NUMBER:
25
TOLERANCES:
x.x ±0.1
x.xx ±0.01
x.xxx ±0.004
x' ±1'
UNLESS SPECIFIED
ALL DIMENSIONS
ARE IN INCHES
FILENAME:
~/thesis/qcad/basering
MATERIAL:
ALUMINUM (6061)
NOTES:
BREAK SHARP EDGES
DATE:
8 JANUARY 1995
DRAWN BY:
Rajesh 'Q' Bilimoria
SCALE:
1:3

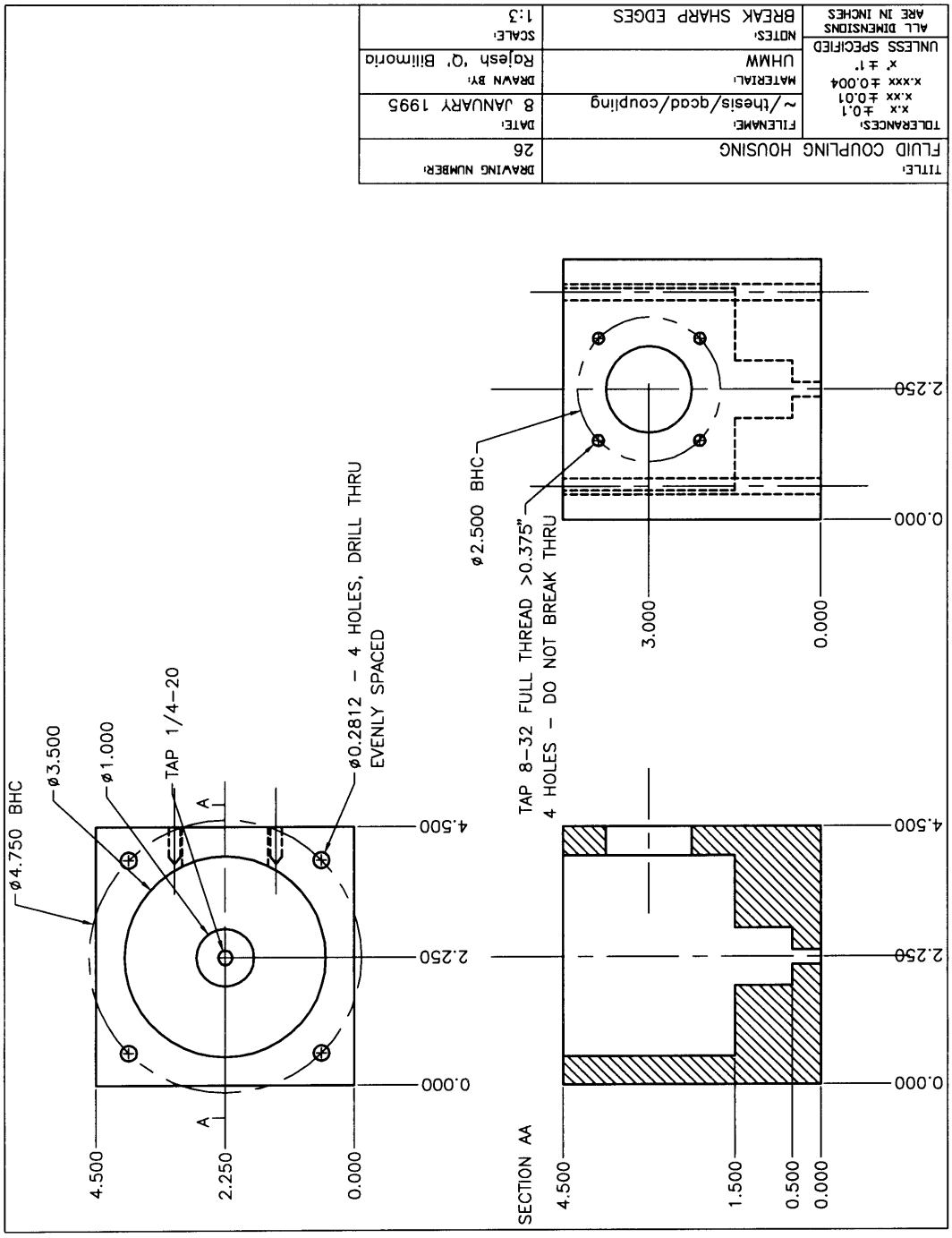
TITLE: FLUID COUPLING HOUSING
DRAWING NUMBER: 26
TOLERANCES: x.x ±0.1, x.xx ±0.01, x.xxx ±0.004, x° ±1°
UNLESS SPECIFIED
ALL DIMENSIONS ARE IN INCHES
FILENAME: ~/thesis/qcad/coupling
MATERIAL: UHMW
NOTES: BREAK SHARP EDGES
DRAWN BY: Rajesh 'Q' Billimoria
DATE: 8 JANUARY 1995
SCALE: 1:3
ø4.750 BHC
ø3.500
ø1.000
TAP 1/4-20
ø0.2812 - 4 HOLES, DRILL THRU EVENLY SPACED
4.500
2.250
0.000
SECTION AA
TAP 8-32 FULL THREAD >0.375"
4 HOLES - DO NOT BREAK THRU
ø2.500 BHC
3.000
1.500
0.500

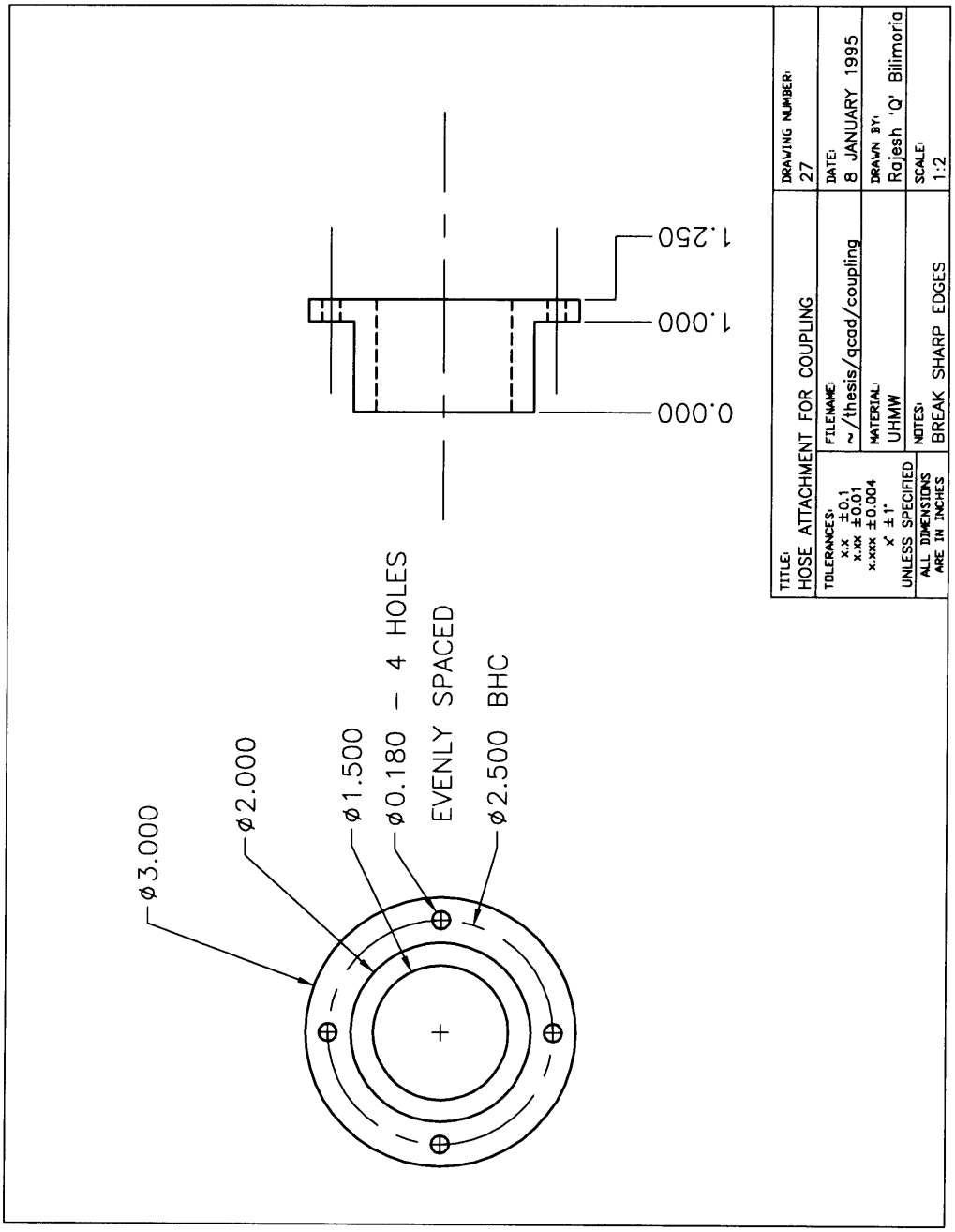
ø3.000
ø2.000
ø1.500
ø0.180 - 4 HOLES
EVENLY SPACED
ø2.500 BHC
1.250
1.000
0.000
TITLE:
HOSE ATTACHMENT FOR COUPLING
DRAWING NUMBER:
27
TOLERANCES:
x.x ±0.1
x.xx ±0.01
x.xxx ±0.004
x' ±1'
UNLESS SPECIFIED
ALL DIMENSIONS ARE IN INCHES
FILENAME:
~/thesis/qcad/coupling
MATERIAL:
UHMW
NOTES:
BREAK SHARP EDGES
DATE:
8 JANUARY 1995
DRAWN BY:
Rajesh 'Q' Bilimoria
SCALE:
1:2

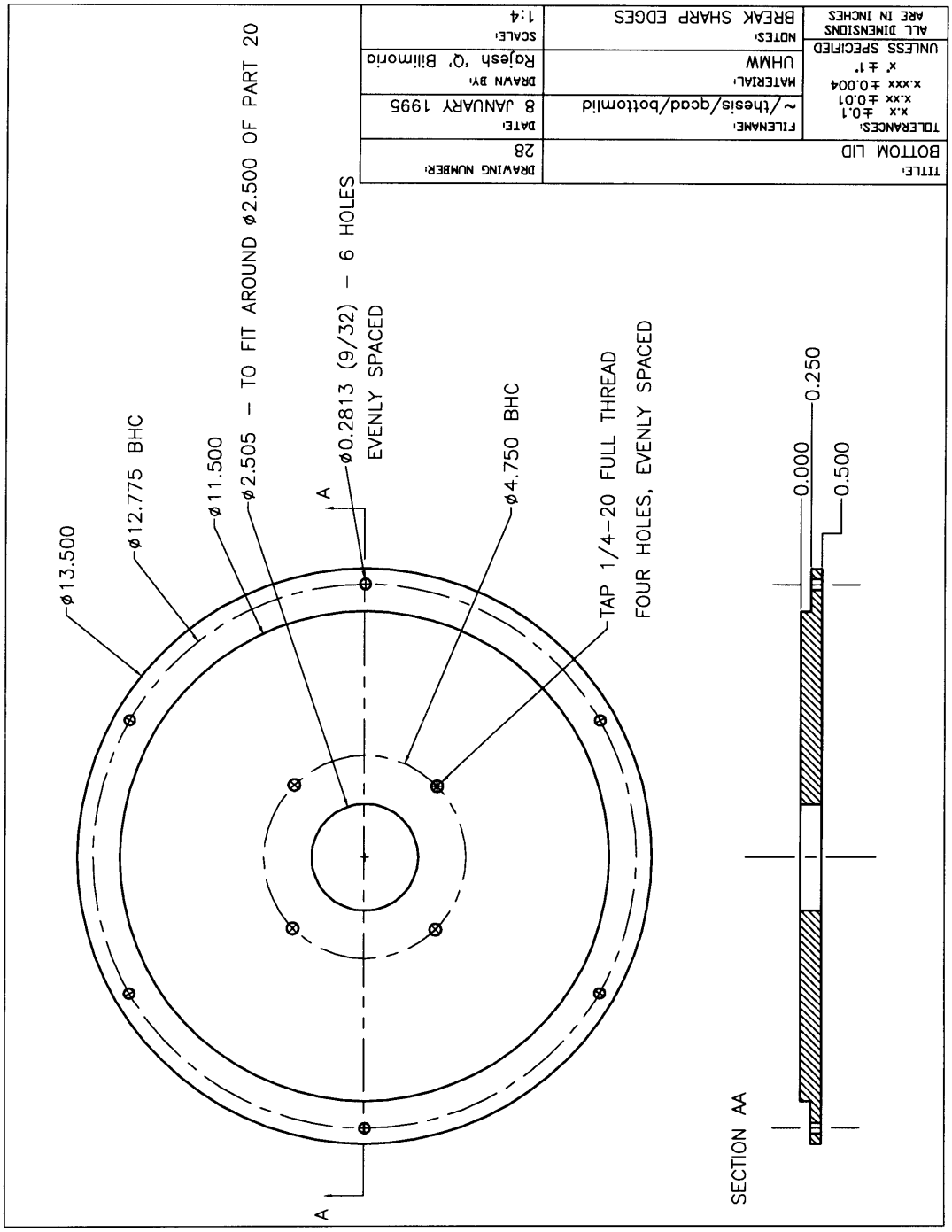
ø13.500
ø12.775 BHC
ø11.500
ø2.505 – TO FIT AROUND ø2.500 OF PART 20
ø0.2813 (9/32) – 6 HOLES
EVENLY SPACED
ø4.750 BHC
TAP 1/4–20 FULL THREAD
FOUR HOLES, EVENLY SPACED
A
A
SECTION AA
0.000
0.250
0.500
TITLE: BOTTOM LID
DRAWING NUMBER: 28
DATE: 8 JANUARY 1995
DRAWN BY: Rajesh 'Q' Bilimoria
SCALE: 1:4
FILENAME: ~/thesis/qcad/bottomlid
MATERIAL: UHMW
NOTES: BREAK SHARP EDGES
TOLERANCES: x.x ±0.1 x.xx ±0.01 x.xxx ±0.004 x' ±1'
UNLESS SPECIFIED
ALL DIMENSIONS ARE IN INCHES

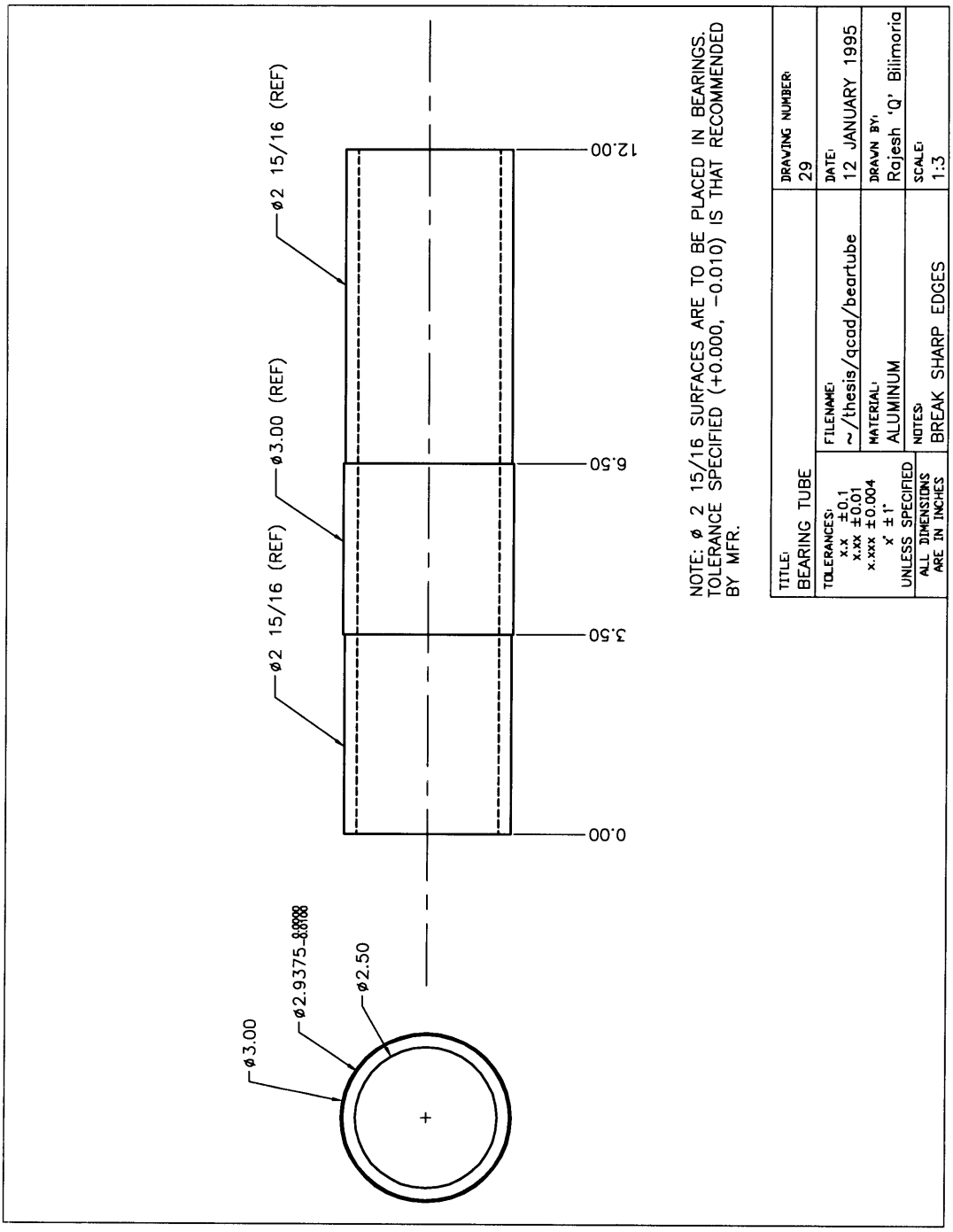
ø3.00
ø2.9375
ø2.50
ø2 15/16 (REF)
ø3.00 (REF)
ø2 15/16 (REF)
0.00
3.50
6.50
12.00
NOTE: ø 2 15/16 SURFACES ARE TO BE PLACED IN BEARINGS. TOLERANCE SPECIFIED (+0.000, -0.010) IS THAT RECOMMENDED BY MFR.
TITLE:
BEARING TUBE
DRAWING NUMBER:
29
TOLERANCES:
x.x ±0.1
x.xx ±0.01
x.xxx ±0.004
x° ±1°
UNLESS SPECIFIED
ALL DIMENSIONS ARE IN INCHES
FILENAME:
~/thesis/qcad/beartube
MATERIAL:
ALUMINUM
NOTES:
BREAK SHARP EDGES
DATE:
12 JANUARY 1995
DRAWN BY:
Rajesh 'Q' Bilimoria
SCALE:
1:3

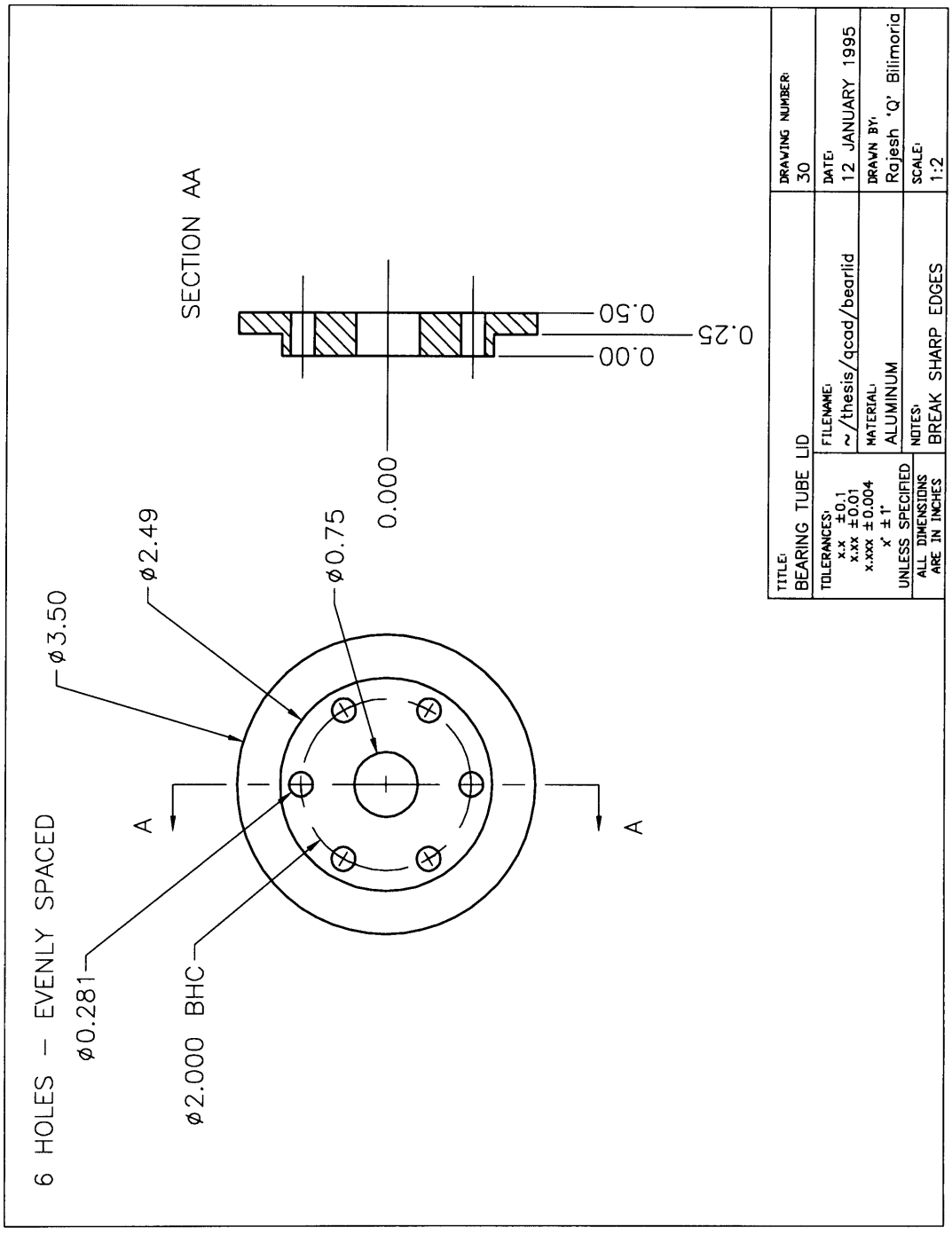
6 HOLES – EVENLY SPACED
ø0.281
ø2.000 BHC
ø3.50
ø2.49
ø0.75
A
A
0.000
SECTION AA
0.50
0.00
0.25
TITLE: BEARING TUBE LID
DRAWING NUMBER: 30
TOLERANCES: x.x ±0.1 x.xx ±0.01 x.xxx ±0.004 x° ±1° UNLESS SPECIFIED ALL DIMENSIONS ARE IN INCHES
FILENAME: ~/thesis/qcad/bearlid
DATE: 12 JANUARY 1995
MATERIAL: ALUMINUM
DRAWN BY: Rajesh 'Q' Bilimoria
NOTES: BREAK SHARP EDGES
SCALE: 1:2

Bibliography

Annis, Karen J. *Segregation Control of Binary Size Particles in a Comminution Device*. S.M. Thesis, Massachusetts Institute of Technology, 1991.

Committee on Comminution and Energy Consumption, National Advisory Board, National Academy of Science. Reprint No. NMAB-364, May, 1981.

Ghaddar, C. K. *Fracture Efficiency Within Particle Beds*. S.M. Thesis, Massachusetts Institute of Technology, 1991.

Kurfess, A. D. *Fracture Criterion for Brittle and Plastic Spheres.* S.M. Thesis, Massachusetts Institute of Technology, 1989.

Laffey, K. M. *Fracture Within Particle Beds Under Compressive Loading*. S.M. Thesis, Massachusetts Institute of Technology, 1987.

Larson, A. *The Effect of Size and Geometry in Single Particle Crushing.* S.M. Thesis, Massachusetts Institute of Technology, 1986.

Misra, S. D. *Particle Breakage and Material Transport in the Design of a High-Efficiency Comminution Device*. S.M. Thesis, Massachusetts Institute of Technology, 1991.

Mular, Andrew L. and Bhappu, Roshan B., eds. *Mineral Processing Plant Design*. New York: Society of Mining Engineers, 1980.

Pflueger, J. *The Behavior of Particle Beds in Simulation*. S.M. Thesis, Massachusetts Institute of Technology, 1988.

Phadke, Madhav S. *Quality Engineering Using Robust Design*. Englewood Cliffs: Prentice-Hall, 1989.

Savage, S. B. and Lun, C. K. K. "Particle Size Segregation in Inclined Chute Flow of Dry Cohesionless Granular Solids." *J. Fluid. Mech.*, 189:311-335. 1988.

Schiaffino, Stefano. *Fluidization and Segregation in Bi-Disperse Solid-Liquid Particulate Systems*. S.M. Thesis, Massachusetts Institute of Technology, 1993.

Snow, R. H. and Paulding, B. W. "Prediction of Fragment Size Distribution from Calculations of Stress in Spheres and Disks." *H. Heywood Memorial Symposium.* Loughborough University of Technology.

Wisnewski, Michael G. *Impulsive Segregation of a Bi-Disperse Mixture Between Outwardly Moving Walls.* S.M. Thesis, Massachusetts Institute of Technology, 1994.